

MELT RATE IMPROVEMENT FOR DWPF MB3:
Melt Rate Furnace Testing (U)

M. E. STONE
J. E. JOSEPHS

Westinghouse Savannah River Company
Savannah River Site
Aiken, SC 29808



SAVANNAH RIVER SITE

This document was prepared in conjunction with work accomplished under Contract No. DE-AC09-96SR18500 with the U.S. Department of Energy.

DISCLAIMER

This report was prepared as an account of work sponsored by an agency of the United States Government. Neither the United States Government nor any agency thereof, nor any of their employees, makes any warranty, express or implied, or assumes any legal liability or responsibility for the accuracy, completeness, or usefulness of any information, apparatus, product or process disclosed, or represents that its use would not infringe privately owned rights. Reference herein to any specific commercial product, process or service by trade name, trademark, manufacturer, or otherwise does not necessarily constitute or imply its endorsement, recommendation, or favoring by the United States Government or any agency thereof. The views and opinions of authors expressed herein do not necessarily state or reflect those of the United States Government or any agency thereof.

This report has been reproduced directly from the best available copy.

Available for sale to the public, in paper, from: U.S. Department of Commerce, National Technical Information Service, 5285 Port Royal Road, Springfield, VA 22161, phone: (800) 553-6847, fax: (703) 605-6900, email: orders@ntis.fedworld.gov online ordering: <http://www.ntis.gov/ordering.htm>

Available electronically at <http://www.doe.gov/bridge>

Available for a processing fee to U.S. Department of Energy and its contractors, in paper, from: U.S. Department of Energy, Office of Scientific and Technical Information, P.O. Box 62, Oak Ridge, TN 37831-0062, phone: (865) 576-8401, fax: (865) 576-5728, email: reports@adonis.osti.gov

WSRC-TR-2001-00146, Revision 0

**Keywords: Melt rate, DWPF
Macrobatch 3**

Retention: Permanent

**MELT RATE IMPROVEMENT FOR DWPF MB3:
*Melt Rate Furnace Testing (U)***

**M. E. Stone
J. E. Josephs**

Publication Date: March 15, 2001

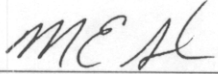
**Westinghouse Savannah River Company
Savannah River Site
Aiken, SC 29808**



SAVANNAH RIVER SITE

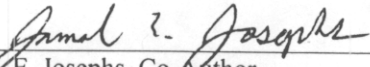
PREPARED FOR THE U.S. DEPARTMENT OF ENERGY UNDER CONTRACT NO. DE-AC09-96SR18500

APPROVALS



M. E. Stone, Co-Author

4/30/01
Date




J. E. Josephs, Co-Author

4-30-01
Date



D. P. Lambert, Technical Reviewer

4/30/01
Date



S. L. Marra, Manager

5/7/01
Date



E. W. Holtzscheiter, Manager

5/7/01
Date

ACKNOWLEDGEMENTS

The authors would like to thank the other members of the melt rate team, which includes Denny Bickford, Hector Guerrero, Carol Jantzen, Dan Lambert, Troy Lorier, Sharon Marra, David Peeler, Jim Sproull, and Doug Witt, for their insightful technical direction. We also appreciate the assistance of the many SRTC technicians, their supervisors and interns that have supported these tasks, especially Frances Williams, Joe Wheeler, Sarah Brown, Tony Burckhalter, Jon DuVall, Sammie King, Debbie Marsh, Mary Moss, Daniel Pittman, Irene Reamer, Pat Toole, Vickie Williams, and Phyllis Workman. The technical support from John Vienna, Joe Perez, and Pavel Hrma (PNNL) was invaluable. We especially appreciated the direction and support from the DWPF and HLW engineers especially Dick O'Driscoll, Richard Edwards, Hank Elder, Dan Iverson, Michael Norton, and John Occhipinti.

The glass shop technicians, Gary Dobos and Curt Sexton, provided capable and timely help in sectioning the crucibles and beakers and preparing glassware to support the use of the borescope to view the melt rate furnace experiments. Gene Daniels (SRTC) provided data analysis with the JMP4 program, Tim Jones and Nick Odom (SRTC) expertly assisted with modifications to the melt rate furnace, and the clerical support provided by Stacie Owens was invaluable. Jeff Siler aided the installation of the camera on the borescope. Technical management and guidance of this task came from Sharon Marra and Bill Holtzscheiter.

TABLE OF CONTENTS

ACKNOWLEDGEMENTS	v
LIST OF FIGURES	vii
LIST OF TABLES	vii
INTRODUCTION.....	1
EXECUTIVE SUMMARY	1
DISCUSSION	2
<i>Melt Rate Furnace Test Methods.....</i>	2
Equipment Description	2
Equipment Operation.....	3
Nomenclature of Runs	3
Melt Rate Determination	3
Bridging	4
<i>Macrobatch 3: Baseline Tests</i>	7
Macrobatch 2 versus Macrobatch 3	10
<i>Alternative Melter Feed Tests</i>	10
Changes in the Sludge Washing Process	10
Changes in the Nitric Acid / Formic Acid Ratio during the SRAT Process	11
Changes in the Amount of Acid Addition during the SRAT Process	11
Sugar Addition.....	11
<i>Alternative Frit Tests</i>	12
Melt Rate Versus Alkali Content: Mole Percentage Basis	14
Frit 320-A Testing	16
Mechanism for Increased Melt Rate with Higher Alkali Content	16
Frit 165 Testing	16
CONCLUSIONS	16
REFERENCES.....	17
APPENDICES A - H.....	19

LIST OF FIGURES

Figure 1. Batch Height Data from Borescope.....	4
Figure 2. Temperature Charts for G-MB3-MRF-2 and BONE-MB3-MRF-2	5
Figure 3. Sectioned Crucible from 200-MB3-MRF-8	6
Figure 4. Bridging During Melt Rate Furnace Tests	6
Figure 5. Isotherm for Runs with 794 Gram Batch Weight.....	7
Figure 6. Isotherm for Runs with 566 Gram Batch Weight.....	8
Figure 8. Glass Pool Height as a Function of Run Time	9
Figure 9. Melt Rate Versus Alkali Content	13
Figure 10. Melt Rate as a Function of Predicted Glass Viscosity.....	14
Figure 11. Melt Rate Versus Total Alkali Content of Frit: Mole Percent Basis	15

LIST OF TABLES

Table 1. Melt Rate Test Results.....	1
Table 2. Melt Rate as a Function of Run Time	9
Table 3. Melt Rate for Baseline Runs.....	10
Table 4. Comparison of Melt Rate of Macrobatches 2 and 3.....	10
Table 5. Melt Rate of Underwashed, Baseline, and Overwashed Feed	11
Table 6. Comparison of Formic Acid Only to Baseline Process	11
Table 7. Comparison of Melt Rate with Sugar Addition	12
Table 8. Melt Rates during Alternative Frit Tests	13
Table 9. Compositions of BONE, BONE3, and D	14
Table 10. Melt Rate of Frit 320-A	16
Table 11. Melt Rate of Frit 165 and Frit 200 during Initial Tests.....	16
Table 12. Melt Rate Test Results.....	17

INTRODUCTION

The Defense Waste Processing Facility (DWPF) would like to increase its canister production rate. The goal of this study is to improve the melt rate in DWPF specifically for Macrobatches 3. However, the knowledge gained may result in improved melting efficiencies translating to future DWPF macrobatches and in higher throughput for other Department of Energy’s (DOE) melter. Increased melting efficiencies decrease overall operational costs by reducing the immobilization campaign time for a particular waste stream. For melt rate limited systems, a small increase in melting efficiency translates into significant hard dollar savings by reducing life cycle operational costs.

EXECUTIVE SUMMARY

Melt rate testing was conducted with Macrobatches 3 sludge simulant to determine if modifications to the current waste vitrification process could improve melt rate. The modifications fall into two categories: changes in the sludge preparation process and changes in the frit composition. The tests indicated that melt rate is significantly impacted by the alkali content of the melter feed.

The testing in this report summarized the melt rate furnace experiments that were used to measure the melt rate of various frit and process changes. Reproducibility of runs was generally good, but problems with bridging were noted during the runs. Although bridging does not appear to have impacted the results of the tests, the possibility that bridging has affected the results cannot be ruled out. Larger scale tests should reduce the amount of bridging and add confidence in the test results. The results of the tests are tabulated in Table 1.

Table 1. Melt Rate Test Results

Alternative Frit Tests			Alternative Feed Tests	
Frit	Original Designation	Melt Rate (in / hr)	SRAT Product Type	Melt Rate (in / hr)
304	D	1.13	Baseline	0.57
165 (Si Def)	n/a	1.06	Underwashed	0.68
320	BONE	1.05	Overwashed	0.47
320-A	BONE3	1.04	Formic Only	0.59
313	M	1.01		
326	BONE2	0.95		
165	n/a	0.95		
307	G	0.93		
325	BICK	0.87		
322	MIMI	0.87		
324	KMA2A	0.79		
200 (Baseline)	n/a	0.75		
314	N	0.66		
323	KMA2	0.62		
315	O	0.62		
303	C	0.51		

DISCUSSION

The melt rate testing to improve the throughput of the DWPF facility began in FY00. The FY00 tests focused on improving the melt rate of the Macrobatch 2 (MB2) sludge batch currently being processed at DWPF. The tests with MB2 feed indicated that the melt rate could be improved by changing the frit composition from Frit 200 to Frit 165 and by addition of sugar to the melter feed [3]. The current test program documented in this report was designed to utilize the experience gained during testing with MB2 melter feed to evaluate ways to improve the melt rate for the next sludge batch, Macrobatch 3 (MB3) [1].

The results obtained during the MB3 tests was comparable to the MB2 results with one exception: the batch height during the run. During MB2 tests, the batch height was observed to rise during the initial part of the run before collapsing and slumping into a glass pool. No rise in batch height was noted during runs with MB3 feed, with the exception of the run with sugar added. The difference in expansions is most likely the result of improvements made to the feed preparation process [5].

Melt Rate Furnace Test Methods

Equipment Description

The melt rate furnace was designed by Denny Bickford, fabricated at Clemson University, and modified at TNX to support the melt rate tests. The furnace was heated by two 1925-watt plate heaters and had a one cubic foot inner chamber surrounded by five to six inches of ceramic fiber insulation. A digital pulse relay controller and a type K thermocouple along the sidewall of the furnace controlled the furnace temperature. An offgas eductor was utilized to pull an air sweep across the top of the furnace.

The furnace was designed to heat the bottom of the beaker while insulating the sides and top to create a vertical temperature profile in the beaker similar to the one dimensional heat transfer from the glass pool to the cold cap. The top of the furnace had a 6" diameter hole through the insulation, as shown in Appendix A. A 1200 ml stainless steel beaker with a Kaowool insulating sleeve, shown in Appendix A, was inserted into the hole so that the bottom of the beaker was nearly flush with the top of the heated chamber. A 1" thick insulation board was placed over the beaker to prevent excessive heat loss from the top.

The type K thermocouples inserted into the beaker were connected to a temperature indicator that logged the readings every 5 seconds. The four to eight lower thermocouples in the beaker were 0.040" in diameter and were positioned around a 3/4" radius from the center of the beaker during initial tests. Six lower thermocouples were bundled into a central thermocouple (T/C) tree during the last ten runs. The upper thermocouple was 5" above the bottom of the beaker to measure the vapor space temperature. This thermocouple was 1/8" in diameter and was located at the center of the beaker.

A borescope camera system was utilized during the final ten runs to allow viewing of the top surface of the batch during the run, as shown in Appendix A. A double walled quartz tube with cooling air was used to cool the borescope during the run and a thermocouple was used to monitor its temperature. The light source for the borescope was a fiber-optic cable attached to a quartz rod. The quartz rod was inserted through the top insulating board to illuminate the side of the beaker opposite to the borescope.

The melt rate furnace was previously used during testing with Macrobatch 2 [3]. Several modifications were made to the furnace between the Macrobatch 2 tests and the Macrobatch 3 tests. The hole through the furnace top board was enlarged from 4" to 6" to allow an insulating sleeve to be used around the beaker. During Macrobatch 2 tests, the beaker was held in place and insulated on the sides by the top board of the furnace. The top board of the furnace developed cracks and shrinkage of the board was noted during tests. The insulating effect on the beaker varied due to damage to the top insulation board, therefore, a replaceable insulating sleeve was fabricated to provide uniform conditions for all tests. The sleeve also allowed multiple runs per day versus the one run per day during Macrobatch 2 testing.

Other modifications included the installation of a high temperature interlock to allow overnight operation and a modification to the offgas system to improve the air sweep over the top of the furnace, as well as the borescope mentioned above.

Equipment Operation

Prior to beginning the runs, the furnace was ramped to approximately 1150°C with an insulation board over the top hole. The beaker filled with dry melter feed, sleeve, felt liner, and beaker T/C's were assembled at ambient temperature prior to insertion into the melt rate furnace. When the furnace reached setpoint, the beaker assembly was inserted into the furnace. The vapor space thermocouple was then inserted through the top insulation board.

When the vapor space temperature reached the designated temperature or the specified run time was reached, the vapor space thermocouple was removed and then the beaker was removed from the furnace and quenched in air. The insulation board was placed back over the furnace and the furnace was allowed to ramp back to setpoint. After the furnace returned to setpoint, the next beaker assembly was inserted.

If the borescope was utilized during the run, the quartz tube was inserted into the top board prior to insertion of the beaker in the melt rate furnace. The light source and camera were inserted after the beaker was placed in the furnace. If the temperature limit for the borescope (150° C) was exceeded, the camera was removed. The quartz tube and light source were left in place to seal the holes in the top board. The borescope (if still in place) and the light source were removed from the beaker one minute prior to the completion of the run.

Nomenclature of Runs

A unique run number was assigned to each melt rate furnace runs by combining the frit designation with the SRAT product type as follows: FRIT DESIGNATION – SRAT PRODUCT TYPE – MRF, where MRF stands for Melt Rate Furnace. If multiple runs of the with the same frit and SRAT product were performed, a number was added to the end to enumerate the run. For example, the second run using Frit G and Baseline SRAT product would be designated “G-MB3-MRF-2” while the first run using Frit 200 and underwashed SRAT product would be “200-MB3-UNDERWASHED-MRF”.

Melt Rate Determination

Several methods were utilized to measure the melt rate from the tests. The first method was to utilize the temperature data from the run to determine the rate of rise in isotherms in the beaker. Isotherm charts were developed for each run, as shown in Appendix F. A melt rate can be calculated assuming that the rate of rise of glass is indicated by the rate of rise in the isotherm. The results using this method were not valid due to bridging during the melting process. Bridging increases the temperature rapidly in the section of the beaker beneath the bridge by insulating the lower section from the colder batch above the bridge. For example, an experiment with bridging may have an 800° C temperature at the ½” T/C after a run time of 20 minutes while an experiment without bridging may be at 600° C at the same point with no difference in the amount of glass that has melted. For this reason, the isotherm data could not be used to determine relative melt rates.

The method used to determine the melt rate was to measure the height of the glass pool formed during each test and divide by the run time, the same method used during MB2 testing [3]. The height of the glass pool was measured at the point where the glass has become free of bubbles. This method was complicated by the irregularities in the height of the melt pool due to large bubbles present during many runs.

Two approaches were used to determine the glass height in the runs with irregular height profiles. The linear method involves measuring the batch height at ¼” intervals across the beaker, then averaging the values to obtain an average glass pool height. The average glass pool height was divided by the run time to obtain the melt rate result in inches per hour. The volumetric method involves calculation of the volume of each concentric ring represented by the batch height at ¼” intervals, then summing the volume of the rings

to obtain the volume of glass produced during the run. The glass volume is then divided by the run time to obtain a melt rate in cubic inches per hour.

Bridging

Indications of bridging were noted during many of the runs conducted during testing with Macrobatch 3 feed. The air gap created during bridging would create an insulating effect at low temperatures and slow down the heat transfer to the unreacted feed above the gap. However, studies have shown that thermal radiation can result in effective heat transfer through large voids at high temperatures.[7] In addition, the variation in the linear melt rate noted between duplicate runs was typically 10% or less, even for runs such as G-MB3-MRF which bridged and G-MB3-MRF-2 which did not bridge. The small variation between runs indicates that the problems with bridging likely did not significantly impact the tests. Nevertheless, the possibility that bridging has affected the results cannot be ruled out without larger scale tests.

Bridging was detected in one of four ways: rapid rise of all thermocouples, sudden drop in one or more thermocouples, indication of a gap when sectioning, and/or lack of drop in batch height as seen through the borescope. The temperature charts and batch height measurement from the borescope images for runs G-MB3-MRF-2 and BONE-MB3-MRF-2 illustrate the difference between a run with and without bridging. The borescope image was used as an indirect indication of batch height during the test. As shown in Figure 1, the batch height during run G-MB3-MRF-2 dropped smoothly throughout the run while the batch height for run BONE-MB3-MRF-2 had periods with no drop in batch height followed by a rapid drop. The temperature charts for these two runs shown in Figure 2 also indicate that bridging is occurring in BONE-MB3-MRF-2 and not in G-MB3-MRF-2. The “humps” in the temperature data for BONE-MB3-MRF-2 coincides with periods that no drop in batch height was noted while the sudden dips coincide with rapid drops in the batch height. The temperature chart for G-MB3-MRF-2 does not show sudden swings in temperature. Figure 3 shows the appearance of a sectioned crucible that indicates severe bridging.

Figure 1. Batch Height Data from Borescope

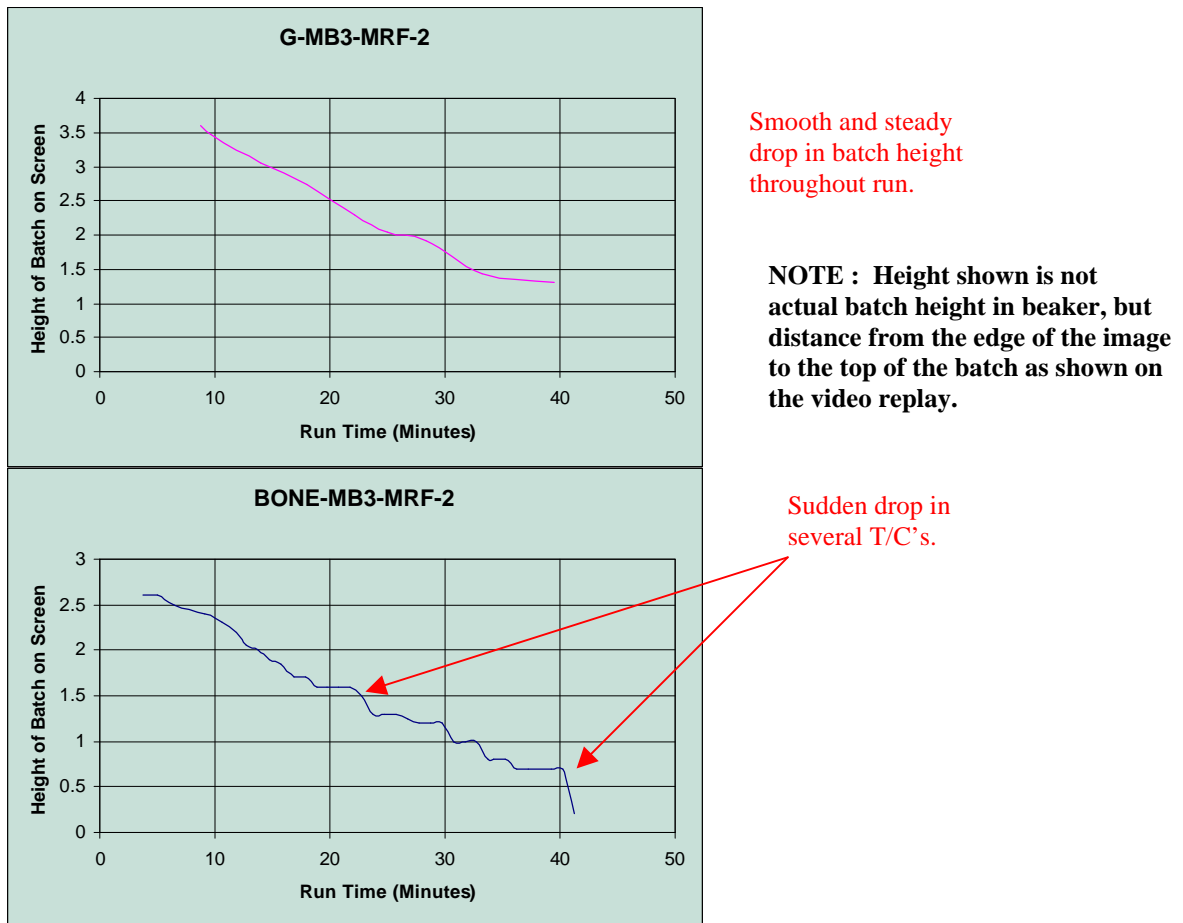
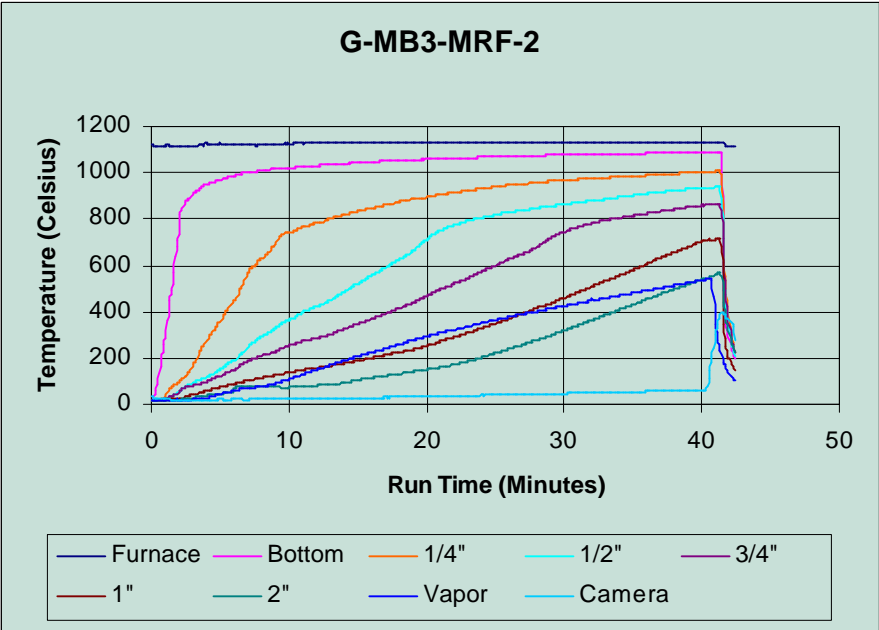
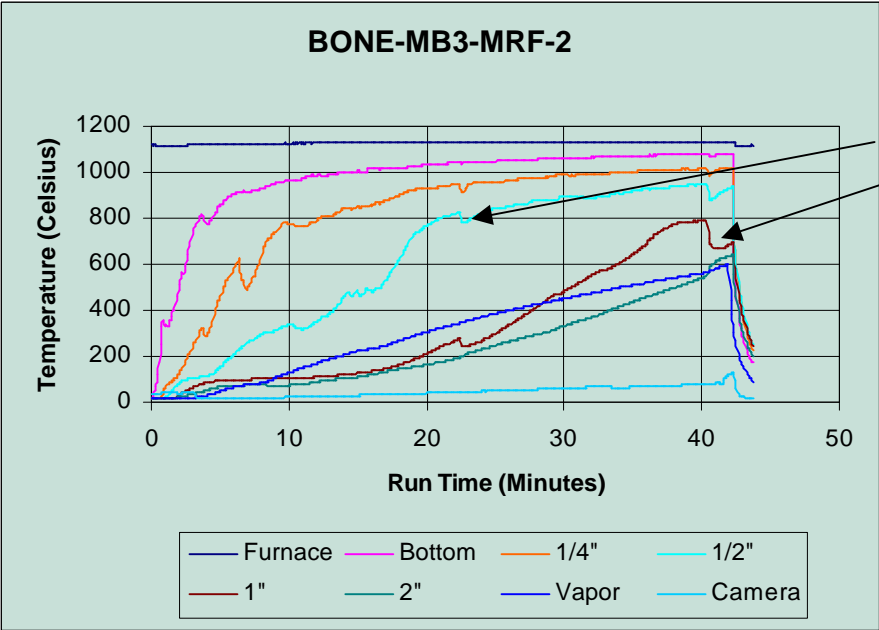


Figure 2. Temperature Charts for G-MB3-MRF-2 and BONE-MB3-MRF-2

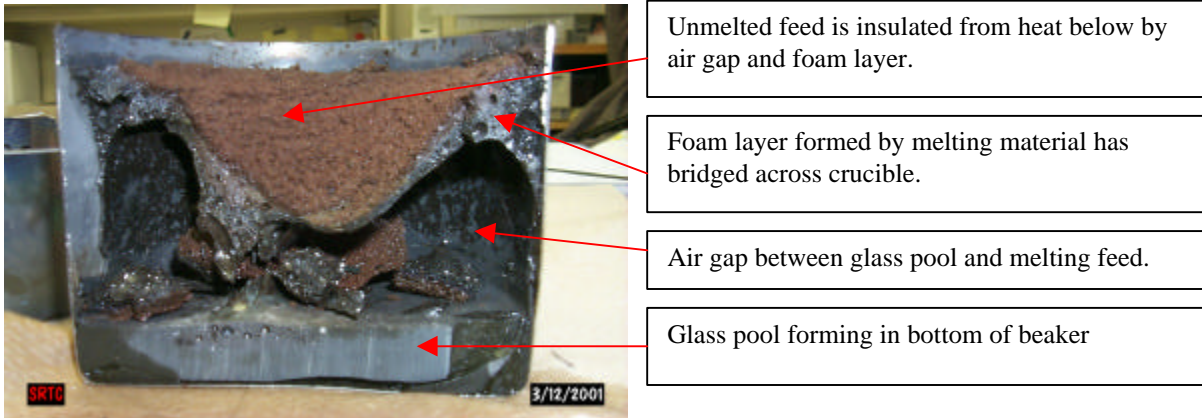


Smooth temperature profile throughout run



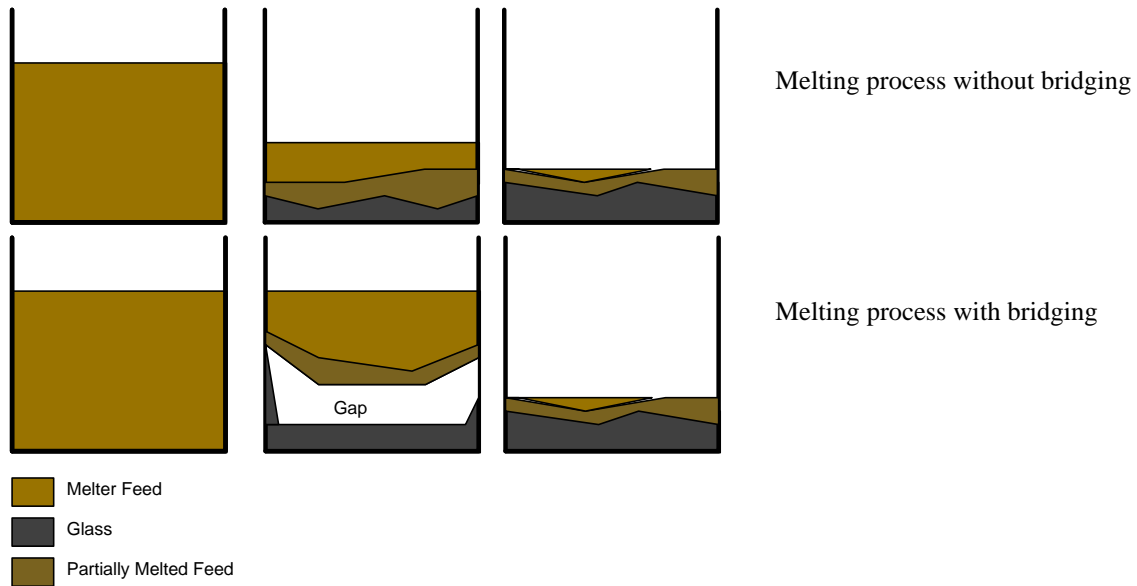
"Humps" in temperature data are followed by sudden dips.

Figure 3. Sectioned Crucible from 200-MB3-MRF-8



The volume occupied by the melter feed was typically three times greater than the volume of the final glass product. Therefore, a significant volume reduction occurred when the feed melted. As shown in Figure 4, when bridging occurred, the feed would remain suspended above the melted glass as the feed at the bottom of the beaker melted and slumped down into a glass pool.

Figure 4. Bridging During Melt Rate Furnace Tests



Numerous factors impact the potential for bridging, but only four factors can be controlled during melt rate testing: amount of water in feed, particle size of dried feed, T/C number and placement, and beaker diameter. The amount of water in the feed was significantly reduced during the testing and the number and placement of thermocouples was also varied in attempts to reduce the amount of bridging. These variations do not appear to have significantly changed the amount of bridging noted during the testing. The diameter of the beaker is the primary factor in determining whether or not bridging will occur with a given feed material. Due to cost and schedule considerations in producing melter feed, the diameter of the beaker is currently four inches. The tests indicate that a larger diameter beaker is required to reduce the occurrence of bridging.

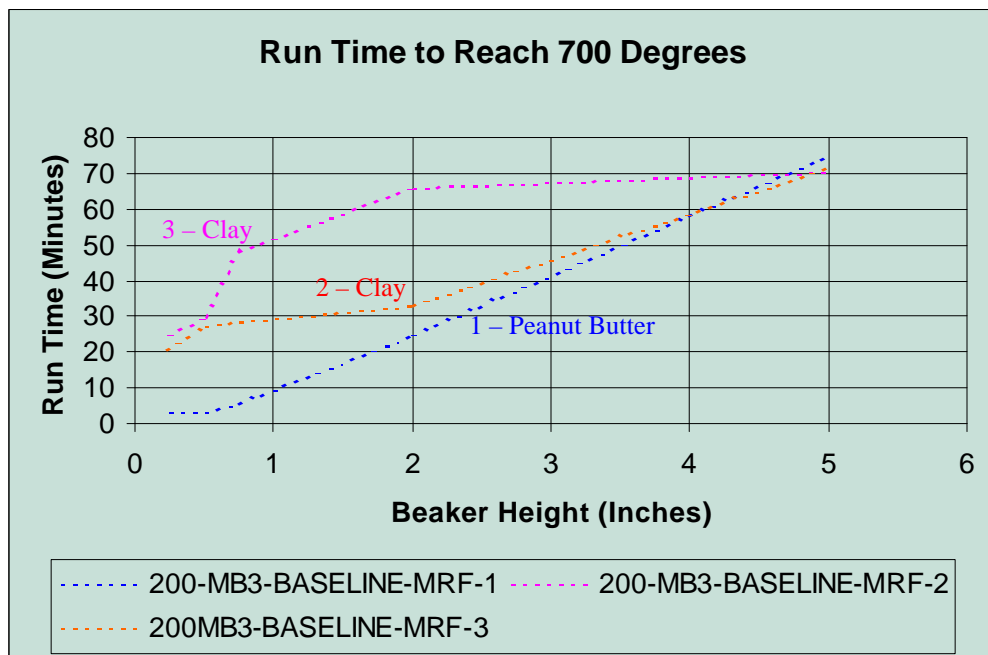
Macrobatch 3: Baseline Tests

Tests were conducted with Frit 200 and Baseline SRAT product [4] to establish a baseline for comparison with other runs. The tests were also used to gauge the reproducibility of runs in the melt rate furnace. A total of eleven baseline runs were conducted: three with a batch weight of 794 grams, six with a batch weight of 575 grams, and two with a batch weight of 545 grams. Volume expansions were not noted during any of the baseline process runs, in contrast to testing with Macrobatch 2 when severe volume expansions were noted which limited melt rate[3].

Runs 200-MB3-Baseline-MRF-1,2, and 3 were conducted with a batch weight of 794 grams prior to firing. The first run had the consistency of peanut butter prior to firing while the other two resembled wet clay, as illustrated in Appendix E. Initial batch height between the runs varied from 2.5" to 3".

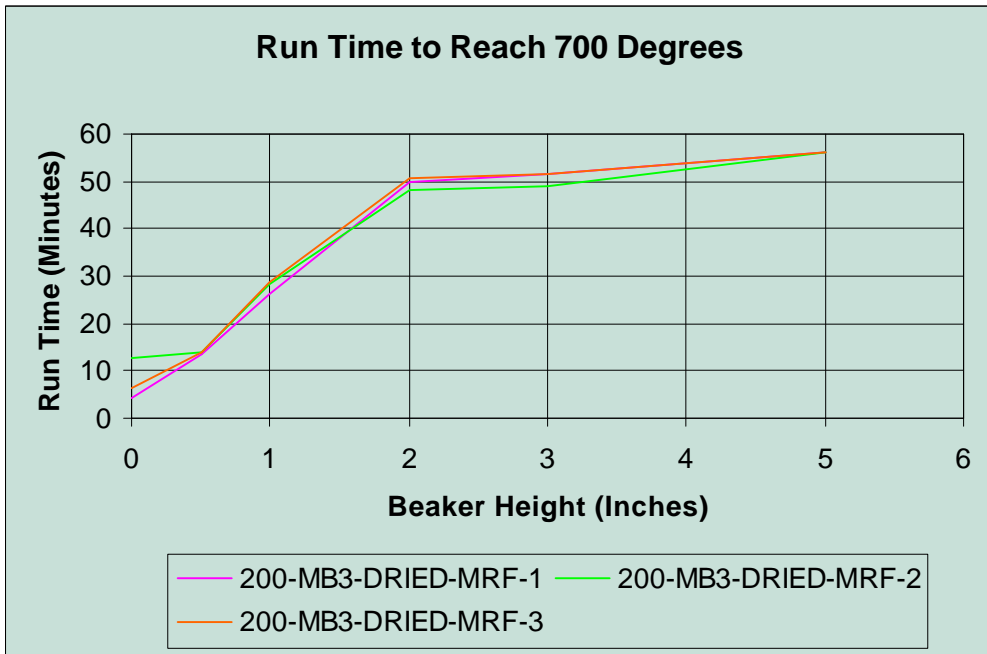
Reproducibility between the runs was less than desired, as indicated by the variation between the 700° C isotherms shown in Figure 5. In addition, 200-MB3-Baseline-MRF-1 had a significant amount of foam attached to the thermocouples when the beaker was removed from the furnace while the other two runs did not. The foam on the thermocouples indicated that bridging was occurring during the run. Run 200-MB3-BASELINE-MRF-2 formed a melt pool with a significant amount of foam on the surface with a run time of 72 minutes, while run 200-MB3-BASELINE-MRF-3 formed a melt pool with a small amount of foam on the surface after a run time of 80 minutes. All runs were kept in the furnace until the vapor space temperature reached 800°C.

Figure 5. Isotherm for Runs with 794 Gram Batch Weight



Concerns with the reproducibility of the first runs led to a change in the test protocol to dry the feed more thoroughly and insert additional thermocouples. Three tests (200-MB3-DRIED-MRF-1,2,3) with a batch weight of 575 grams were designed to determine if reproducibility could be improved by removing the water from the batch prior to vitrification in the melt rate furnace. After drying, the melter feed was ground in a mortar and pestle, then passed through a #10 mesh sieve. Initial batch height for all runs was 3" +/- , and the visual appearance prior to firing was the same for all three runs, as shown in Appendix E. As shown in Figure 6, the variation in the 700° C isotherms was significantly reduced by the dried feed. In addition, the visual appearance of the sectioned beakers was very consistent between the three runs.

Figure 6. Isotherm for Runs with 566 Gram Batch Weight



Runs 200-MB3-DRIED-MRF-4, 5, and 6 were performed to determine what process(es) were occurring during the sudden drop in temperature seen in the middle thermocouples at a run time of 40 minutes. 200-MB3-DRIED-MRF-4 was removed from the melt rate furnace 10 minutes after the temperature drop (run time = 50 minutes), 200-MB3-DRIED-MRF-5 was pulled from the furnace as soon as the drop was detected (run time = 36 minutes), and 200-MB3-DRIED-MRF-6 was pulled from the melt rate furnace prior to the temperature drop (run time = 30 minutes), as shown in Figure 7.

Figure 7. Sectioned Beakers from Runs 200-MB3-DRIED-4,5,and 6



When sectioned, the tests indicated that bridging was occurring during the run and that the temperature drop noted during the runs was likely the result of the collapse of the bridge. At 30 minutes, approximately 0.35" of glass is present with large voids above the glass pool. A 1/4" layer of foam separates the void space from the unreacted feed at the top of the batch. During the temperature drop, the large voids have disappeared and the foam layer has become thicker. At 50 minutes, large bubbles are present in the foam layer and nearly all unreacted feed has been consumed.

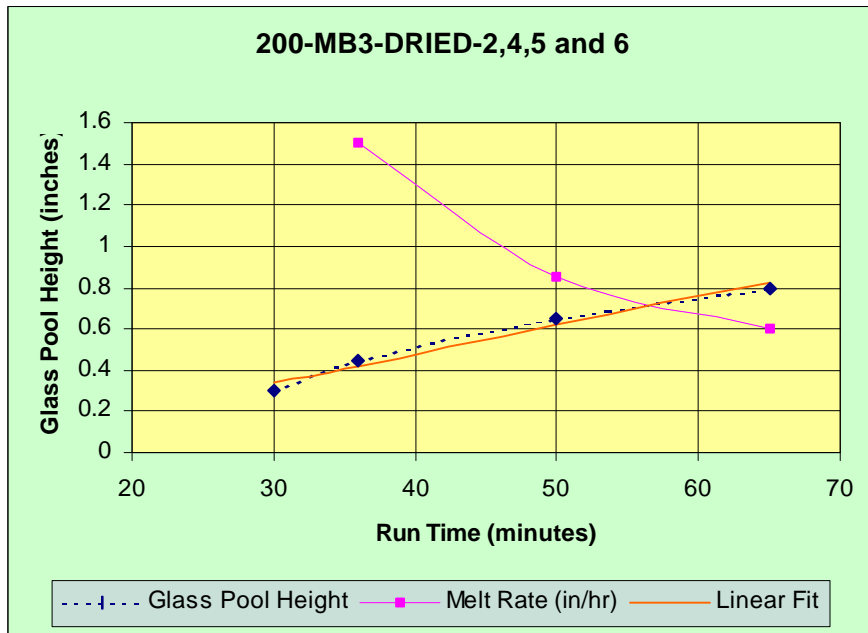
The height of the glass pool was measured at each of the different run times, as shown in Figure 8. The melt rate was calculated by subtracting the previous height from the height and dividing by the difference in run time. The melt rate was also calculated by a linear curve fit on the data and by dividing the total run

time by the final glass height, as shown in Table 2. As shown by the data, the melt rate during the onset of the temperature drop seen during the runs was higher than the melt rate later in the run.

Table 2. Melt Rate as a Function of Run Time

Measurement Method	Value (inches per hour)
Height difference from 30 – 36 minutes	1.5
Height difference from 36 – 50 minutes	0.86
Height difference from 50 – 66 minutes	0.6
Linear Curve Fit	0.83
Final Glass Height / Total Run Time	0.72

Figure 8. Glass Pool Height as a Function of Run Time



Two runs (200-MB3-MRF-7 and 200-MB3-MRF-8) were performed with Frit 200 and the Baseline SRAT product to provide a comparison point for alternative frit compositions. These runs were conducted at an initial batch weight of 545 +/- 5 grams to match the dried weight of the tests with alternative frit compositions. 200-MB3-MRF-7 was performed with eight thermocouples, arranged in pairs. 200-MB3-MRF-8 was performed with a central bundle of six thermocouples and a borescope to view the batch as it melted.

Melt rate for each of the baseline runs was determined by the linear method, as shown in Table 3. The completely dried runs produced good agreement between runs, despite the fact that the many parameters (such as number of thermocouples and run time) varied considerably. The variation between the “peanut butter” runs was significantly higher than the dried feed runs with a 25% difference between the fastest and slowest runs compared to 12% for runs with dried feed.

Table 3. Melt Rate for Baseline Runs

Run Number	Number of Thermocouples	Run Time	Linear Melt Rate
		Minutes	Inches per hour
200-MB3-BASELINE-MRF-1	4	82	0.51
200-MB3-BASELINE-MRF-2	4	71	0.63
200-MB3-BASELINE-MRF-3	4	80	0.56
200-MB3-DRIED-MRF-1	8	66	0.73
200-MB3-DRIED-MRF-2	8	65	0.78
200-MB3-DRIED-MRF-3	8	66	0.77
200-MB3-DRIED-MRF-4	4	50	0.78
200-MB3-DRIED-MRF-5	4	36	0.75
200-MB3-DRIED-MRF-6	4	30	0.70
200-MB3-MRF-7	8	48	0.75
200-MB3-MRF-8	6	42	0.79

Macrobatch 2 versus Macrobatch 3

Determination of the difference between Macrobatch 2 and Macrobatch 3 was performed using Frit 200. A run was performed with Macrobatch 2 SRAT product with the same batch preparation and drying process as the Macrobatch 3 alternative frit tests. The drying process went to completion at a batch weight of 566 grams (versus 545 grams for MB3), but the runs were otherwise conducted in the same manner. The melt rate determination, shown in Table 4, does not indicate a difference in melt rate between the two sludge batches. Volume expansions were not noted during the tests.

Table 4. Comparison of Melt Rate of Macrobatch 2 and Macrobatch 3

Sludge Batch	Linear Melt Rate (in/hr)	Volumetric Melt Rate (in ³ /hr)
MB2	0.80	11.7
MB3	0.75	11.0

Alternative Melter Feed Tests

The sludge currently stored in the waste tanks undergoes numerous process steps prior to vitrification. The sludge is first washed in the tank farm with very dilute caustic solution to remove soluble species. The washed sludge is then transferred to DWPF where it is acidified with nitric and formic acid. After the sludge is refluxed to remove mercury, a slurry of frit and dilute formic acid is added. After concentration by boiling, the processed sludge (now referred to as melter feed) is fed to the melter for vitrification [4]. Changes in the feed preparation process can affect the sodium content, formate content, nitrate content, and/or water content of the melter feed. These parameters can all affect melt rate; therefore, changes in the melter feed process were studied to determine the impact on melt rate. All tests with alternative melter feed were performed with a batch weight of 794 grams and the beakers were removed from the melt rate furnace when the vapor space temperature reached 800° C. All alternative feed tests were conducted with Frit 200.

Changes in the Sludge Washing Process

The washing process conducted in the tank farm determines the amount of soluble species (such as sodium nitrate, sodium nitrite, and sodium hydroxide) present in the feed to DWPF. A reduction in the number of wash cycles (or size of each wash cycle) performed on the sludge increases the amount of soluble species in the sludge fed to DWPF. Conversely, increasing the number of washes decreases the amount of soluble species in the sludge. The amount of acid required during acidification of the sludge in DWPF is increased by an increase in nitrite and hydroxide content, so the washing process also impacts subsequent processing. Two alternatives to the nominal washing process currently planned for Macrobatch 3 were studied: underwashed and overwashed feed. The underwashed feed was prepared to simulate one less wash cycle

than the nominal process while the overwashed feed was prepared to simulate a reduction in the sodium concentration to ½ the nominal process [4].

The underwashed melter feed has a higher sodium concentration than the nominal washed sludge in addition to higher levels of nitrate. The melt rate test conducted with the underwashed sludge indicates that the increase in sodium content increased the melt rate for the underwashed sludge, as shown in Table 5. The redox of the glass is also shown in Table 5. Conversely, the overwashed test indicated that the reduced sodium concentration decreased melt rate, although severe bridging was noted during this run. Melt rate was determined by the linear method only since the glass pool height for these runs was uniform across the beaker cross section.

Table 5. Melt Rate of Underwashed, Baseline, and Overwashed Feed

Sludge Type	Glass Redox (Fe ⁺² /ΣFe)	Melt Rate (in/hr)
Underwashed	0.14	0.68
Baseline (average of three runs)	0.17	0.57
Overwashed	0.12	0.47

Changes in the Nitric Acid / Formic Acid Ratio during the SRAT Process

The ratio of nitric acid to formic acid during the acidification process in the DWPF SRAT cycle is currently used to control the reduction potential (redox) of the glass formed during vitrification. The redox target for the nominal process is 0.2 Fe⁺²/ΣFe, as predicted by the current redox model [6]. Changing the ratio to increase the amount of nitric acid leads to a more oxidizing glass, lowering the ratio of Fe⁺²/ΣFe, while changing the ratio to increase the formic acid amount leads to a more reducing glass. Past studies [3] have shown that a more oxidizing glass melts slower, therefore tests were not conducted with increased amounts of nitric acid.

To determine if a more reducing glass would significantly improve melt rate, melter feed was produced which utilized only formic acid during the SRAT cycle. The predicted redox for this feed was 0.255 Fe⁺²/ΣFe. The melt rate test conducted with this feed indicated no significant improvement in melt rate, as shown in Table 6. The change in glass redox, as shown in Table 6, also indicates minimal improvement over the baseline process.

Table 6. Comparison of Formic Acid Only to Baseline Process

Sludge Type	Glass Redox (Fe ⁺² /ΣFe)	Melt Rate (in/hr)
Formic Only	0.18	0.59
Baseline (average of three runs)	0.17	0.57

Changes in the Amount of Acid Addition during the SRAT Process

The amount of acid used during the SRAT process was 125% of the calculated stoichiometric amount, as recommended during Chemical Process Cell tests with Macrobatches 3. A reduction or increase in the amount of acid added may have an impact on melt rate by changing the amount of formate and nitrate that is fed to the melter. Tests to determine the impact of the acid amount were a lower priority than the tests performed and will be completed at a later date if required [1].

Sugar Addition

Sugar additions were shown to improve the melt rate during Macrobatches 2 tests by reducing the size of the volume expansions that occurred during the melting process. The addition of sugar to the Macrobatches 3 baseline SRAT product did not improve the melt rate during melt rate furnace run 200-MB3-SUGAR-MRF, as shown in Table 7. [5]

Table 7. Comparison of Melt Rate with Sugar Addition

	Linear Melt Rate (in/hr)	Volumetric Melt Rate (in ³ /hr)
5.83 grams of Sugar Added	0.70	9.2
Baseline Process	0.75	11.0

Alternative Frit Tests

The Macrobatch 2 melt rate study indicated changing the frit formulation had a significant impact on melt rate. That study also indicated that Frit 200 was not the optimal frit composition for sludge only MB2 processing [3]. Therefore, process models were used to develop and perform a preliminary evaluation on 27 alternate frit formulations for Macrobatch 3 tests [11]. Based on the preliminary evaluation and crucible studies, fourteen frit formulations were selected for testing in the melt rate furnace, along with Frit 165 with ½ of the silica removed [10]. The compositions of the formulations are shown in Appendix D.

Frit 200 and Frit 165 were on hand from previous tests, all other frits were fabricated in platinum crucibles and ground in a carbon steel mill. The steel grinding plates were abraded by the glass during the size reduction process, requiring the iron filings to be magnetically separated from the frit. After removal of the tramp iron, the frit was sampled to verify that the makeup was accurate and that the contaminants had been reduced to acceptable levels. [9]

After all frits had been tested in the melt rate furnace, seven frits were selected for additional testing: D, M, G, BONE, BONE2, 165, and KMA-2. Silica deficient 165 and BICK were not selected because these frits are two component frits and the increase in melt rate was not sufficient to warrant the additional handling required. Although the melt rates with these frits were comparable to some of the frits selected, the improvement offered by these frits was not sufficient to warrant the additional handling required in DWPF.

Additional quantities of frits were fabricated in platinum crucibles and ground using hardened carbon steel plates in the mill. After magnetically separating the iron filings, the frits were sampled to verify that the impurities had been removed. Results are shown in Attachment D. The run time for each beaker during these tests was 42 minutes, based on the time required for the run with Frit D. Running the beakers for the same run time allows a direct comparison to be made between two sectioned beakers. Bridging was noted in several of the runs, but the overall results matched well with the first runs.

During the melt rate furnace tests with these frits, a camera mounted on a borescope was used to record the surface of the batch during melting. The camera confirmed that sudden drops in the batch caused the sudden dips in the temperature data. In addition, the video allowed the batch height to be indirectly measured during the run, with the best results achieved for G-MB3-MRF-2 and BONE-MB3-MRF-2. The video (and temperature data) indicated that very little, if any, bridging occurred during the G-MB3-MRF-2 run, but bridging to some extent was present in all other runs. The melt rate for duplicate runs was typically had a difference of less than 10%.

The results of the tests are shown in the Table 8, with average values shown for frits that have two runs. Preliminary analysis of the data indicated that melt rate is proportional to the total alkali content of the frit and viscosity, as shown by Figures 9 and 10. Viscosity is not independent from alkali content and statistical analysis with JMP4 program (shown in Appendix H) indicated that alkali content was the dominant factor. The statistical analysis was conducted on the 22 runs performed during the alternative feed study to eliminate the impact of batch weight. The data set was not ideal for the statistical study, but the results show a strong correlation between alkali content and melt rate while the relationships with other factors, such as viscosity was an order of magnitude lower. The impacts of silica and boron on melt rate were also analyzed with the JMP4 program, but no significant correlation was detected.

Table 8. Melt Rates during Alternative Frit Tests

New Frit Designation	Old Frit Designation	Melt Rate Linear Basis In/hr	Melt Rate Volume Basis In ³ /hr	Alkali Content Wt% Oxide
304	D	1.13	15.1	23.87
N/A	165-Si Deficient	1.06	13.5	20.0
320	BONE	1.05	14.0	20.0
313	M	1.01	13.8	19.49
326	BONE-2	0.95	13.0	19.0
N/A	165	0.95	12.9	20.0
307	G	0.93	12.6	15.41
325	BICK	0.87	13.5	16.65
322	MIMI	0.87	12.6	15.0
324	KMA2-A	0.79	12.1	13.47
N/A	200	0.75	11.0	16.0
314	N	0.66	10.5	12.06
323	KMA2	0.62	9.1	13.47
315	O	0.62	9.0	10.03
303	C	0.51	8.4	10.12

Figure 9. Melt Rate Versus Alkali Content

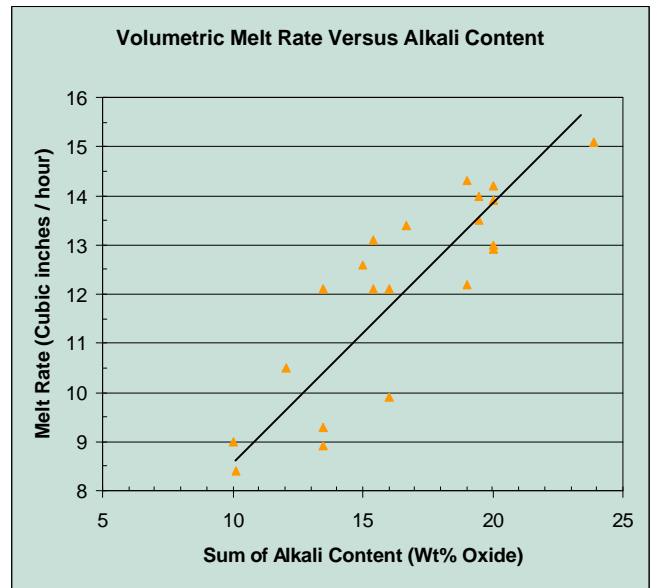
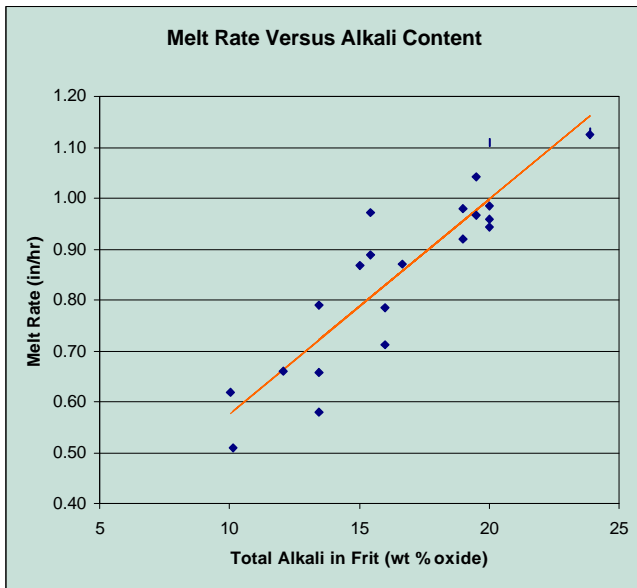
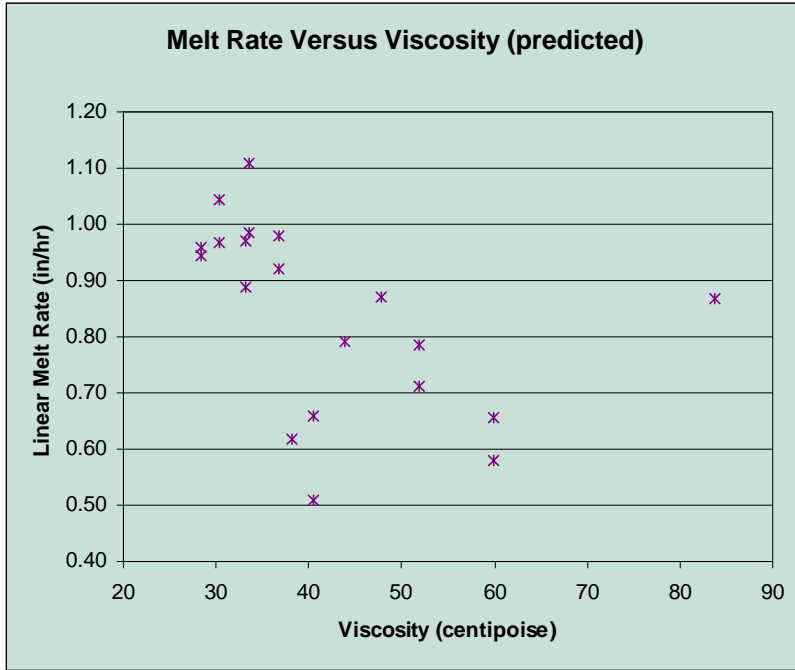


Figure 10. Melt Rate as a Function of Predicted Glass Viscosity



Melt Rate Versus Alkali Content: Mole Percentage Basis

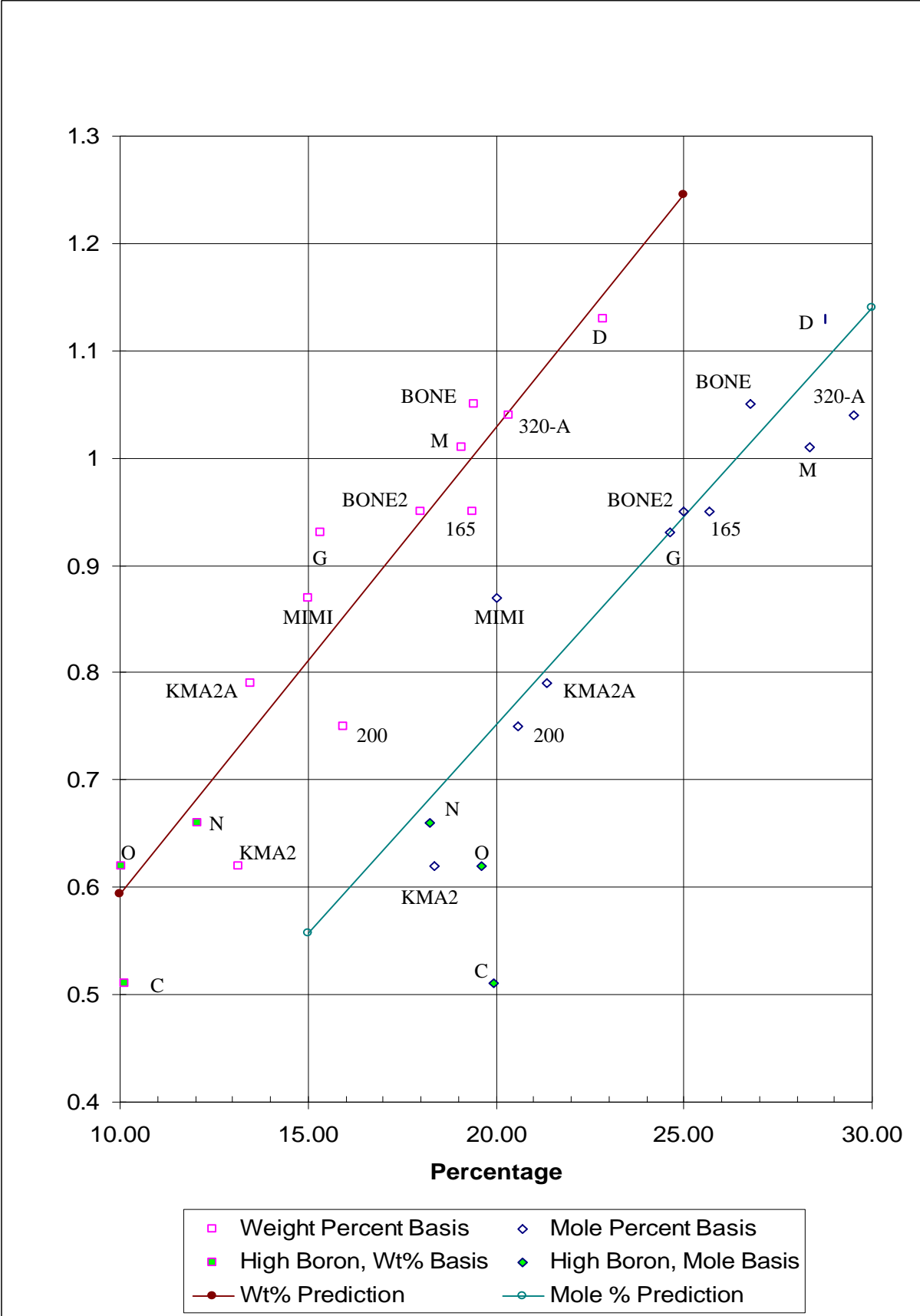
Two alkali elements are present in the frit compositions, sodium and lithium. KMA2 and KMA2A are identical frits, except that the amounts of lithium and sodium are switched, with KMA2 having more sodium and KMA2A having more lithium. The melt rate of KMA2A is significantly higher than KMA2, indicating that lithium has a stronger impact on melt rate than sodium. The higher impact from lithium is likely the result of the lower molecular weight, resulting in more moles of alkali in the glass from a given weight percent of alkali if lithium is used versus sodium

In order to cancel this effect, the frit compositions were converted to a molar basis. The melt rate was then plotted versus mole fraction of total alkali and versus weight percent total alkali, as shown in Figure 11. The scatter in the data is significantly reduced by conversion to a molar basis. In addition, a frit composition (BONE3) was formulated that limits the total weight percent alkali in the frit to 20% while increasing the alkali molar percentage by raising the lithium content of Frit BONE to 11% while lowering sodium content to 9%. The melt rate was then predicted from a linear regression based on mole percentage. Frit BONE3 is predicted to have a melt rate comparable to Frit D, the fastest melting frit during the tests, as shown in Table 9.

Table 9. Compositions of BONE, BONE3, and D

Frit Component	BONE (sample results)		BONE3 (320-A)		D (sample results)	
	Weight Percent	Mole Percent	Weight Percent	Mole Percent	Weight Percent	Mole Percent
Al ₂ O ₃	0.00	0.00	0.0	0.0	1.84	1.11
B ₂ O ₃	8.14	6.91	8.0	6.56	6.96	6.15
Li ₂ O	7.75	15.34	11.0	21.06	5.65	11.67
Na ₂ O	11.98	11.40	9.0	8.28	17.2	17.07
SiO ₂	71.88	66.19	72.0	64.09	66.6	63.94
Total Alkali	19.73	26.74	20.0	29.34	22.85	28.74
Melt Rate	1.05		1.11*		1.13	

* Predicted melt rate.



Frit 320-A Testing

Frit 320-A was fabricated and tested in the melt rate furnace in the same manner the other alternative frits. A melt rate of 1.04 was indicated by the test, as shown in Table 10. The results indicate that Frit 320-A has a melt rate comparable to Frit 320.

Table 10. Melt Rate of Frit 320-A

	Frit 320-A (Predicted)	Frit 320-A (measured)	Frit 320	Frit 304
Melt Rate (in/hr)	1.11	1.04	1.05	1.13

Mechanism for Increased Melt Rate with Higher Alkali Content

The impact of alkali on melt rate could be the result of several mechanisms. The tests conducted during this study were not designed to indicate the mechanism of melt rate improvement, therefore, the mechanism that causes the higher melt rate with higher alkali content has not been determined. Possible mechanisms include reduction in the latent heat of vitrification when alkali is increased, reduction in activation energy for the melting process, and/or an increase in the heat transfer coefficient of the melting batch. Understanding the mechanism would increase confidence in translation of the results to the DWPF process.

Frit 165 Testing

During testing with Macrobatches 2, Frit 165 was shown to improve melt rate versus Frit 200. As a result, the initial tests conducted with Macrobatches 3 were designed to verify that the melt rate of Macrobatches 3 feed could be improved by switching to Frit 165. Three runs were conducted with Frit 165, dried to a batch weight of 794 grams, during the initial stages of the testing. Frit 165 without zirconia was also tested to determine the impact of removing the zirconia. All runs were held in the melt rate furnace until the vapor space temperature reached 800° C. Melt rate was determined by the linear method only because the glass pool height was uniform across the beaker cross-section.

The results of these tests indicated that Frit 165 improved melt rate and that removing zirconia from Frit 165 also improved melt rate relative to Frit 165, as shown in Table 11. Subsequent tests with Frit 165 were conducted during the alternative frit study, as shown in the results from testing with dried feed.

Table 11. Melt Rate of Frit 165 and Frit 200 during Initial Tests

Frit	Melt Rate (in/hr)	Melt Rate during Dried Feed Testing (in/hr)
200 (average of three runs)	0.57	0.75
165 (average of three runs)	0.63	0.95
165 without zirconia	0.72	Not tested

CONCLUSIONS

Melt rate was strongly influenced by alkali content during the tests. Additional alkali added to the process either by reduced washing during sludge preparation or by additional alkali in the frit composition improved melt rate. Processes that lowered alkali content, either by substitution of boron or silica in the frit composition or by increased washing during the sludge preparation, lowered melt rate. The mechanism through which high alkali content improves melt rate was not studied; additional tests are required if an understanding of the mechanism is desired.

The run with SRAT product produced with formic acid only indicated that melt rate would not be significantly changed by raising the ratio of formic acid to nitric acid during SRAT processing.

Bridging was noted during the majority of the tests conducted. Although bridging did not lead to poor agreement between duplicate runs, the possibility exists that the bridging noted affected the results. Since

adjustment of the thermocouples and water content of the batch did not eliminate bridging, larger diameter beakers appear to be required to reduce the amount of bridging.

The melt rate results are shown in Table 12. Note that the amount of water in the feed was significantly higher for the alternative feed tests, causing the melt rates during those tests to be lower.

Table 12. Melt Rate Test Results

Alternative Frit Tests			Alternative Feed Tests	
Frit	Original Designation	Melt Rate (in / hr)	SRAT Product Type	Melt Rate (in / hr)
304	D	1.13	Baseline	0.57
165 (Si Def)	n/a	1.06	Underwashed	0.68
320	BONE	1.05	Overwashed	0.47
320-A	BONE3	1.04	Formic Only	0.59
313	M	1.01		
326	BONE2	0.95		
165	n/a	0.95		
307	G	0.93		
325	BICK	0.87		
322	MIMI	0.87		
324	KMA2A	0.79		
200 (Baseline)	n/a	0.75		
314	N	0.66		
323	KMA2	0.62		
315	O	0.62		
303	C	0.51		

REFERENCES

1. Task Technical and QA Plan for Alternative Process Options to Improve Melt Rate, **WSRC-RP-2001-00183**, January 31, 2001.
2. Technical Task Request, **HLW/DWPF/TTR-00-0044**, October 24, 2000.
3. M. E. Stone and D. P. Lambert, "DWPF Macrobatches 2 Melt Rate Tests", **WSRC-TR-2000-00395**, October 5, 2000.
4. M. E. Stone and D. P. Lambert, "Feed Preparation for Macrobatches 3 Melt Rate Study", **WSRC-TR-2001-00126**, April 1, 2001.
5. J. E. Josephs and M. E. Stone, "Melt Rate Improvement for DWPF MB3: Sugar Addition Tests (U)", **WSRC-TR-2001-00158**, March 31, 2001.
6. K. G. Brown, C. M. Jantzen, and J. B. Pickett, "The Effects of Formate and Nitrate on Reduction/Oxidization (Redox) Process Control for the Defense Waste Processing Facility (DWPF) (U)", **WSRC-RP-97-34**, February 5, 1997.
7. X.-G. Liang and W. Qu, "Effective Thermal Conductivity of Gas-Solid Composite Materials and the Temperature Difference Effect at High Temperature", **International Journal of Heat and Mass Transfer, Volume 42 (1999)**, pages 1885-1893.
8. D. K. Peeler and T. H. Lorier, "Melt Rate Improvement for DWPF MB3: Foaming Theory and Mitigation Techniques (U)", **WSRC-RP-2001-00351**, March 30, 2001.
9. T. H. Lorier and D. K. Peeler, "Melt Rate Improvement for DWPF MB3: Frit Preparation (U)", **WSRC-TR-2001-00152**, March 30, 2001.
10. T. H. Lorier, "Melt Rate Improvement for DWPF MB3: Crucible Tests (U)", **WSRC-TR-2001-00151**, March 30, 2001.
11. D. K. Peeler and T. H. Lorier, "Melt Rate Improvement for DWPF MB3: Frit Development and Model Assessment (U)", **WSRC-TR-2001-00131**, March 30, 2001.

12. M. E. Stone, "Run Plan for Macrobatch Three Baseline in the Melt Rate Furnace (U)", **SRT-PTD-2000-00095, Revision 1**, December 19, 2000.
13. J. E. Josephs, "Run Plan for Macrobatch Three Frit 165 in the Melt Rate Furnace (U)", **SRT-PTD-2000-00107, Revision 1**, December 19, 2000.
14. J. E. Josephs, "Run Plan for Macrobatch Three Frit 165 No Zr in the Melt Rate Furnace (U)", **SRT-PTD-2000-00108**, December 19, 2000.
15. J. E. Josephs, "Run Plan for Macrobatch Three Silica Defecient Frit 165 in the Melt Rate Furnace (U)", **SRT-PTD-2000-00109, Revision 1**, December 21, 2000.
16. J. E. Josephs, "Run Plan for Macrobatch Three Formic Only in the Melt Rate Furnace (U)", **SRT-PTD-2000-00110**, December 19, 2000.
17. J. E. Josephs, "Run Plan for Macrobatch Three Underwashed Frit 200 in the Melt Rate Furnace (U)", **SRT-PTD-2000-00111**, December 19, 2000.
18. J. E. Josephs, "Run Plan for Macrobatch Three Overwashed Frit 200 in the Melt Rate Furnace (U)", **SRT-PTD-2000-00112**, December 19, 2000.
19. J. E. Josephs, "Run Plan for Frit O Macrobatch Three in the Melt Rate Furnace (U)", **SRT-GPD-2001-0006**, January 17, 2001.
20. J. E. Josephs, "Run Plan for Frit N Macrobatch Three in the Melt Rate Furnace (U)", **SRT-GPD-2001-0007**, January 17, 2001.
21. J. E. Josephs, "Run Plan for Frit Mimi Macrobatch Three in the Melt Rate Furnace (U)", **SRT-GPD-2001-0008**, January 24, 2001.
22. J. E. Josephs, "Run Plan for Frit M Macrobatch Three in the Melt Rate Furnace (U)", **SRT-GPD-2001-0009**, January 24, 2001.
23. J. E. Josephs, "Run Plan for Frit KMA2A Macrobatch Three in the Melt Rate Furnace (U)", **SRT-GPD-2001-0010**, January 24, 2001.
24. J. E. Josephs, "Run Plan for Frit KMA2 Macrobatch Three in the Melt Rate Furnace (U)", **SRT-GPD-2001-0011**, January 24, 2001.
25. J. E. Josephs, "Run Plan for Frit G Macrobatch Three in the Melt Rate Furnace (U)", **SRT-GPD-2001-0012**, January 24, 2001.
26. J. E. Josephs, "Run Plan for Frit D Macrobatch Three in the Melt Rate Furnace (U)", **SRT-GPD-2001-0013**, January 24, 2001.
27. J. E. Josephs, "Run Plan for Frit C Macrobatch Three in the Melt Rate Furnace (U)", **SRT-GPD-2001-0014**, January 24, 2001.
28. J. E. Josephs, "Run Plan for Frit Bone Macrobatch Three in the Melt Rate Furnace (U)", **SRT-GPD-2001-0015**, January 24, 2001.
29. J. E. Josephs, "Run Plan for Frit Bone 2 Macrobatch Three in the Melt Rate Furnace (U)", **SRT-GPD-2001-0016**, January 24, 2001.
30. J. E. Josephs, "Run Plan for Frit BICK Macrobatch Three in the Melt Rate Furnace (U)", **SRT-GPD-2001-0017**, January 24, 2001.
31. J. E. Josephs, "Run Plan for Frit 165 Macrobatch Three in the Melt Rate Furnace (U)", **SRT-GPD-2001-0022**, February 7, 2001.
32. J. E. Josephs, "Run Plan for Frit 200 Macrobatch Three in the Melt Rate Furnace (U)", **SRT-GPD-2001-0023**, February 7, 2001.
33. M. E. Stone, "Run Plan for Frit 165 Macrobatch Three in the Melt Rate Furnace (U)", **SRT-GPD-2001-0024**, March 5, 2001.
34. M. E. Stone, "Run Plan for Frit 200 Macrobatch Three in the Melt Rate Furnace (U)", **SRT-GPD-2001-0025**, March 5, 2001.
35. M. E. Stone, "Run Plan for Frit BONE2 Macrobatch Three in the Melt Rate Furnace (U)", **SRT-GPD-2001-0026**, March 5, 2001.
36. M. E. Stone, "Run Plan for Frit BONE Macrobatch Three in the Melt Rate Furnace (U)", **SRT-GPD-2001-0027**, March 5, 2001.
37. M. E. Stone, "Run Plan for Frit D Macrobatch Three in the Melt Rate Furnace (U)", **SRT-GPD-2001-0028**, March 5, 2001.
38. M. E. Stone, "Run Plan for Frit G Macrobatch Three in the Melt Rate Furnace (U)", **SRT-GPD-2001-0029**, March 5, 2001.
39. M. E. Stone, "Run Plan for Frit KMA2A Macrobatch Three in the Melt Rate Furnace (U)", **SRT-GPD-2001-0030**, March 5, 2001.

40. M. E. Stone, "Run Plan for Frit M Macrobatches Three in the Melt Rate Furnace (U)", **SRT-GPD-2001-0031**, March 5, 2001.
41. M. E. Stone, "Run Plan for Frit 200 and MB2 SRAT Product Slurry in the Melt Rate Furnace (U)", **SRT-GPD-2001-0032**, March 5, 2001.
42. M. E. Stone, "Run Plan for Frit 200 Macrobatches Three with Sugar in the Melt Rate Furnace (U)", **SRT-GPD-2001-0033**, March 6, 2001.
43. Melt Rate Furnace Laboratory Notebook, **WSRC-NB-2000-00106**
44. Melt Rate Furnace Laboratory Notebook, **WSRC-NB-2001-00009**

APPENDICES A - H

Appendix A	Equipment Diagrams, Sketches and Photographs
Appendix B	Temperature Charts from Melt Rate Furnace Runs
Appendix C	Sectioned Beaker Photographs from Melt Rate Furnace Runs
Appendix D	Frit Compositions
Appendix E	Photographs of Unsectioned Beakers
Appendix F	Isotherm Charts from Selected Melt Rate Furnace Runs
Appendix G	Run Data and Melt Rate Determinations from Melt Rate Furnace Runs
Appendix H	Statistical Regression using JMP4 Software

Appendix A. Equipment Diagrams, Sketches, and Photographs

Figure A-1. Melt Rate Furnace Top

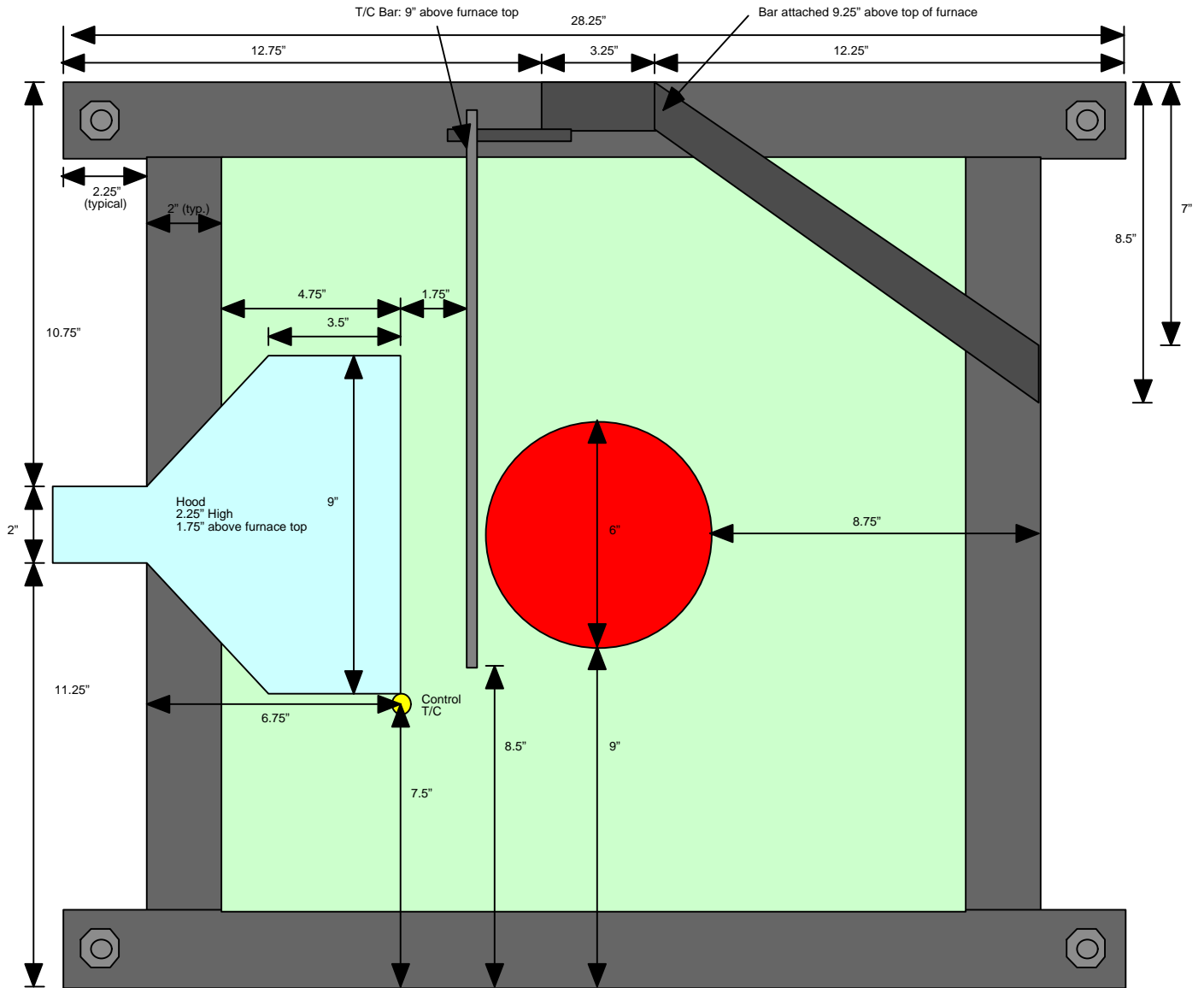
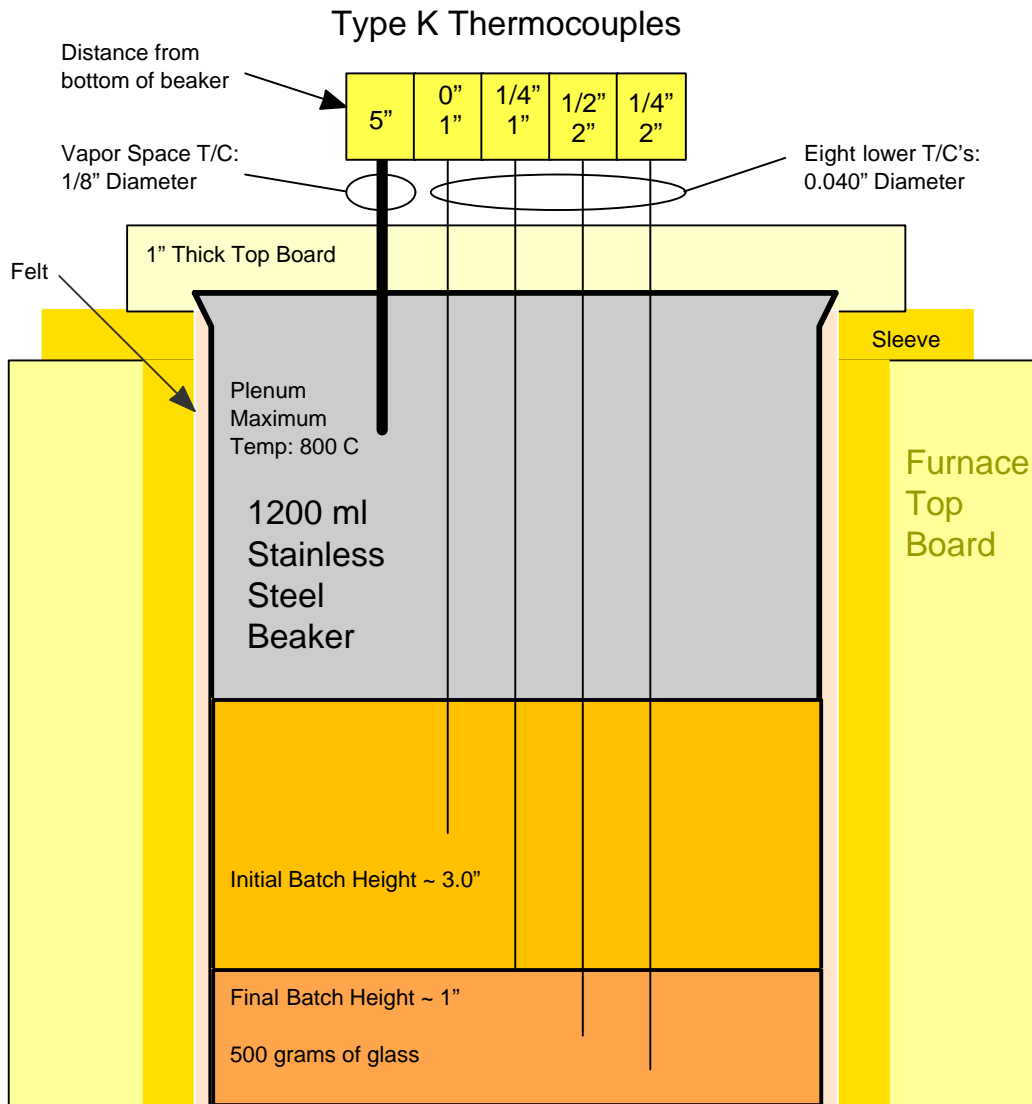


Figure A-2. Insulation Sleeve with Beaker



Furnace Chamber: 1150 Degrees Celsius

Figure A-3. Location of Beaker Thermocouples

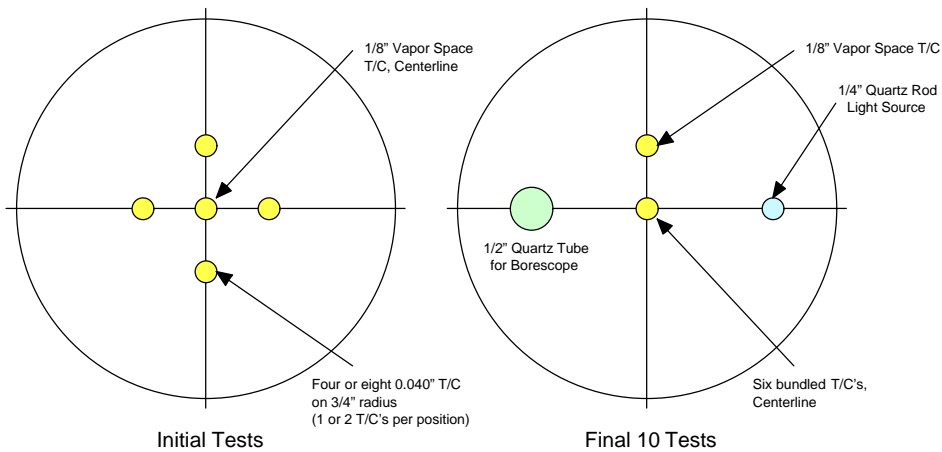


Figure A.3. Borescope Assembly

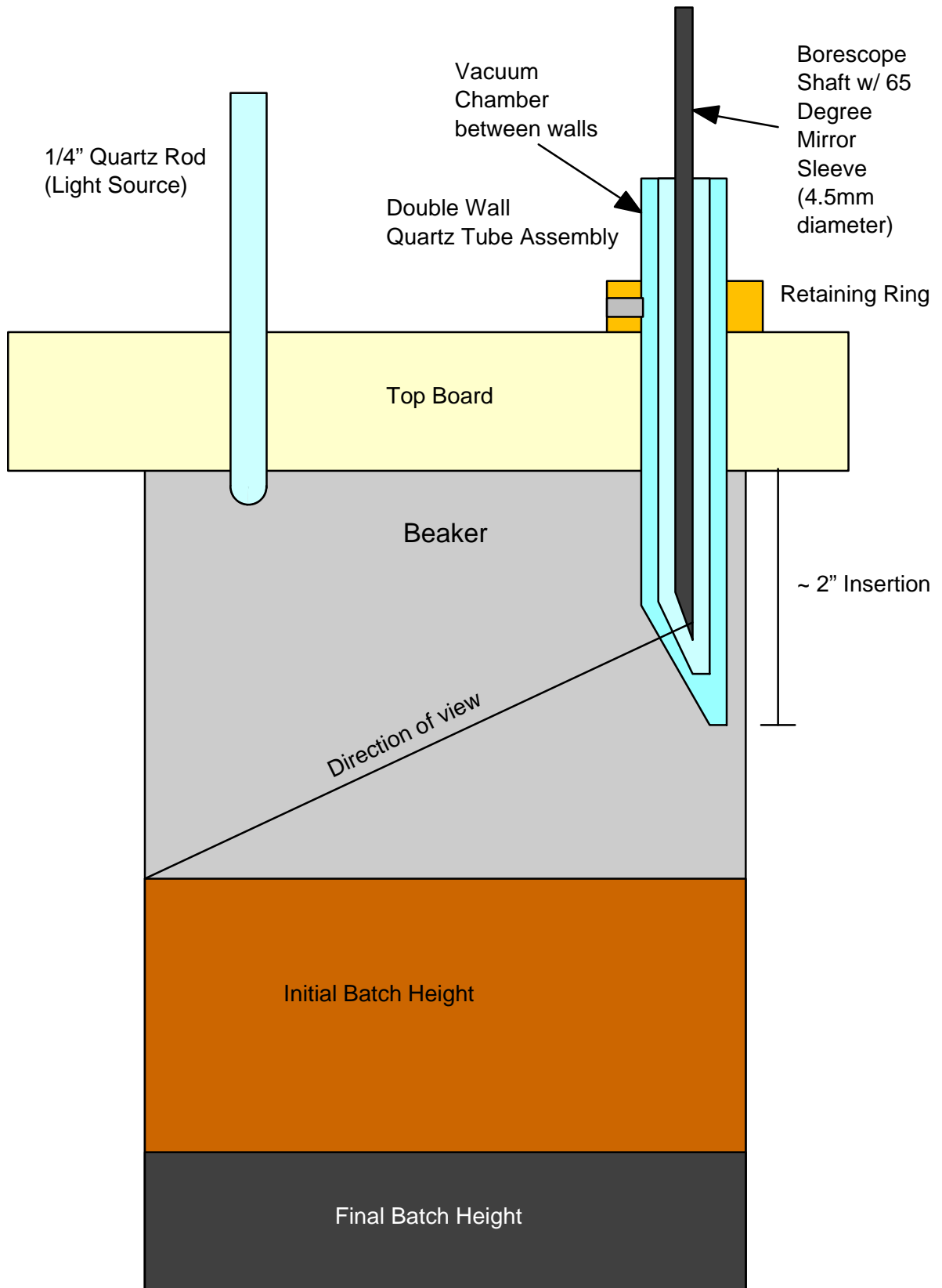


Figure A-4. Melt Rate Furnace Top with Insulating Board

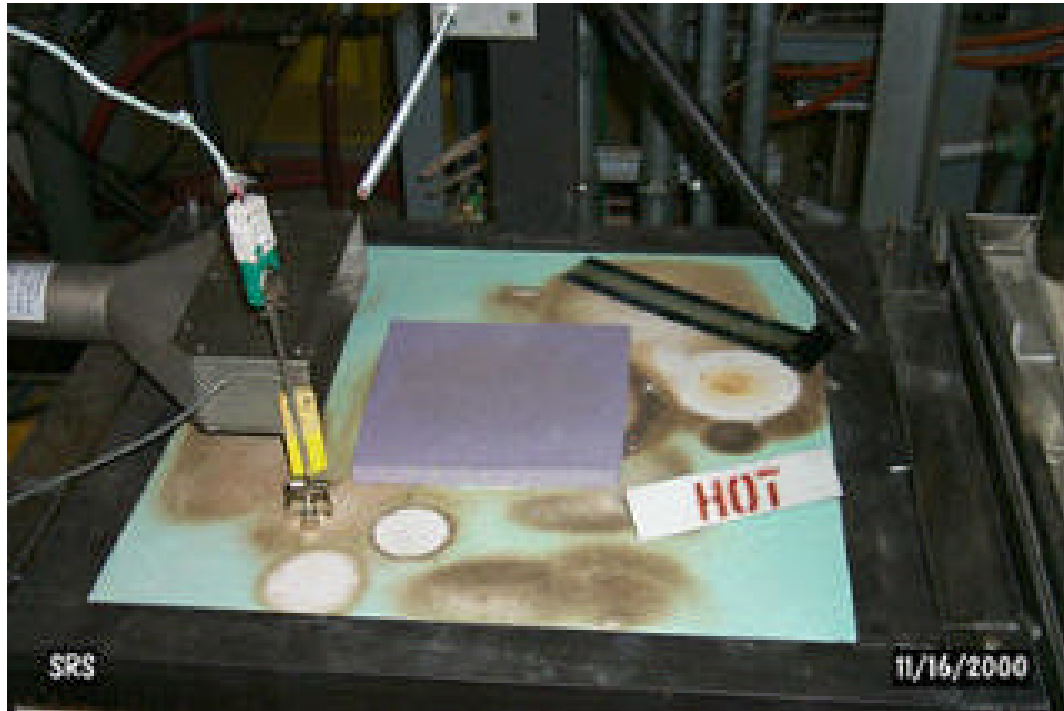


Figure A-5. Melt Rate Furnace Top

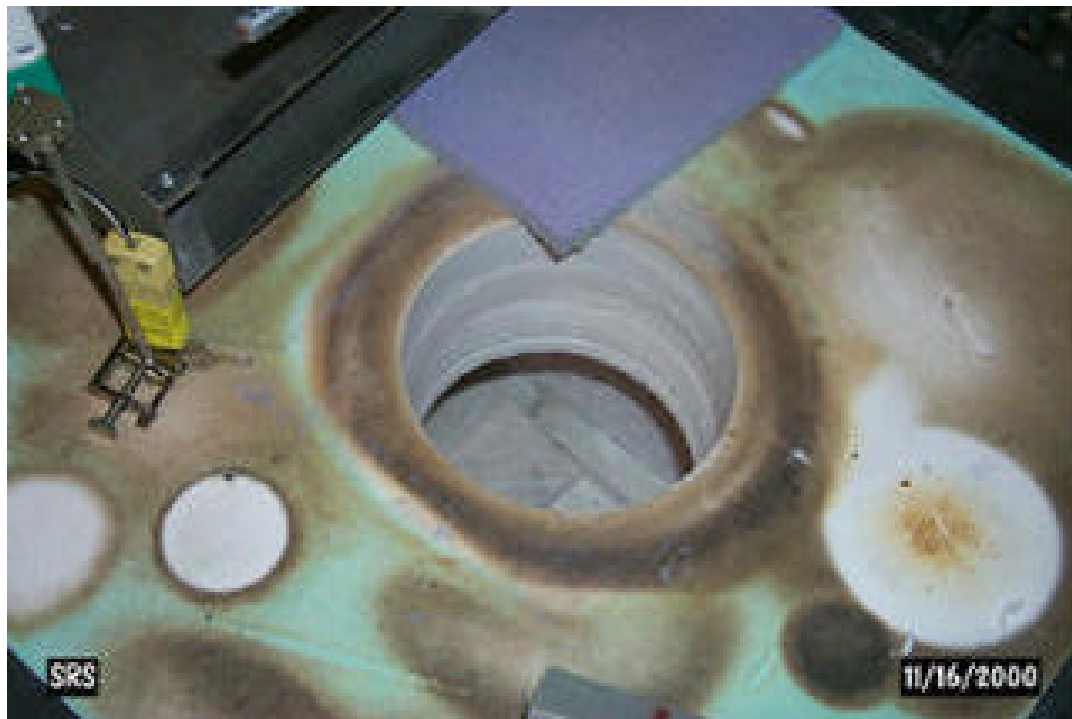


Figure A-6. Insulating Sleeve with Liner



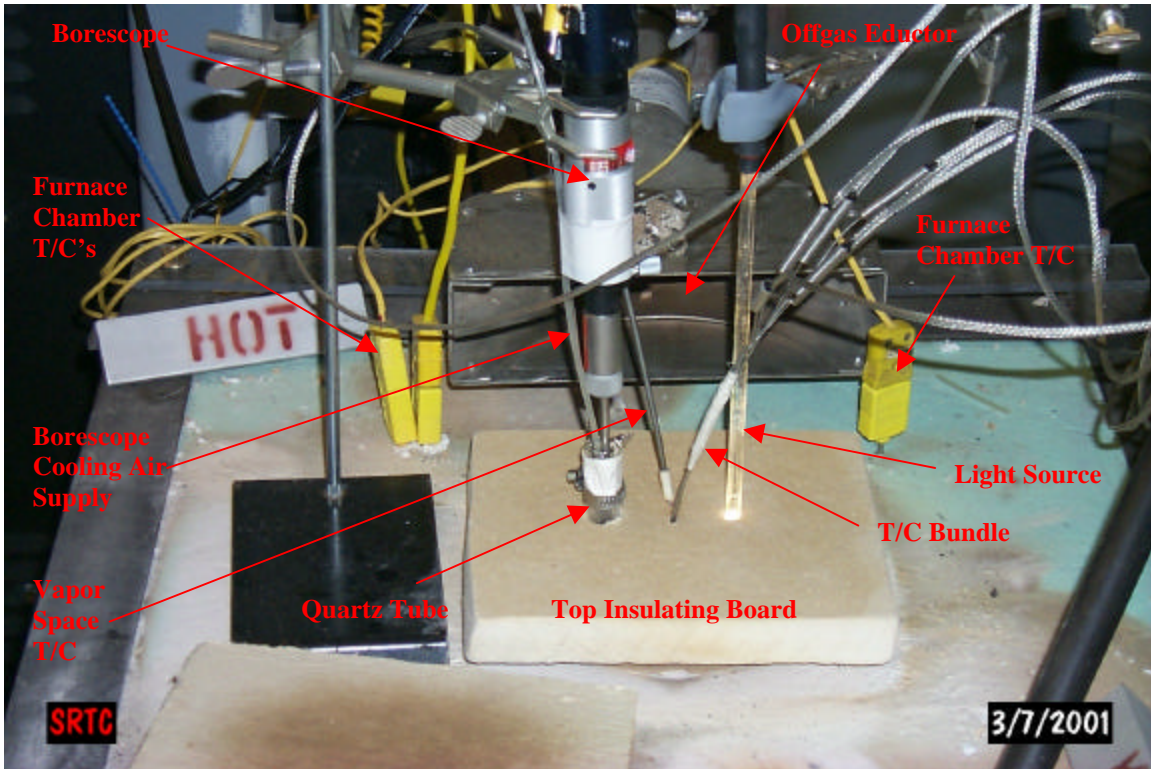
Figure A-7. Insulating Sleeve with Beaker



Figure A-7. Assembled Beaker with Sleeve, Top Board, and Four Beaker T/C's



Figure A-8. Melt Rate Furnace during Run with Borescope



Appendix B. Temperature Charts from Melt Rate Furnace Runs

Figure B-1. 200-MB3-Dried-MRF-1

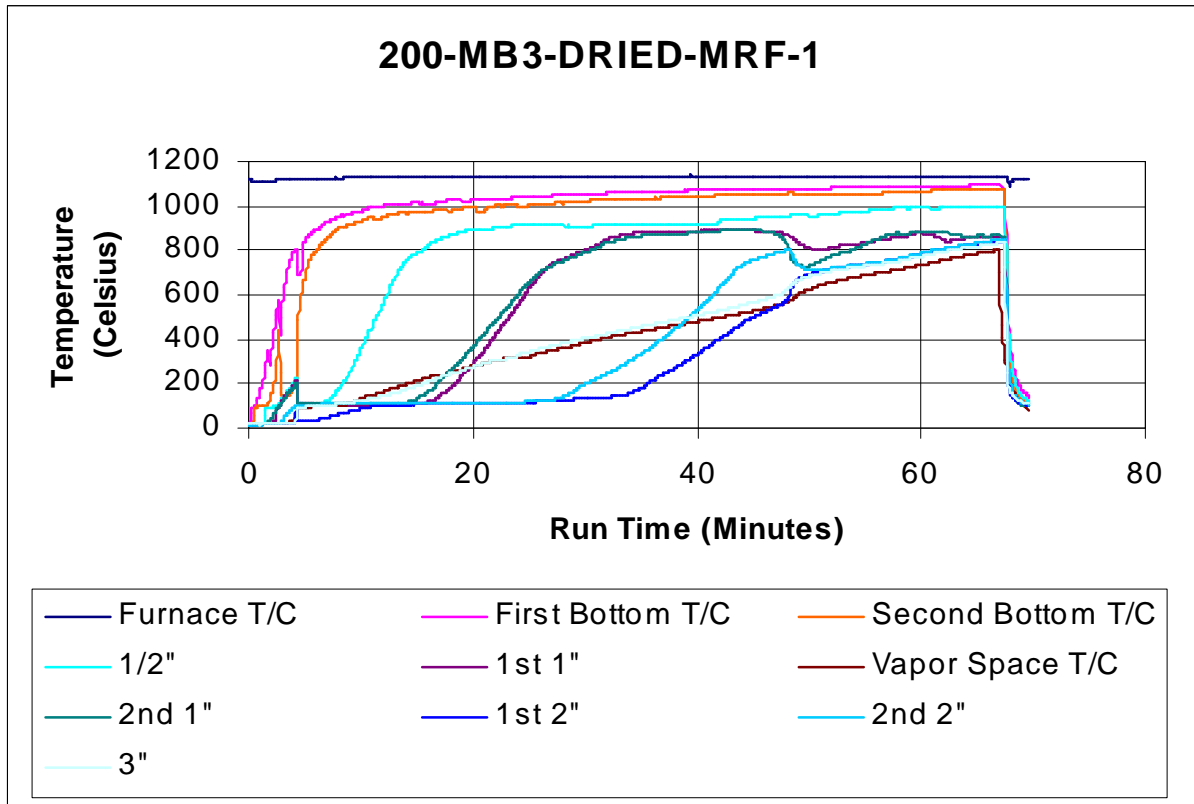


Figure B-2. 200-MB3-Dried-MRF-2

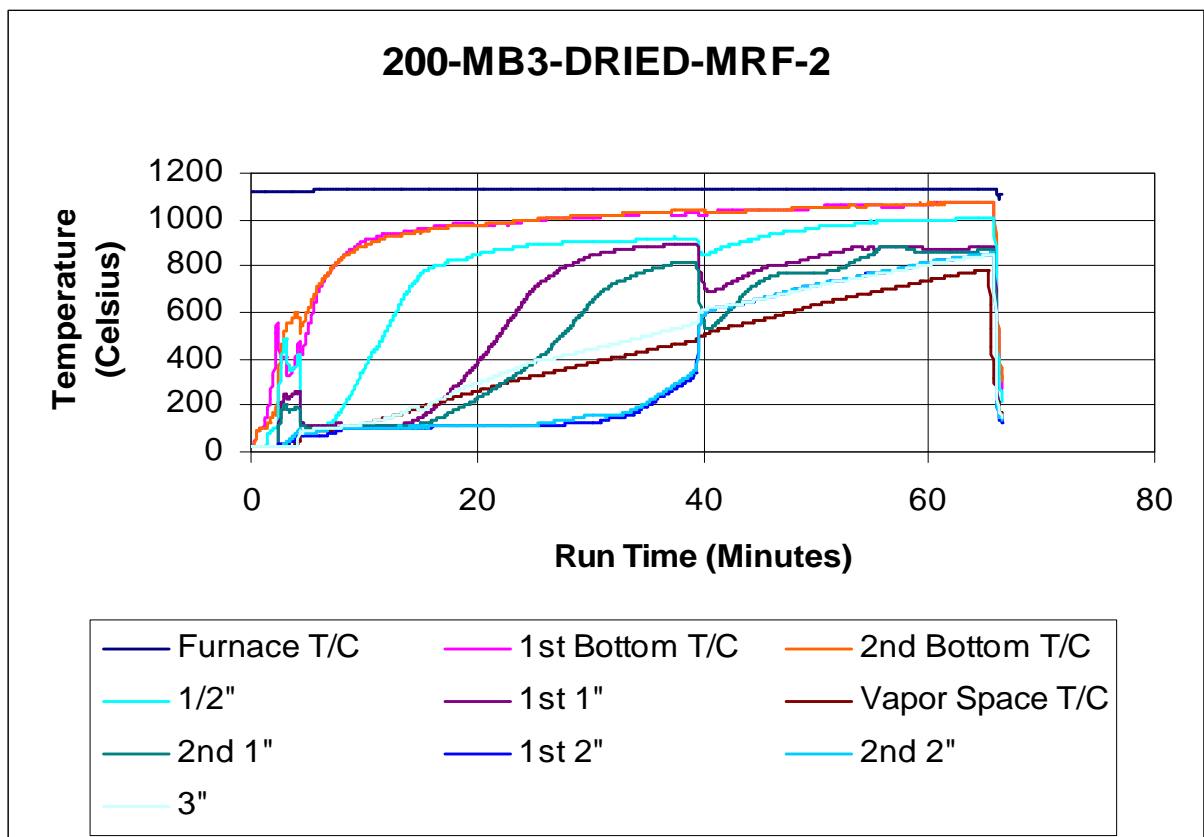


Figure B-3. 200-MB3-Dried-MRF-3

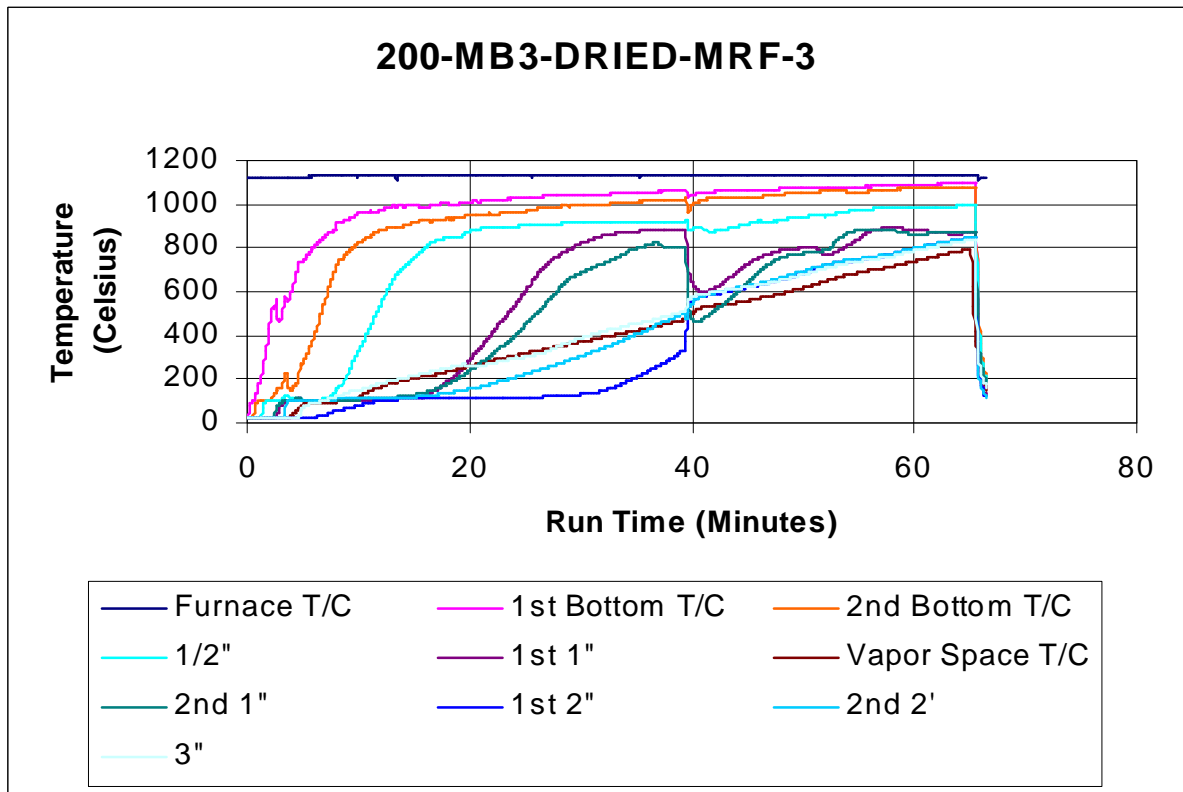


Figure B-4. 200-MB3-Dried-MRF-4

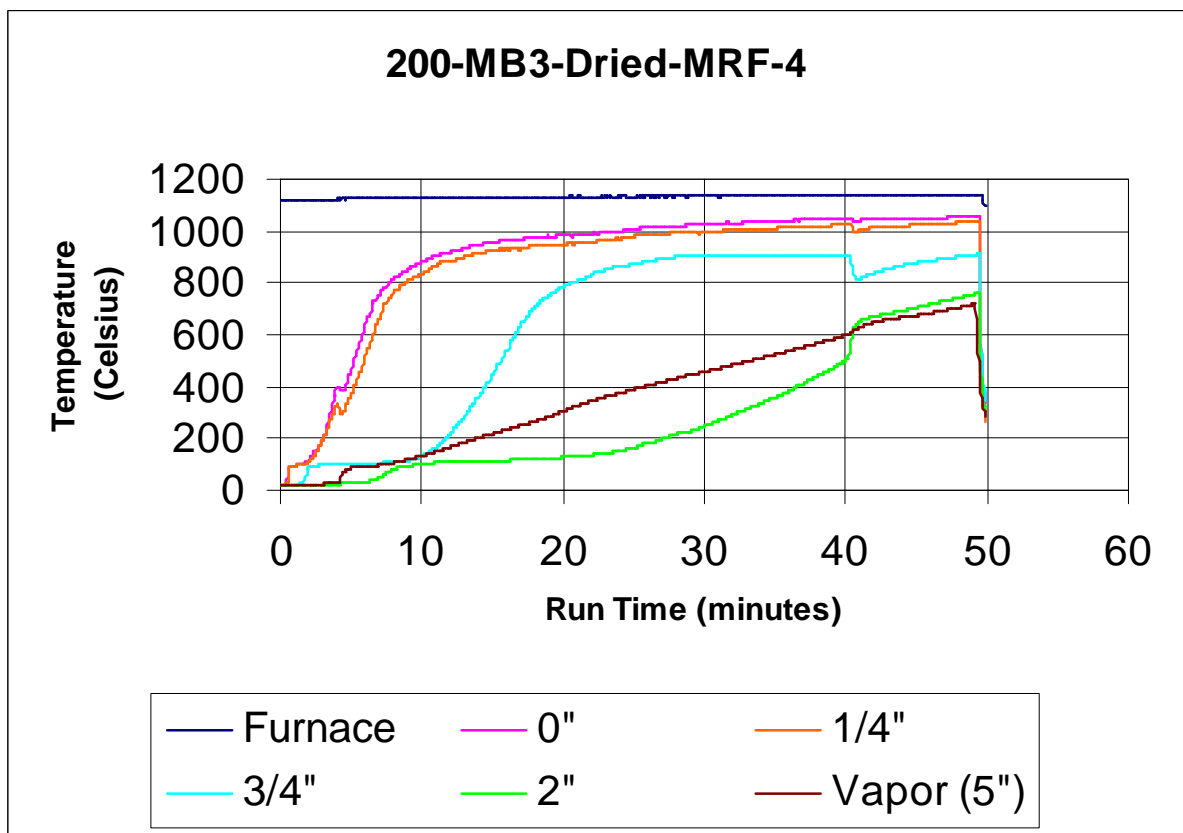


Figure B-5. 200-MB3-Dried-MRF-5

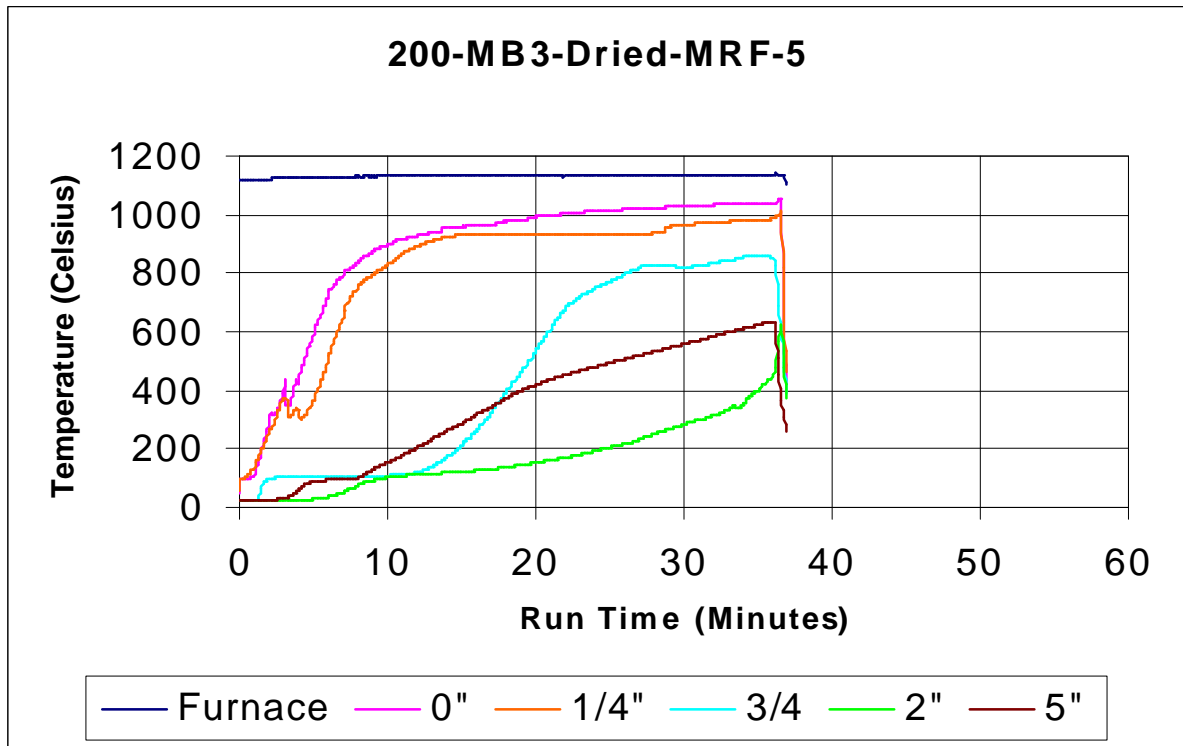


Figure B-6. 200-MB3-Dried-MRF-6

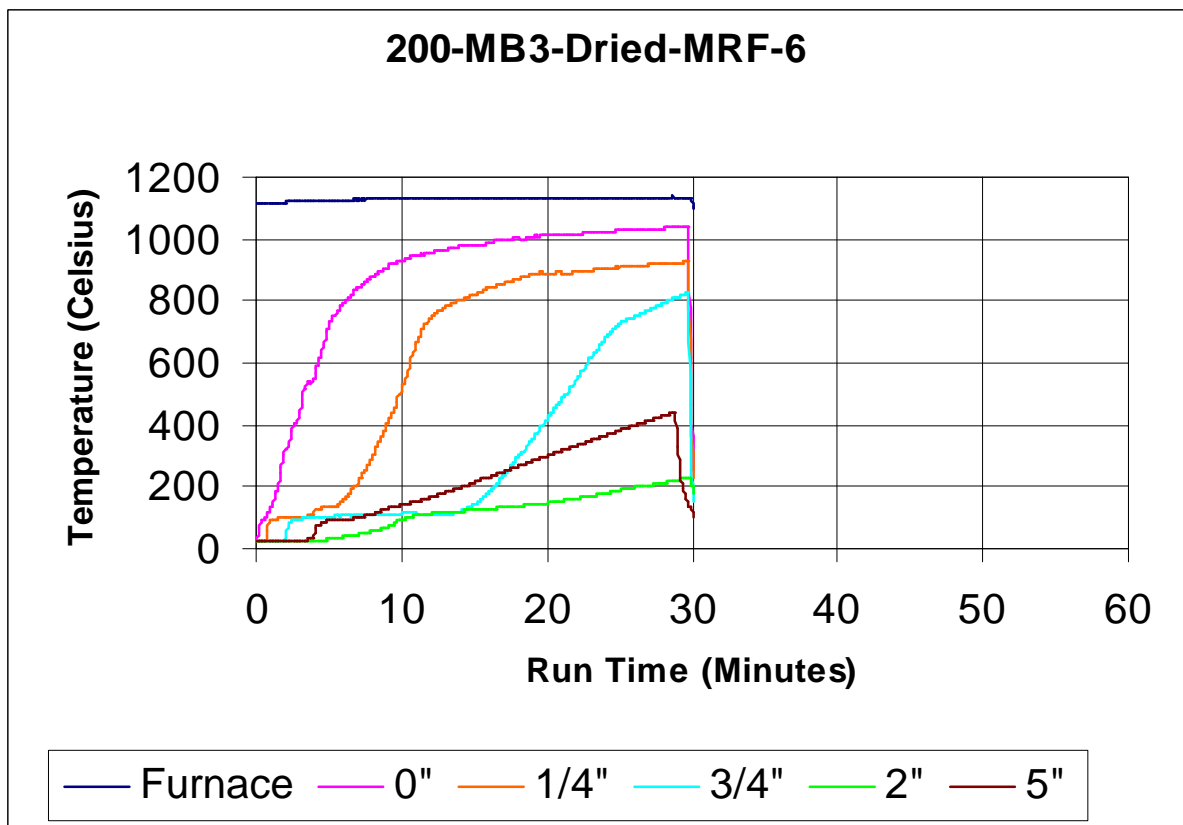


Figure B-7. Bone-MB3-MRF

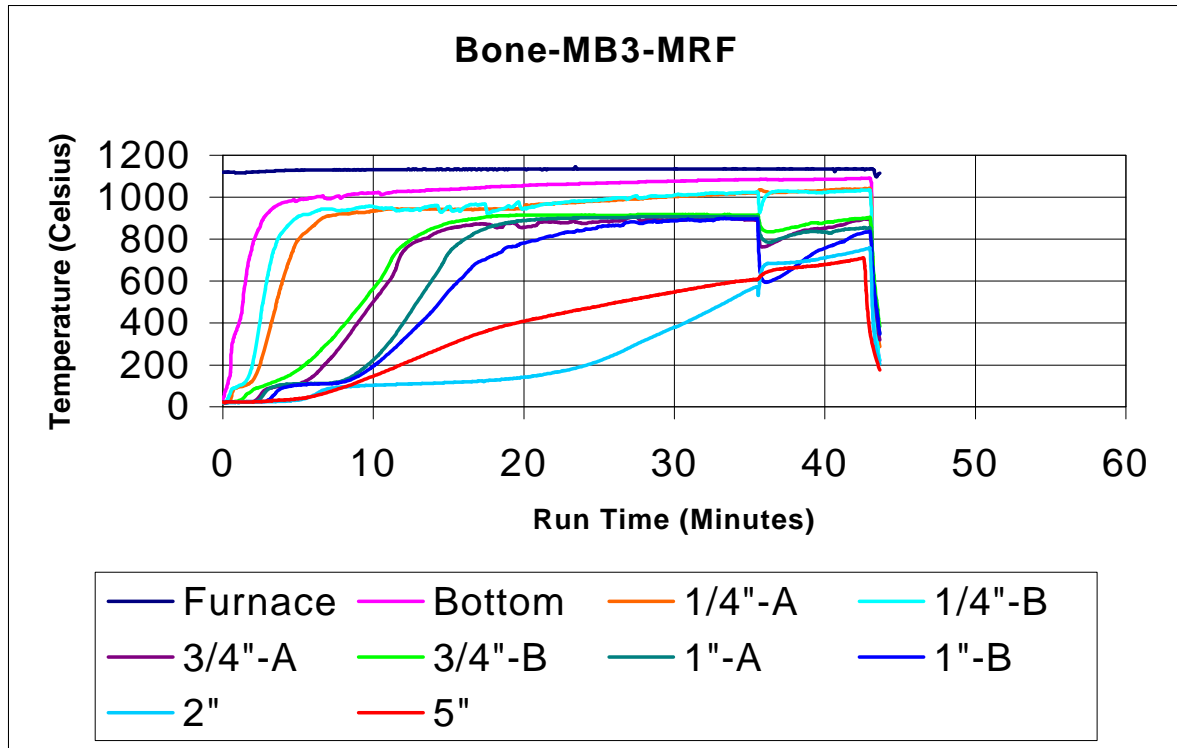


Figure B-8. KMA2-MB3-MRF

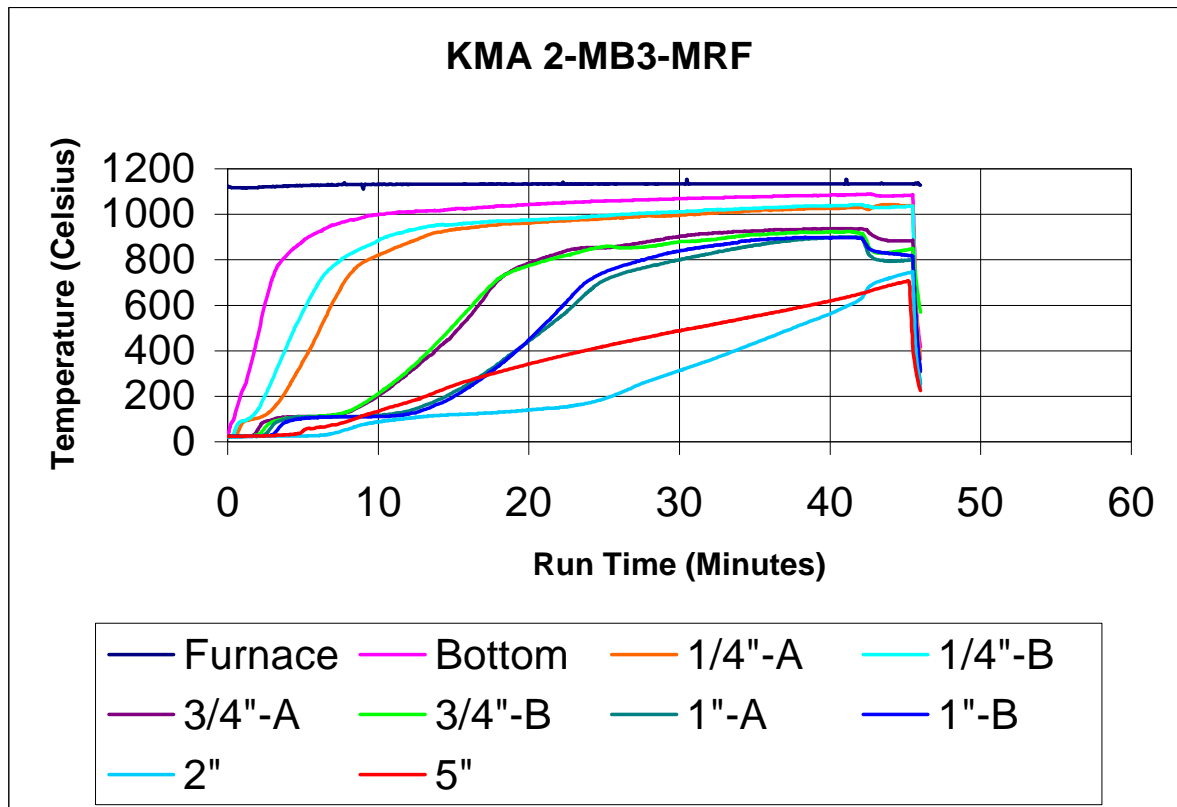


Figure B-9. Bick-MB3-MRF

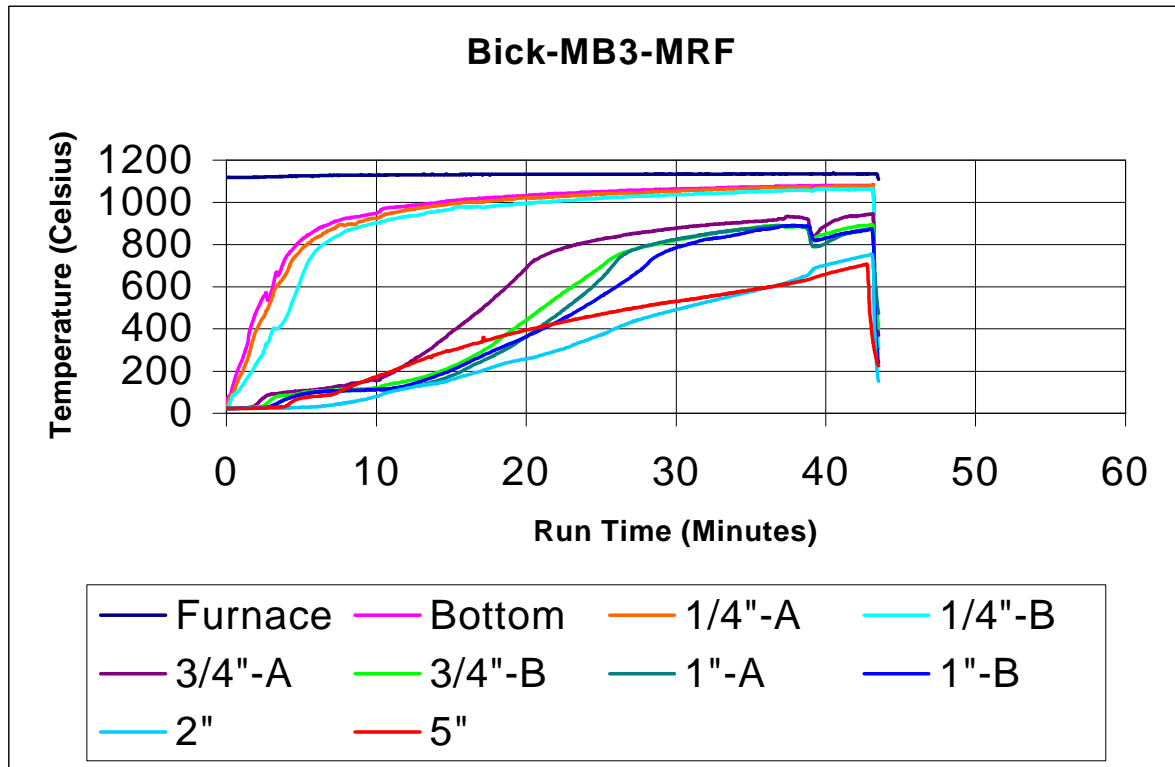


Figure B-10. Mimi-MB3-MRF

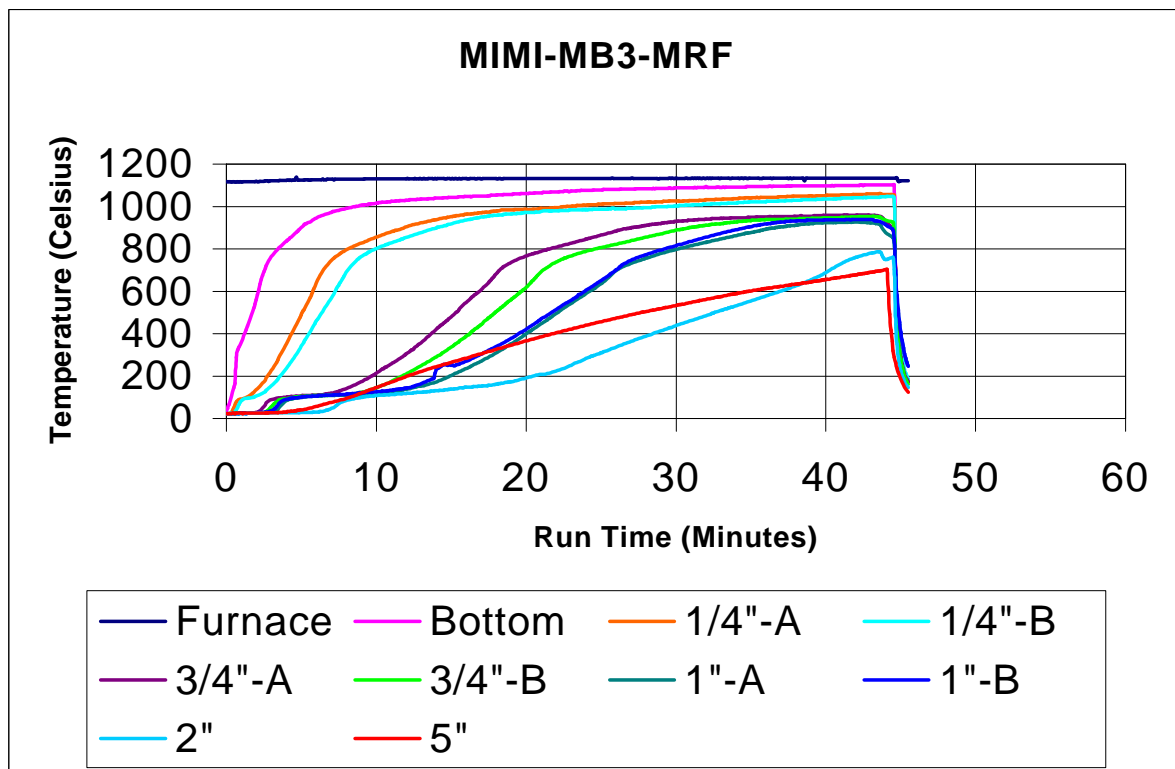


Figure B-11. KMA 2A-MB3-MRF

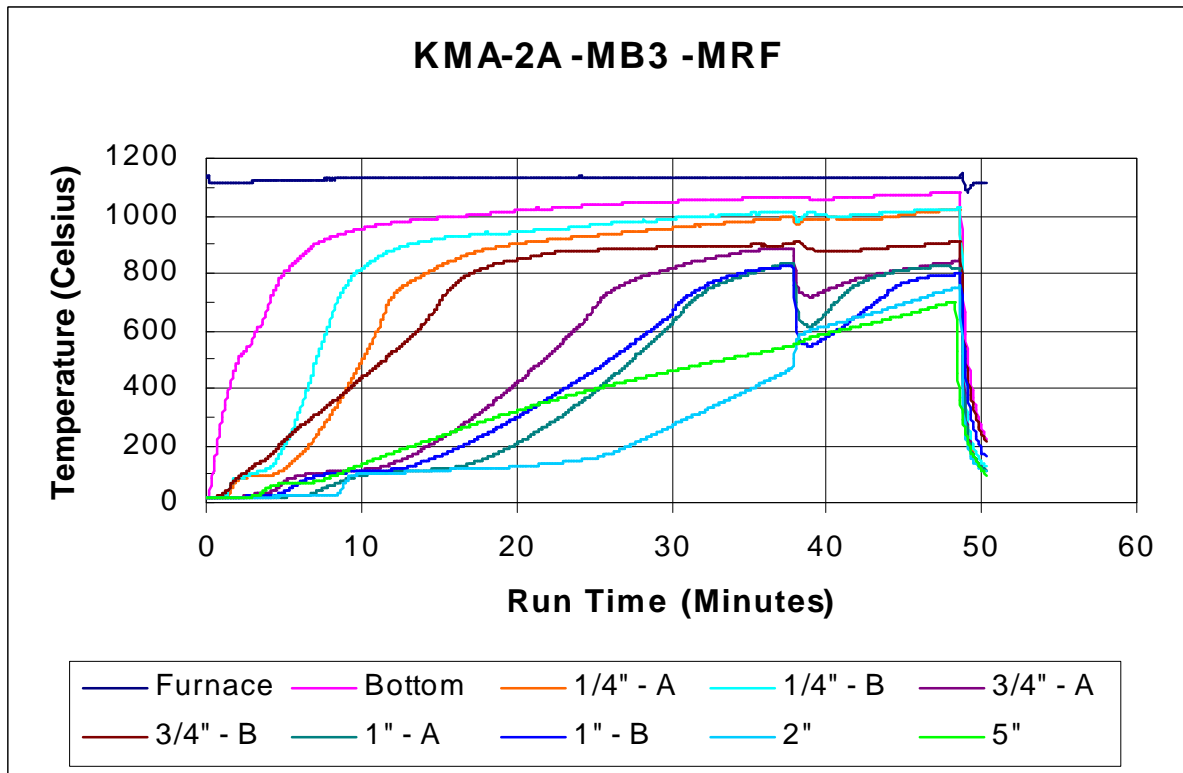


Figure B-12. C-MB3-MRF

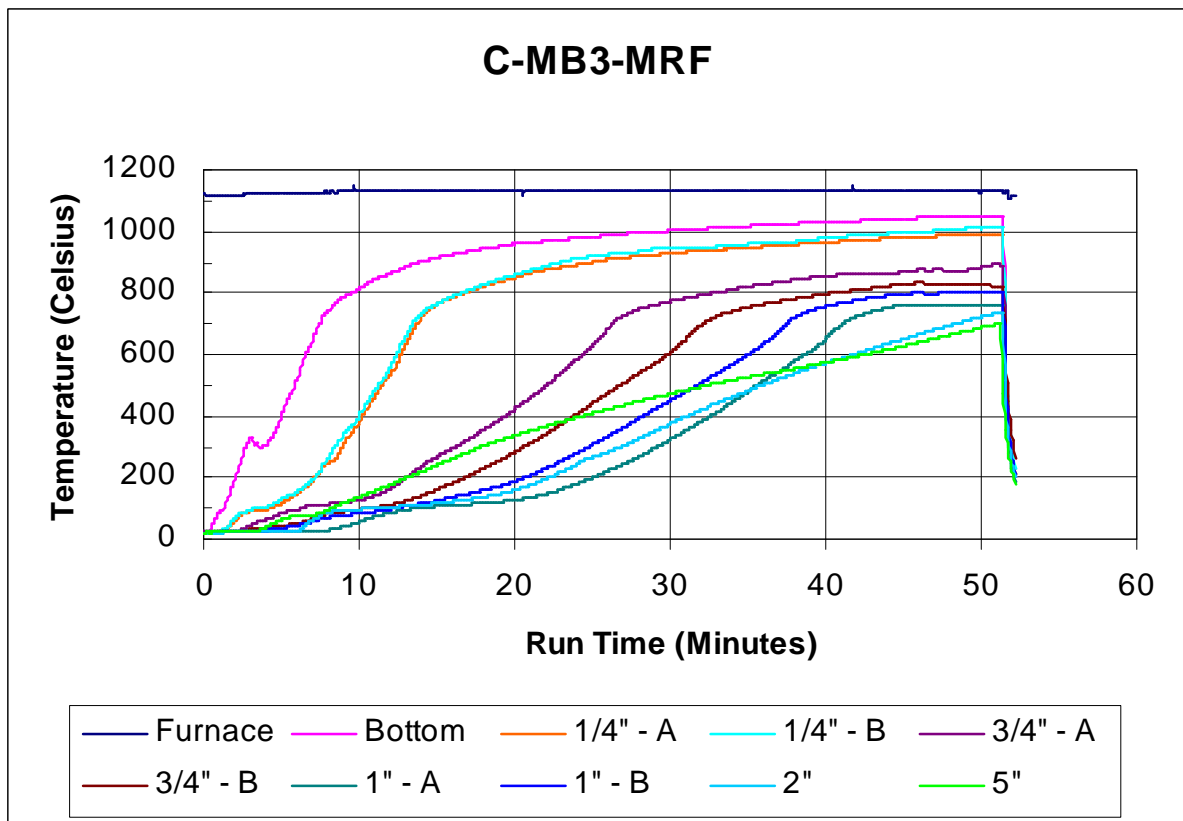


Figure B-13. O-MB3-MRF

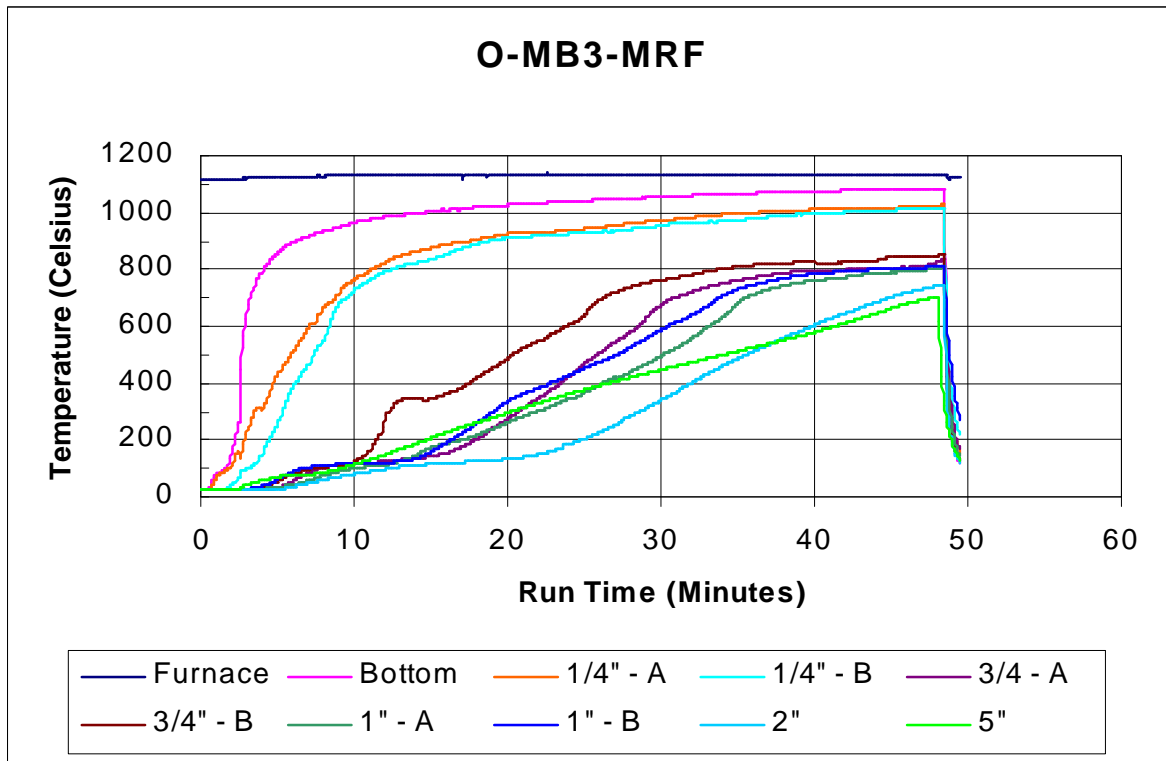


Figure B-14. Bone 2-MB3-MRF

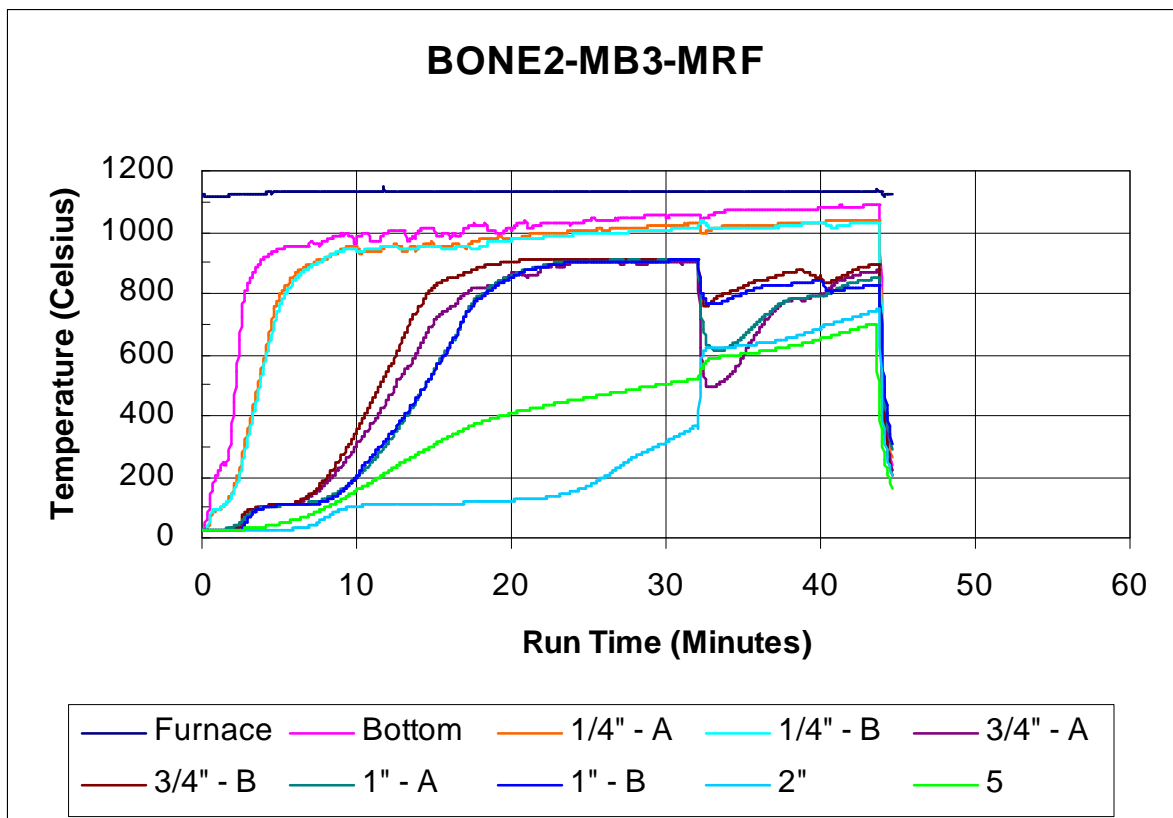


Figure B-15. M-MB3-MRF

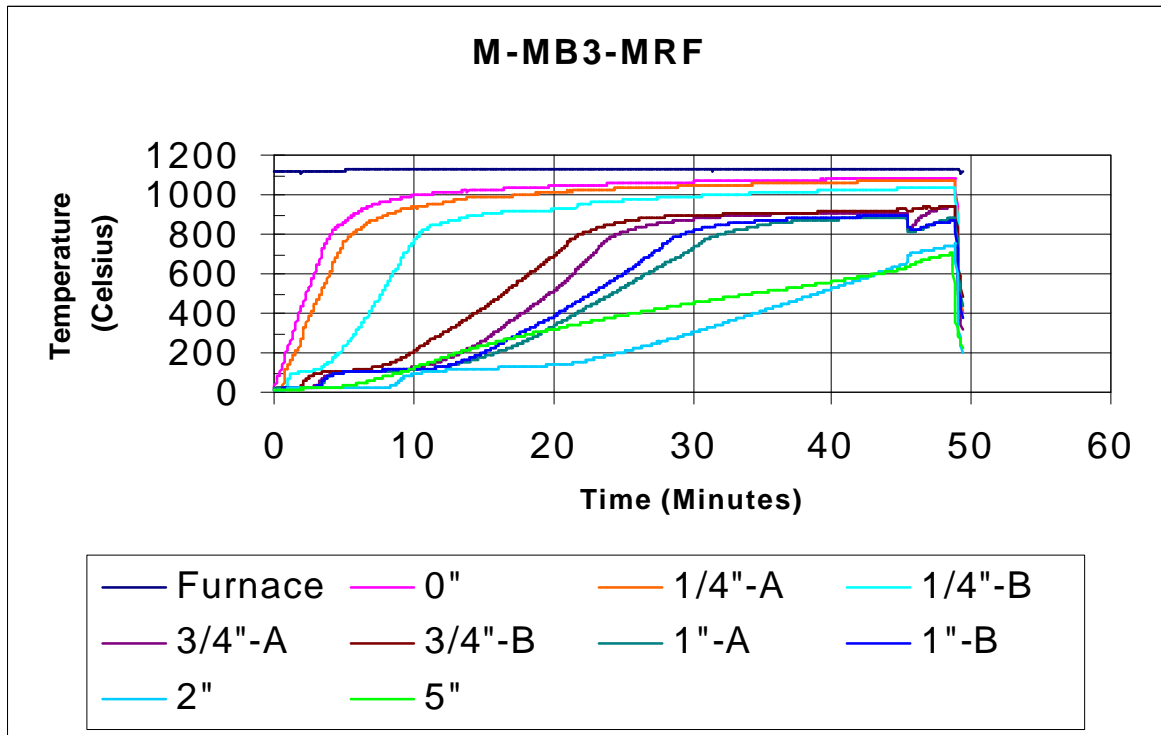


Figure B-16. G-MB3-MRF

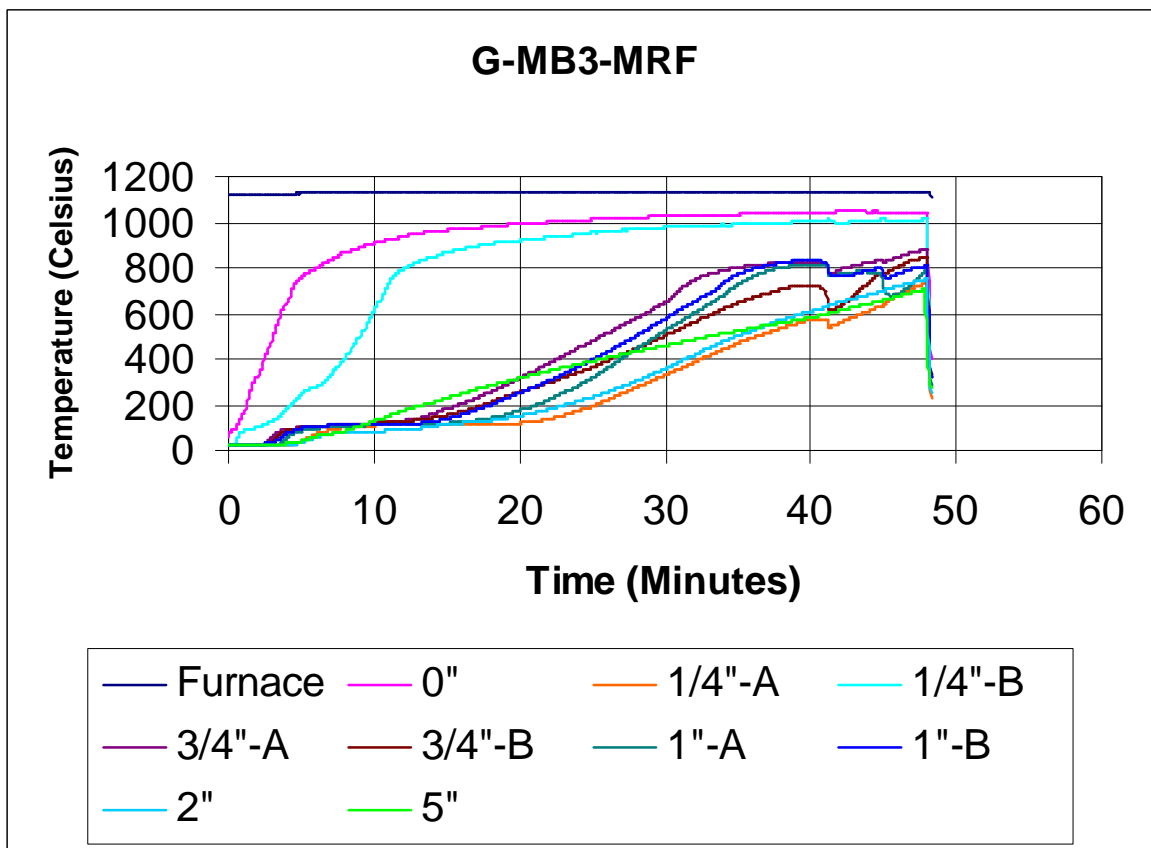


Figure B-17. N-MB3-MRF

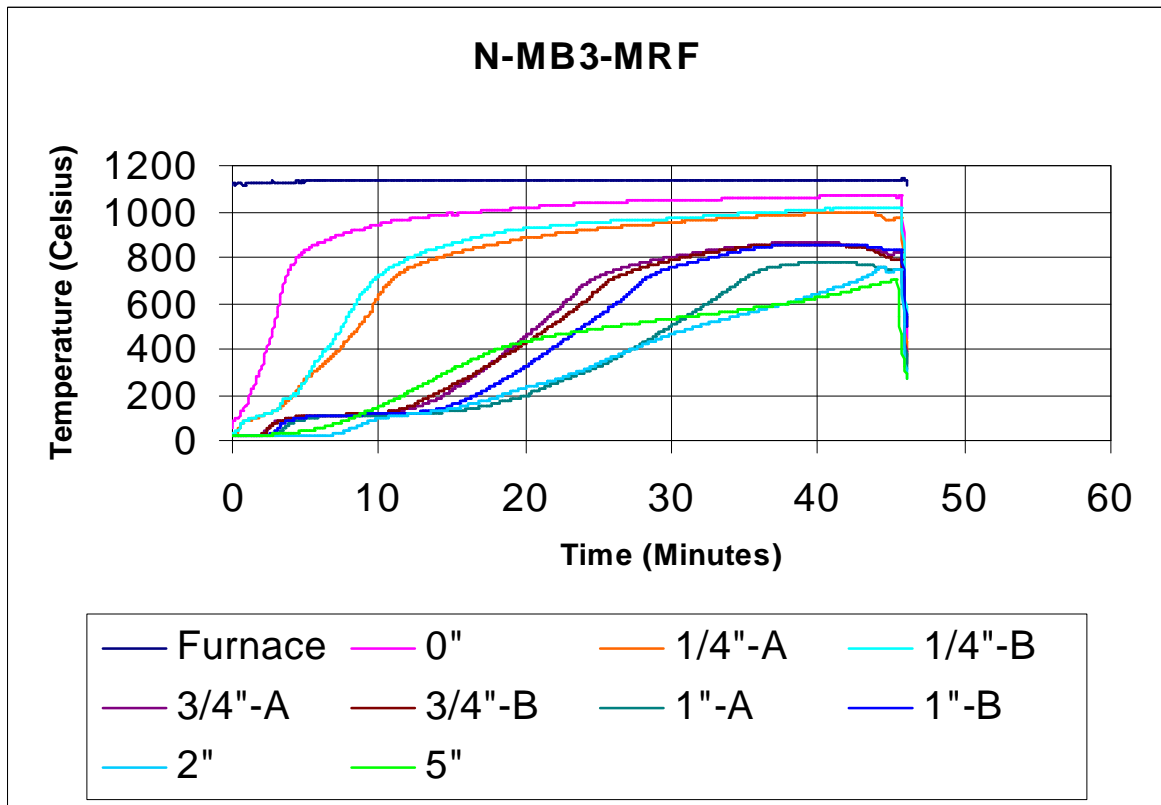


Figure B-18. D-MB3-MRF

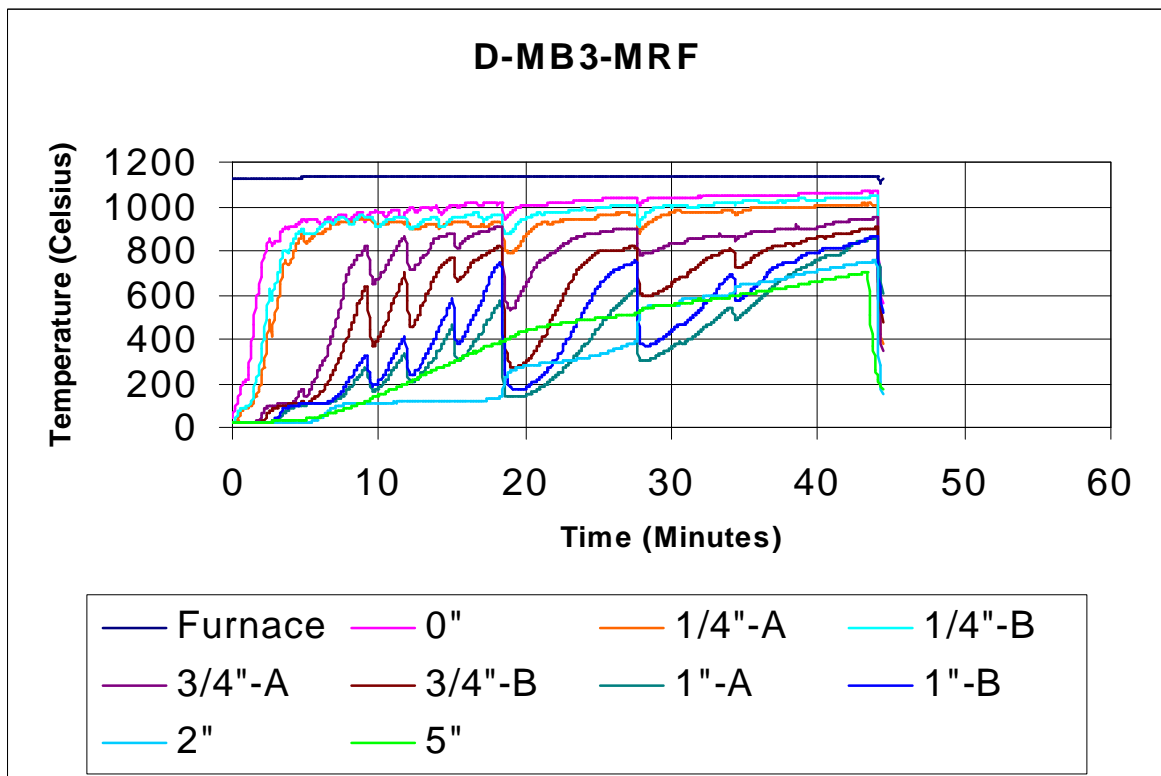


Figure B-19. 165-MB3-MRF-4

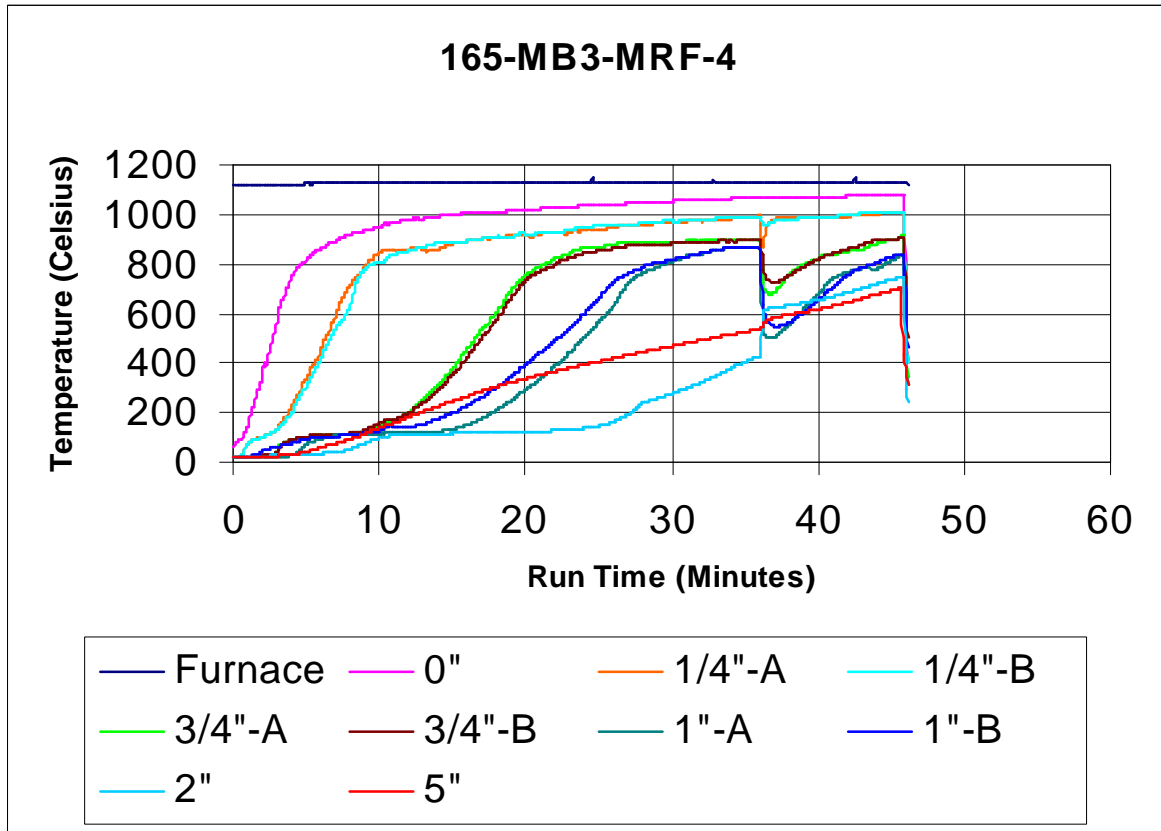


Figure B-20. 200-MB3-MRF-7

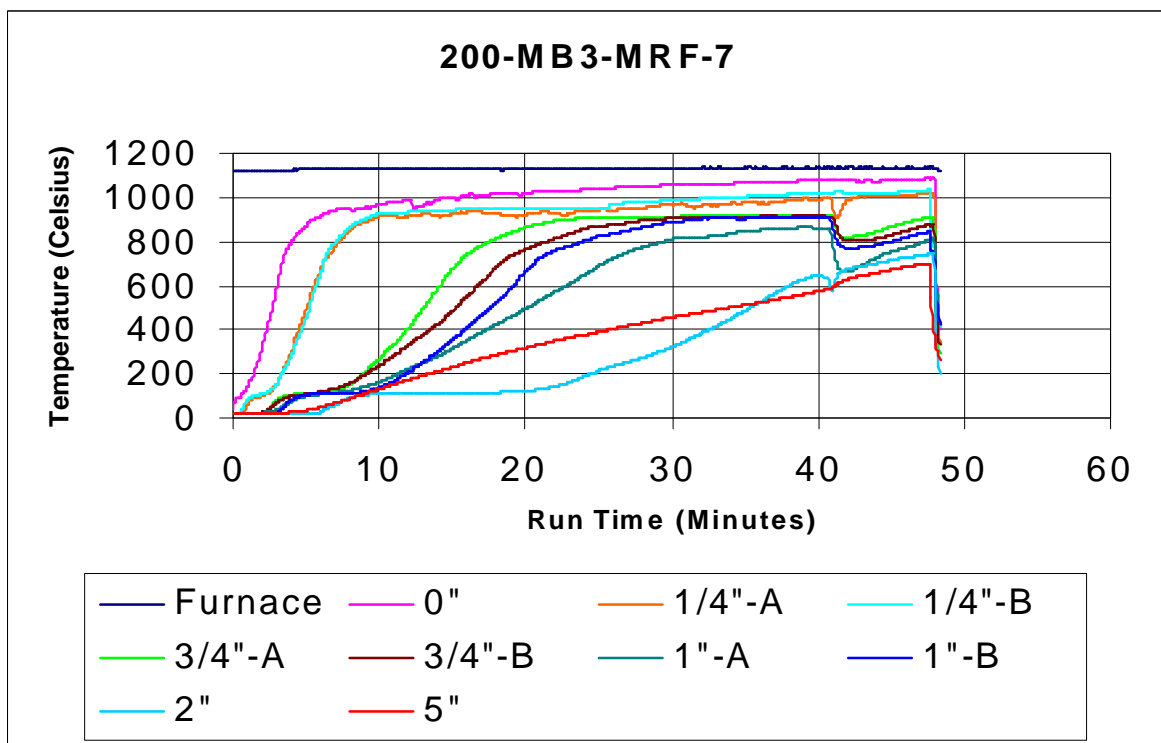


Figure B-21. 165 (Si Def)-MB3-MRF

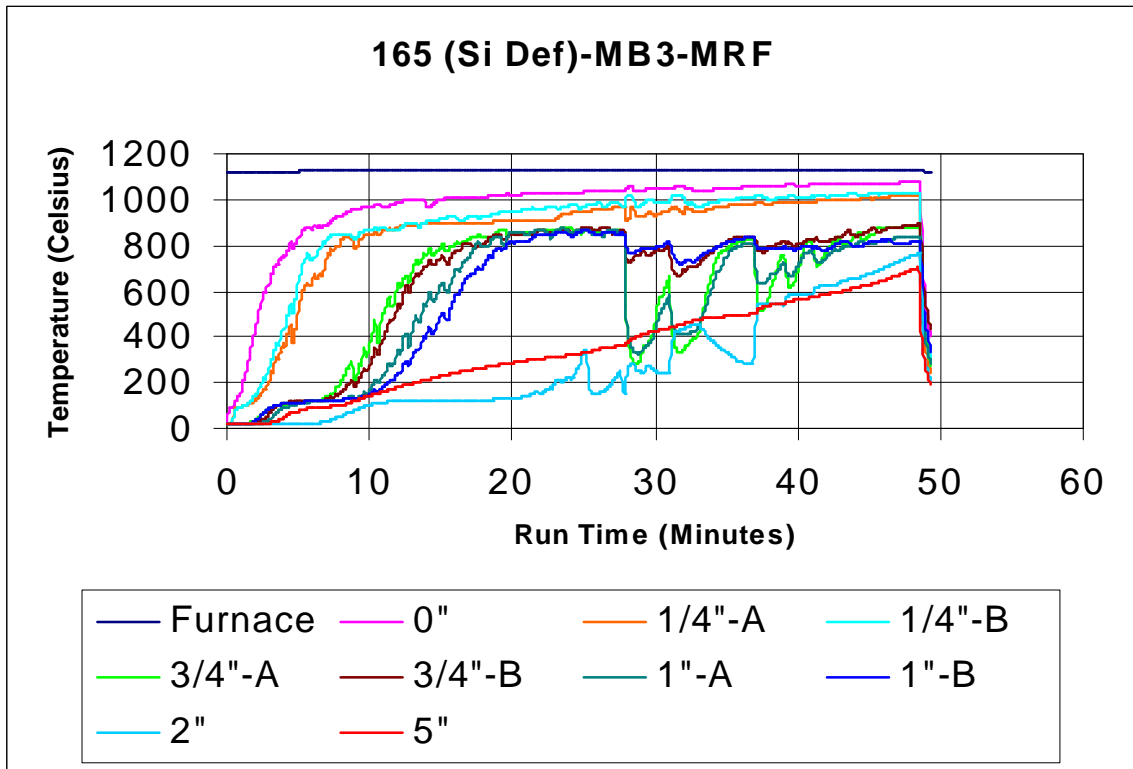


Figure B-22. 200-MB3-Baseline-MRF-1

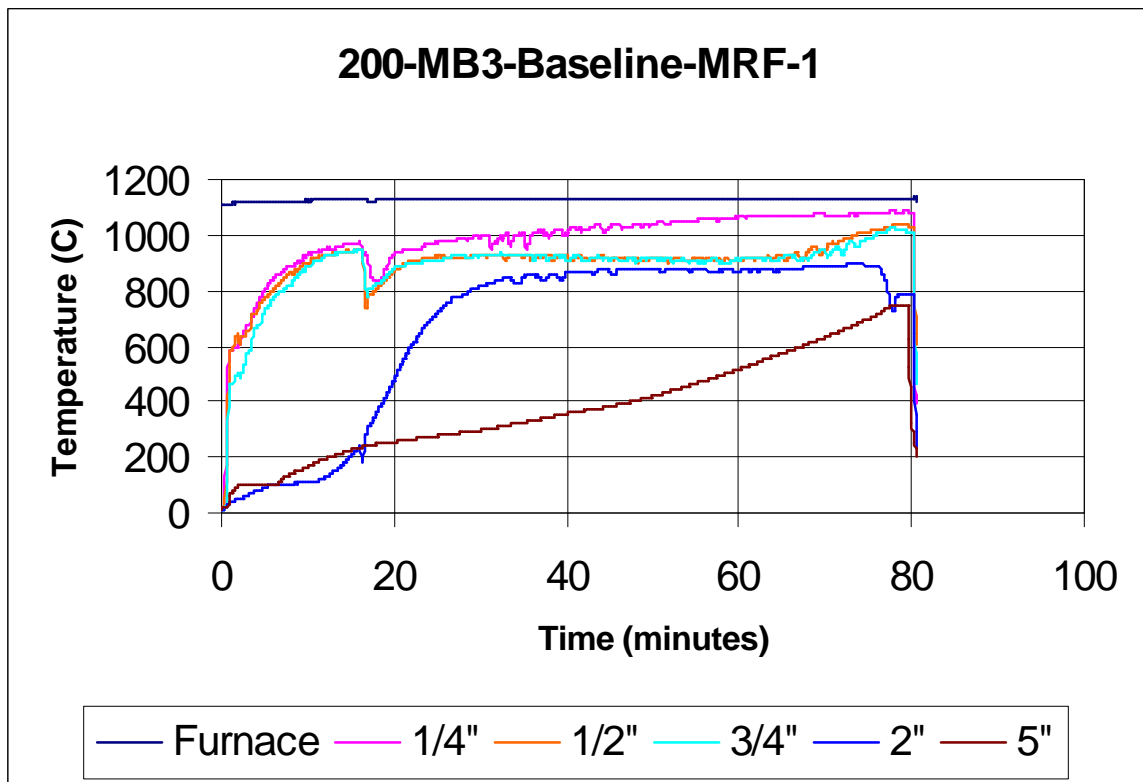


Figure B-23. 200-MB3-Baseline-MRF-2

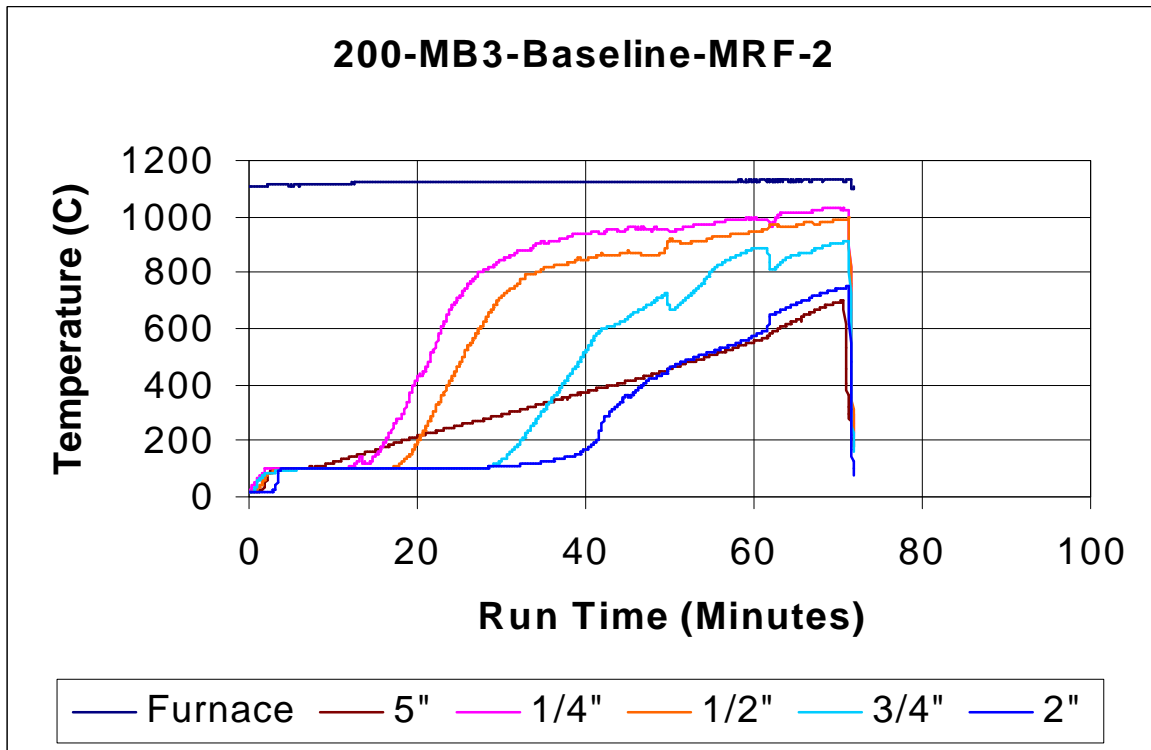


Figure B-24. 200-MB3-Baseline-MRF-3

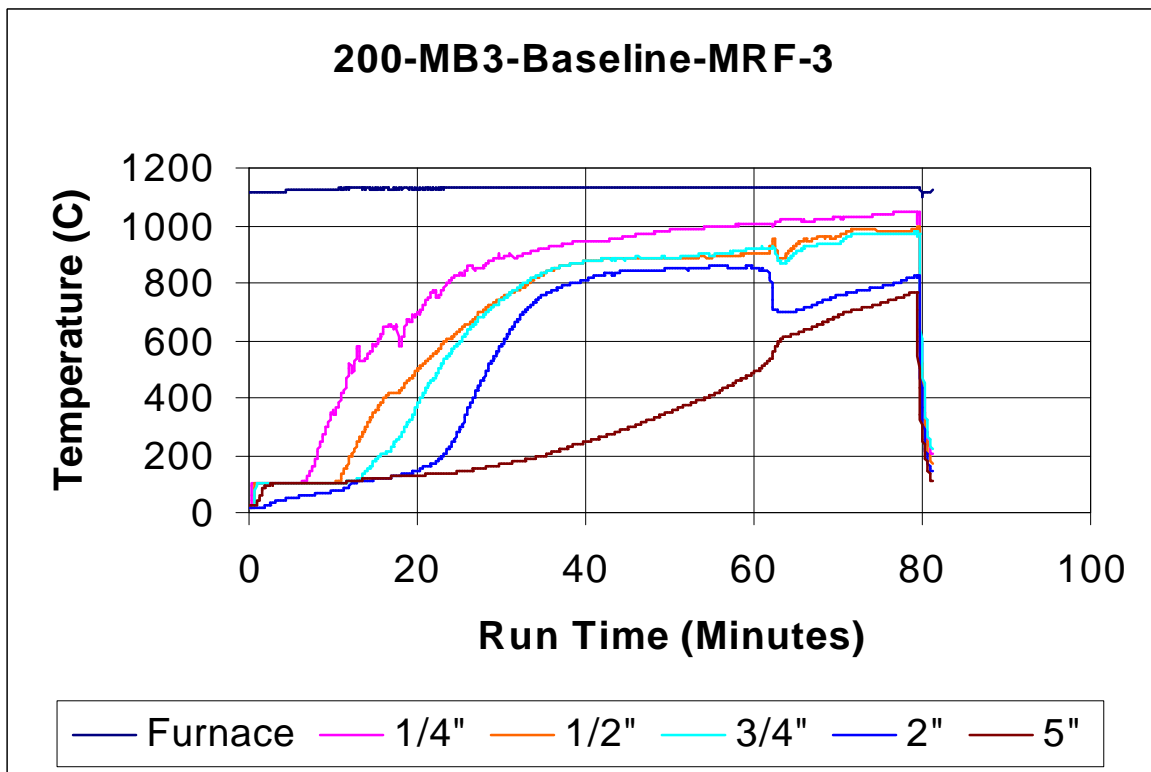


Figure B-25. 165-MB3-Baseline-MRF-1

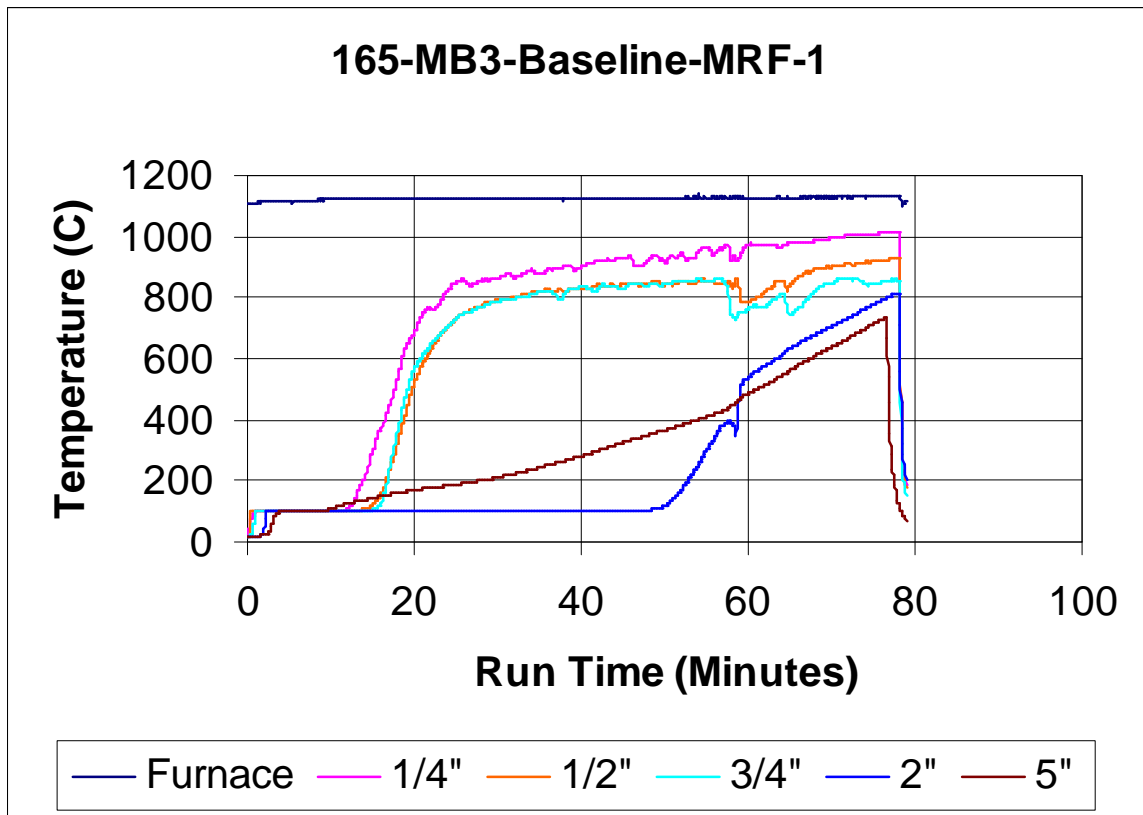


Figure B-26. 165-MB3-Baseline-MRF-2

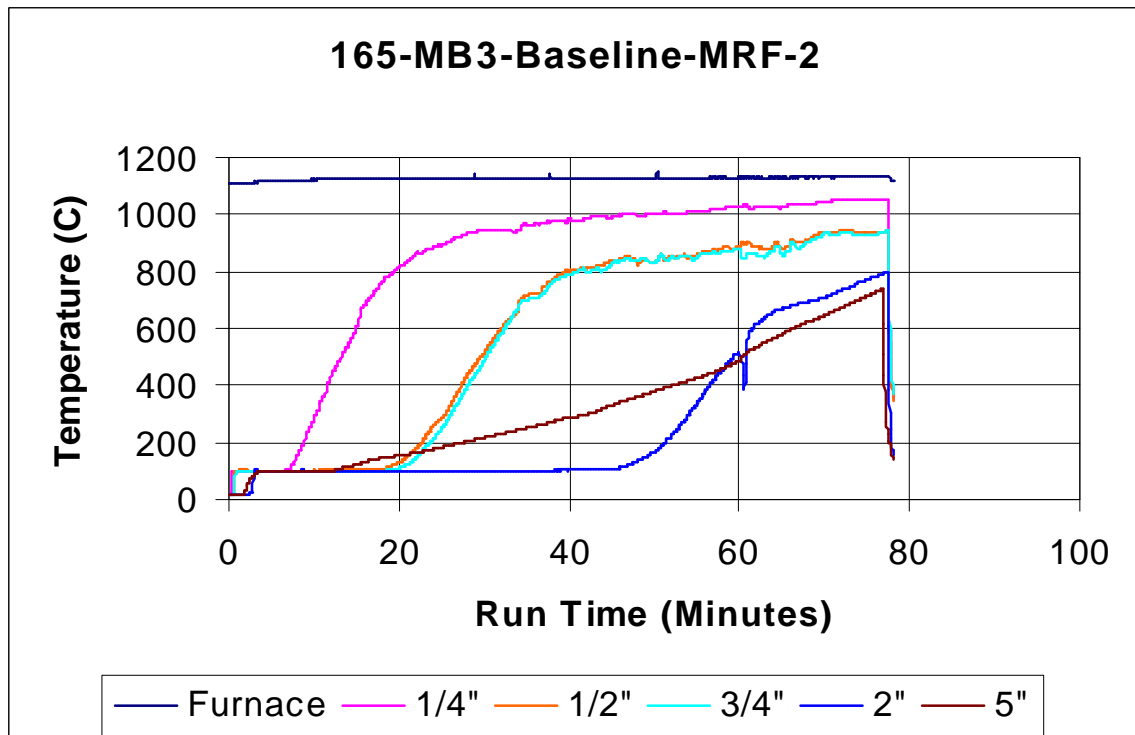


Figure B-27. 165-MB3-Baseline-MRF-3

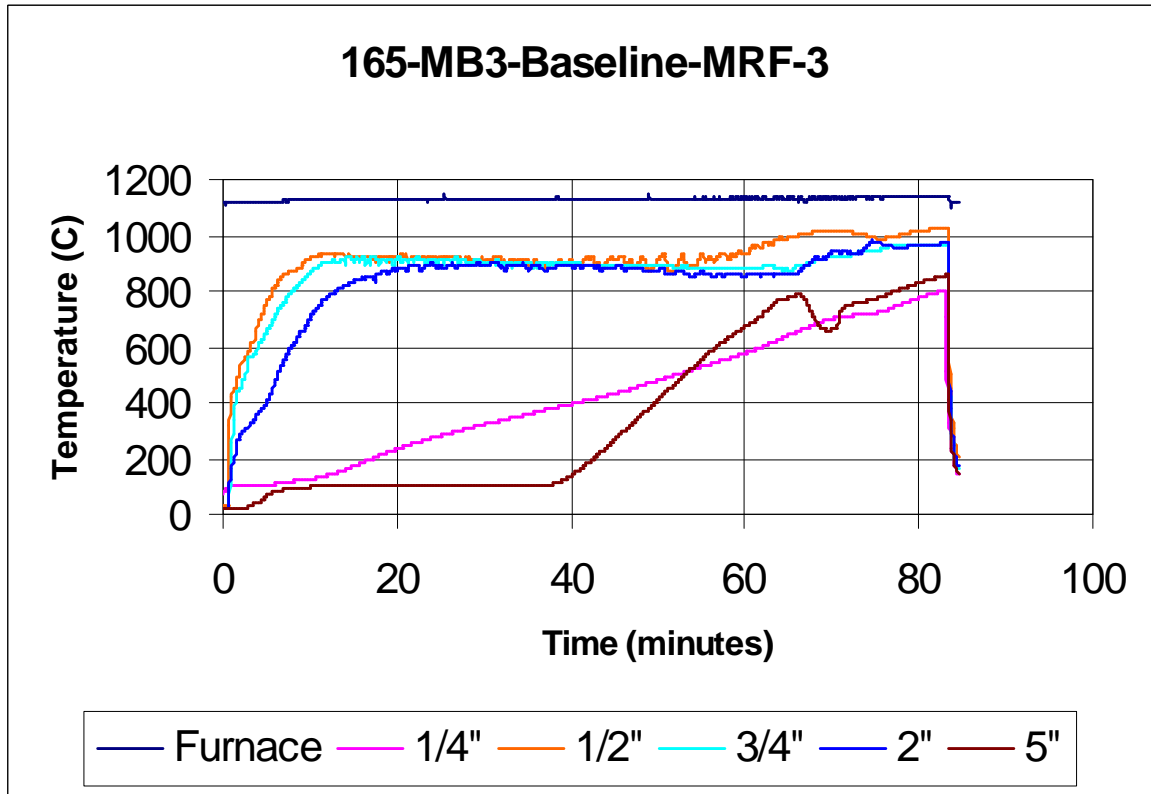


Figure B-28. 165-No Zr-Baseline-MRF

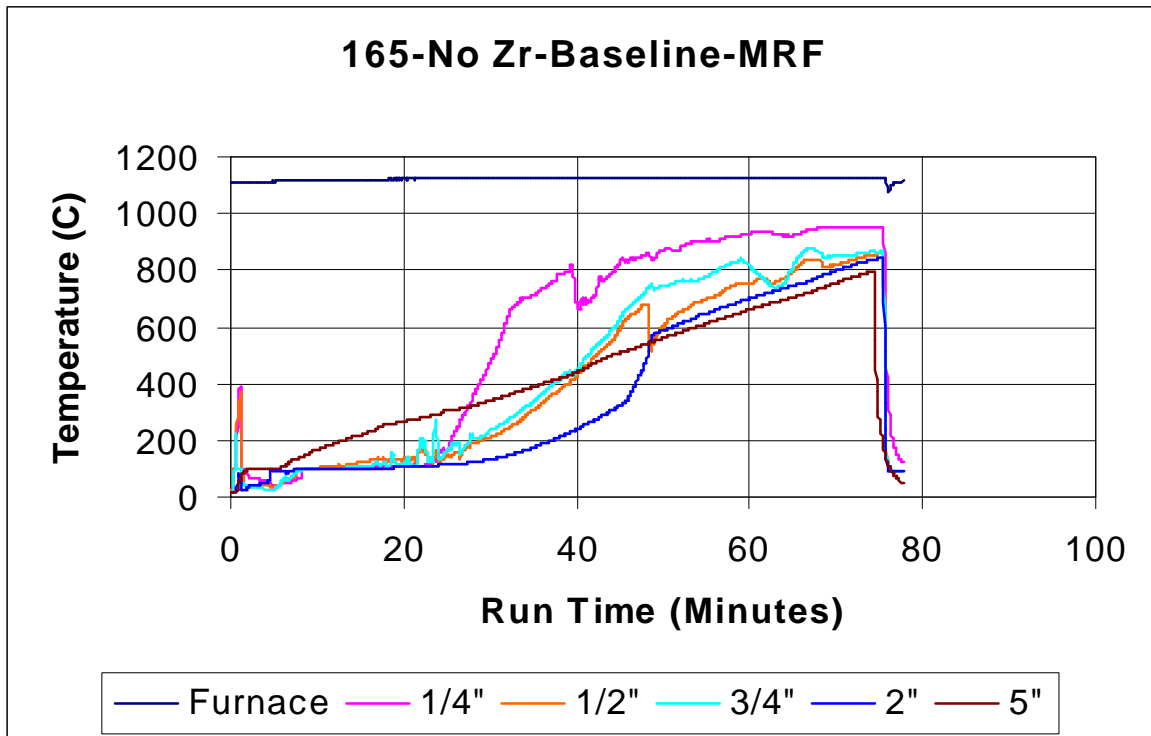


Figure B-29. 200-MB3-Underwashed-MRF

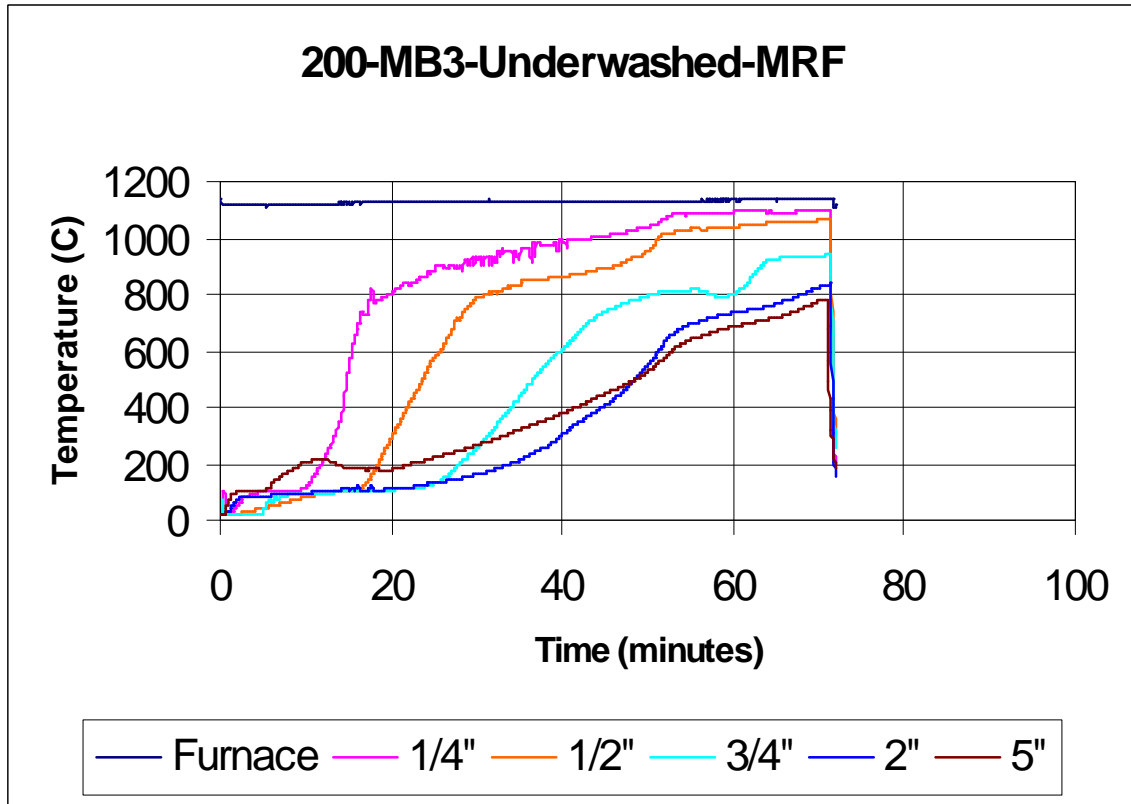


Figure B-30. 200-Overwashed-MRF

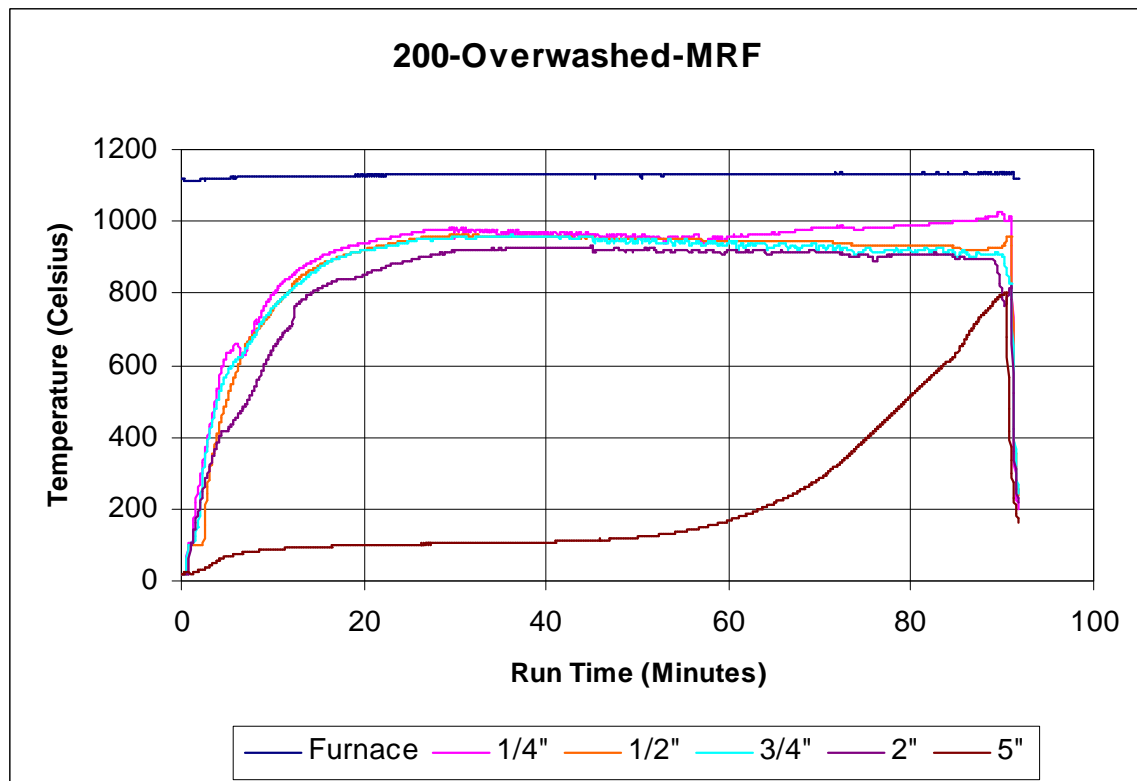


Figure B-31. 200-MB3-Formic Only-MRF

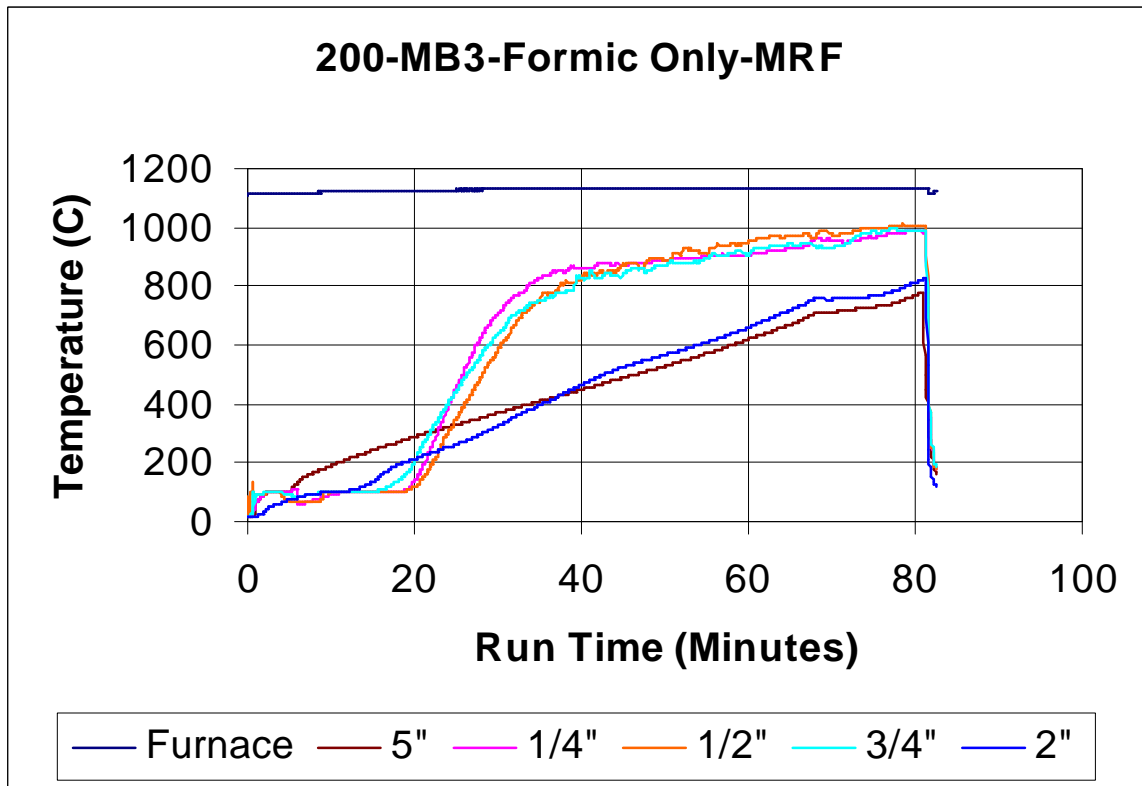


Figure B-32. D-MB3-MRF-2

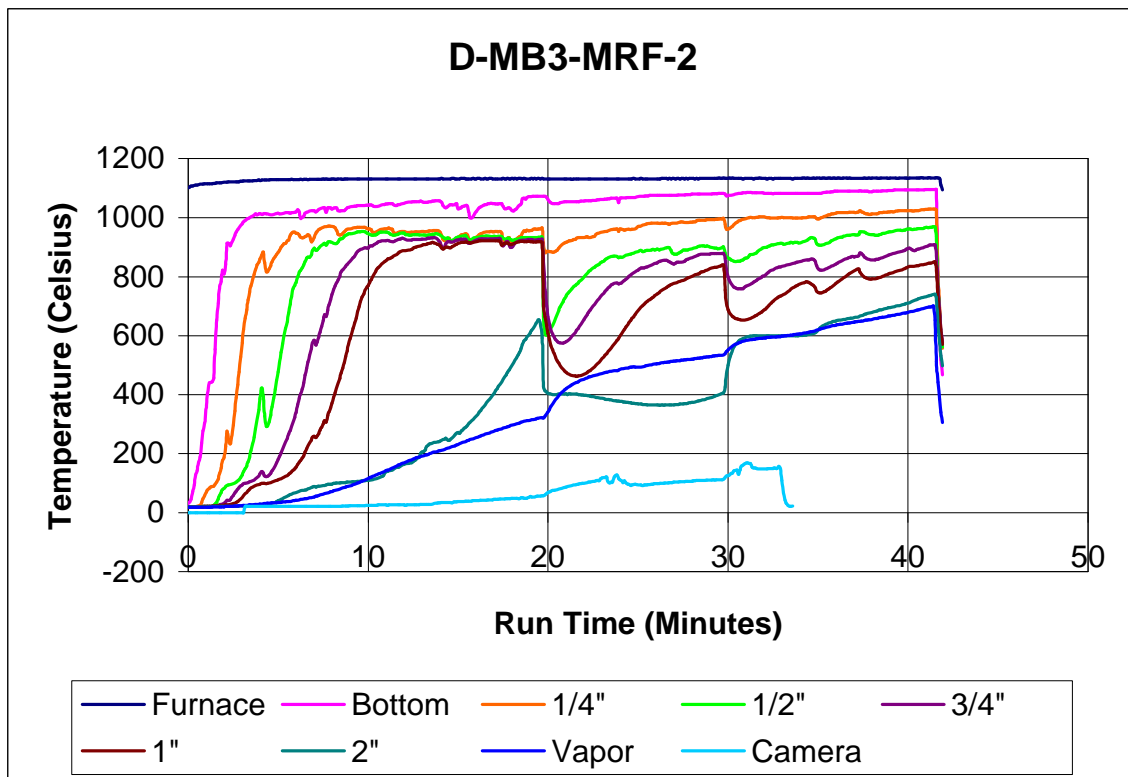


Figure B-35. BONE2-MB3-MRF-2

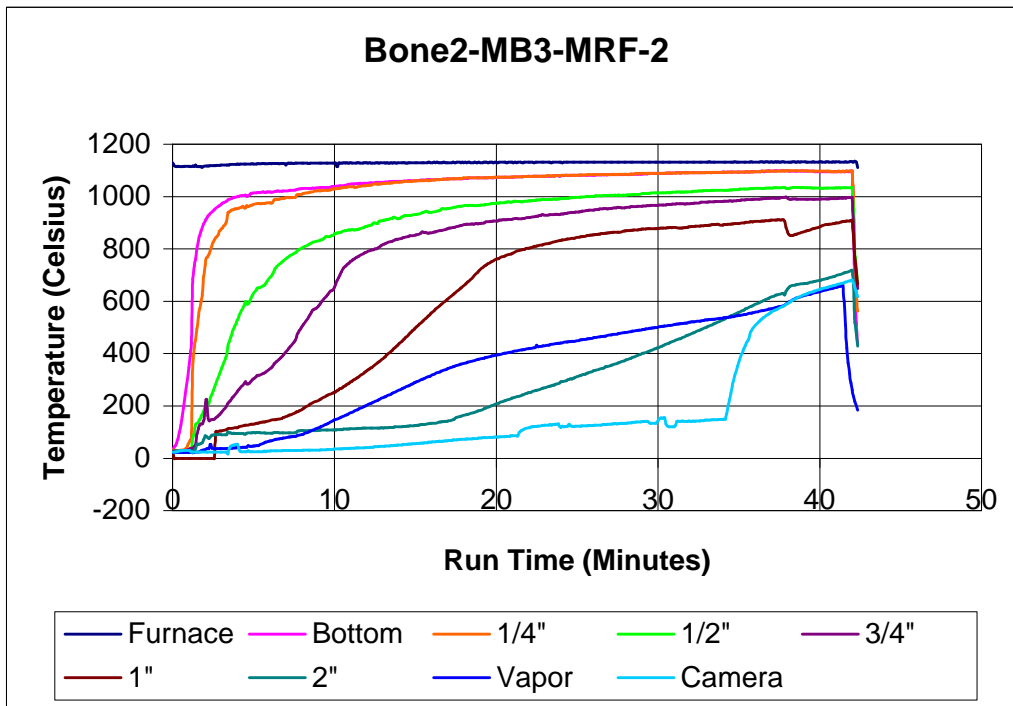


Figure B-36. 200-MB3-MRF-8

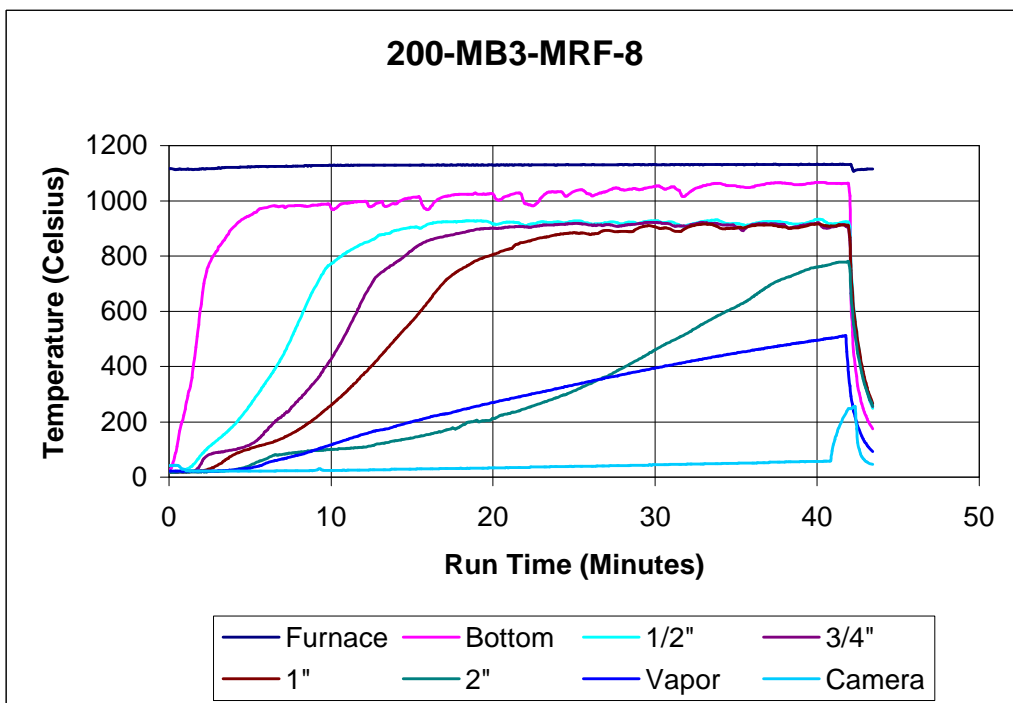


Figure B-41. 200-MB3-SUGAR-MRF

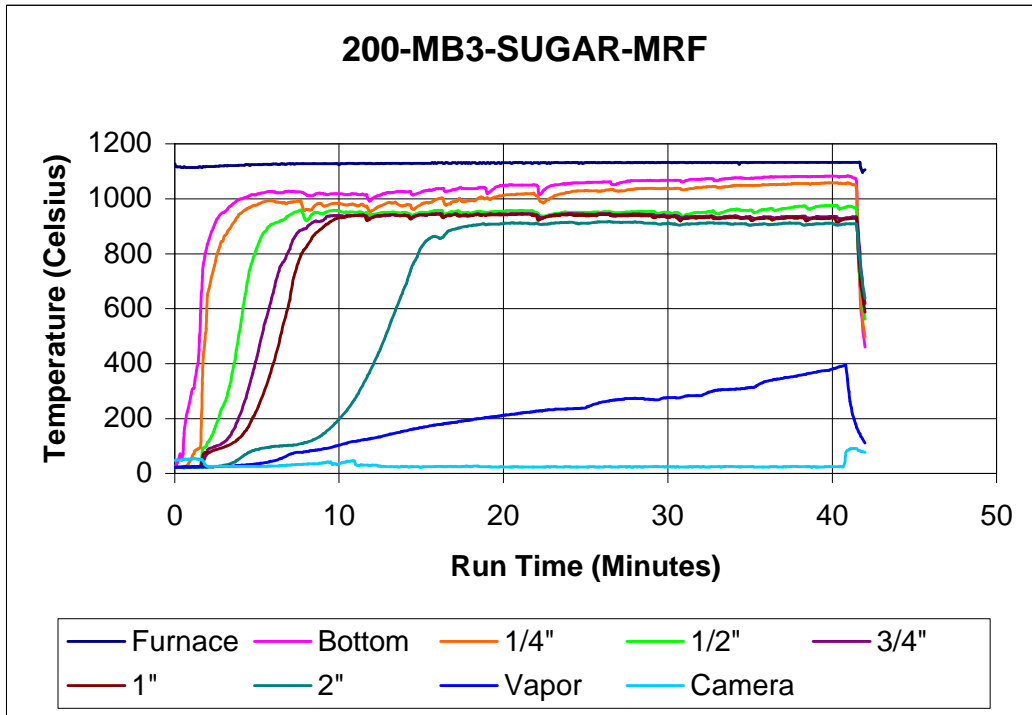
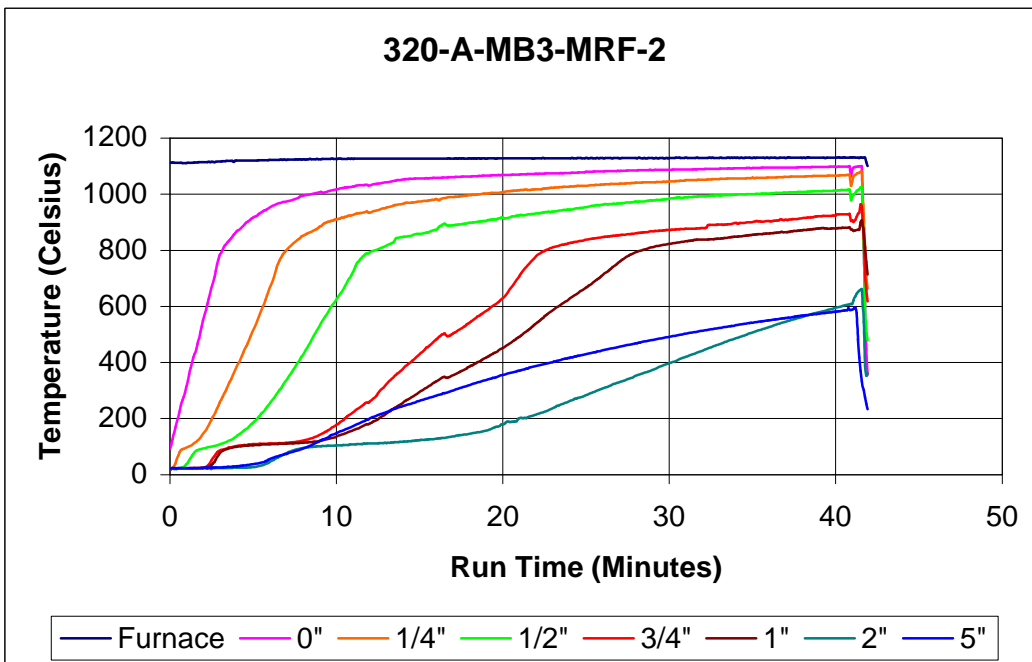


Figure B-42. 320A-MB3-MRF-2



Appendix C. Sectioned Beaker Photographs from Melt Rate Furnace Runs

Figure C-1. 165 (No Zr) – MB3 – MRF

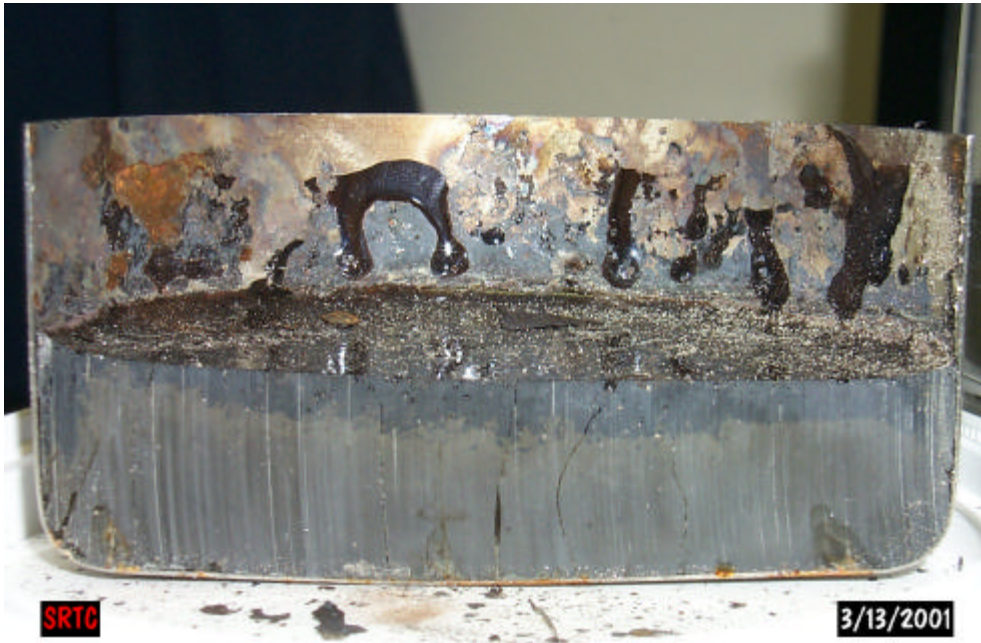


Figure C-2. 200-MB3-BASELINE-MRF-2



Figure C.3. 165-MB3-MRF-1

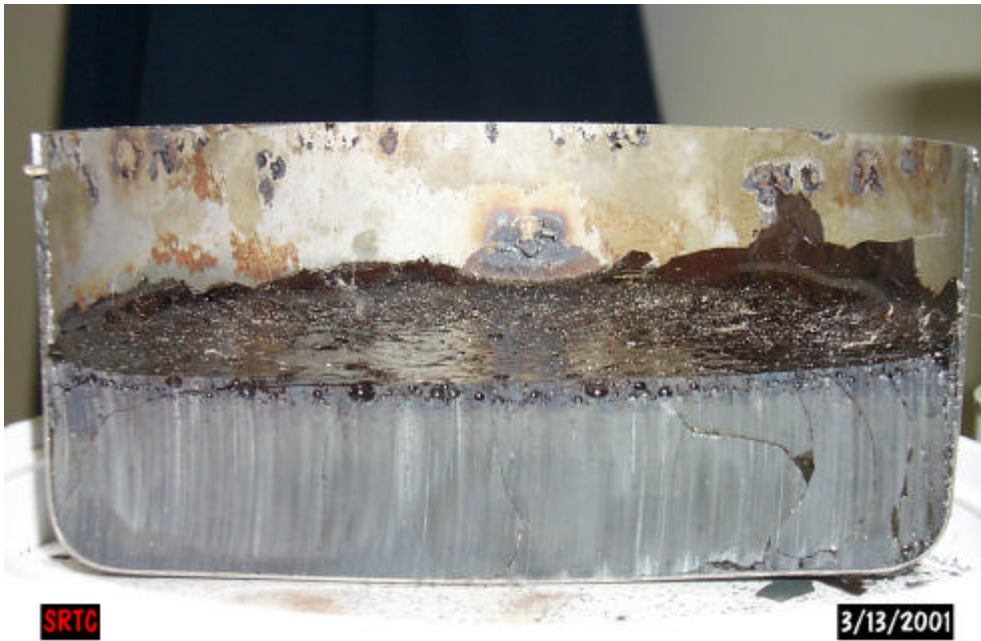


Figure C.4. 165-MB3-MRF-2

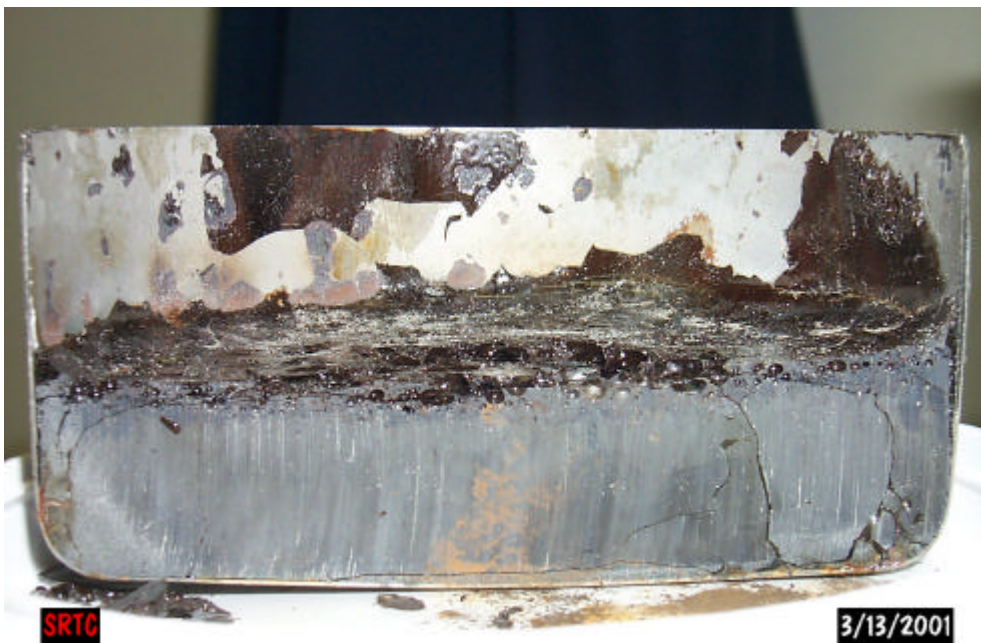


Figure C-5. 200-FORMIC ONLY-MRF

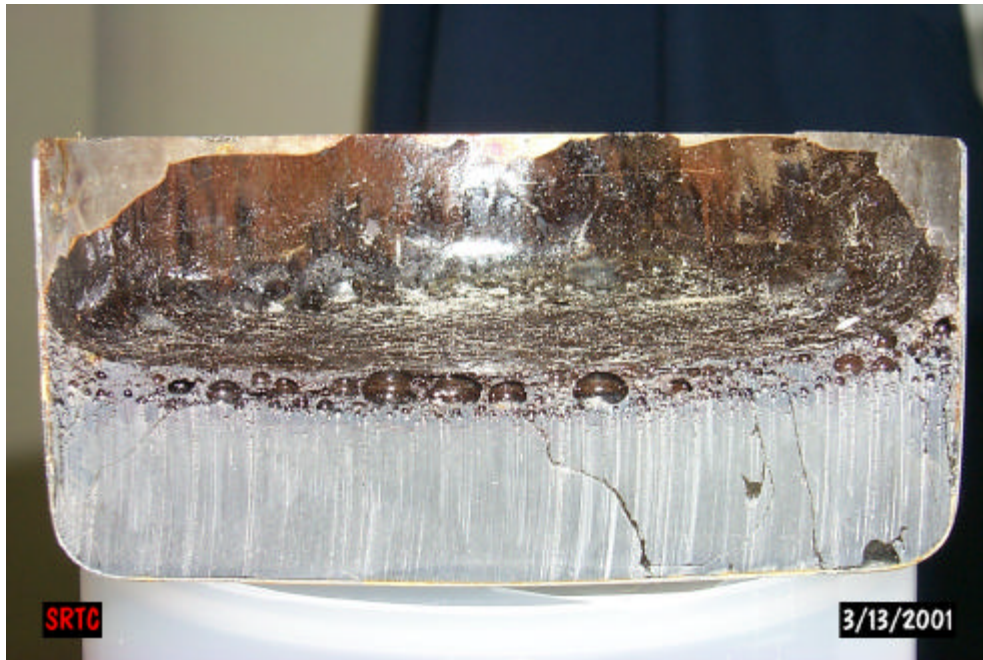


Figure C-6. 200-MB3-BASELINE-MRF-3

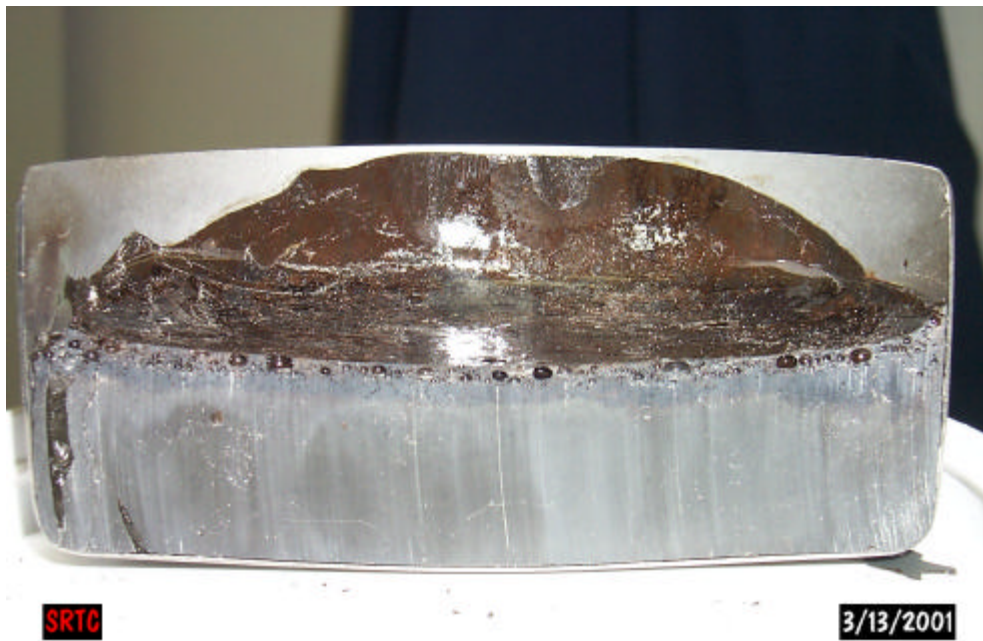


Figure C-7. 165-MB3-MRF-3



Figure C-8. 200-UNDERWASHED-MRF

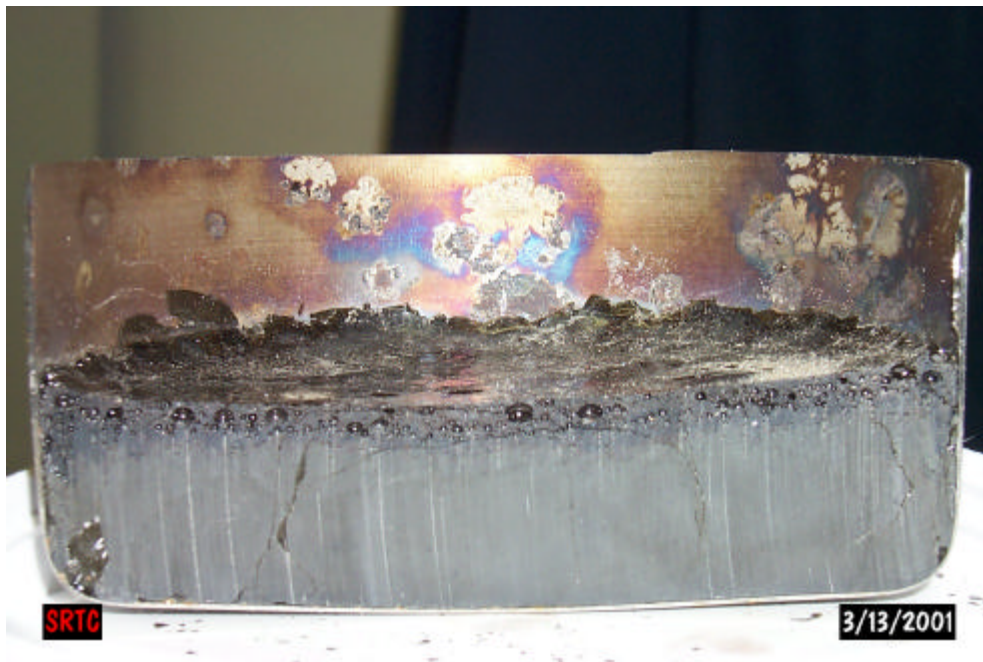


Figure C-9. 200-MB3-BASELINE-MRF-1

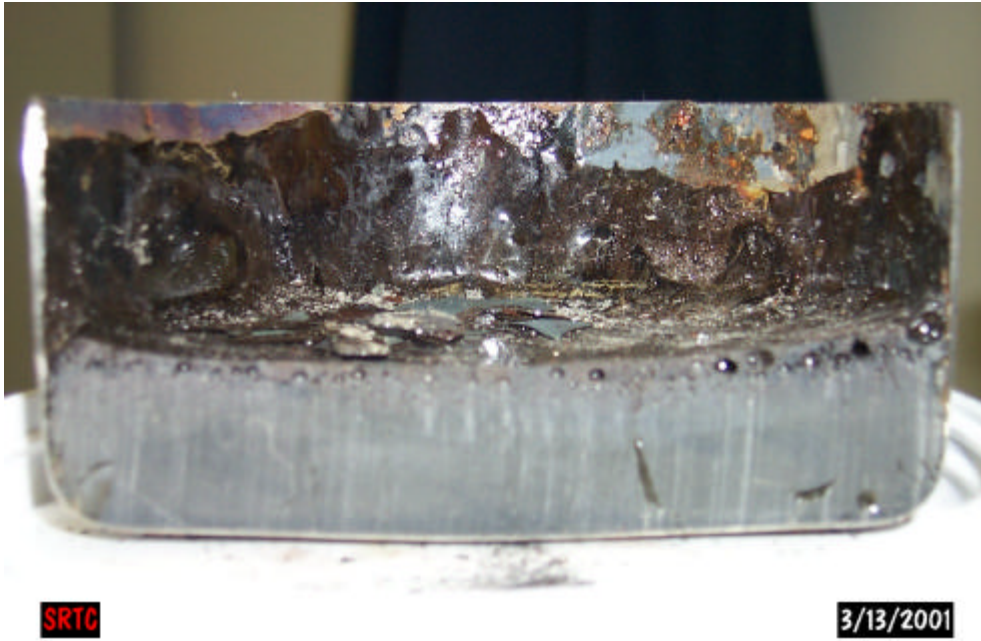


Figure C-10. 200-MB3-DRIED-MRF-1



Figure C-11. 200-MB3-DRIED-MRF-2



Figure C-12. 200-MB3-DRIED-MRF-3

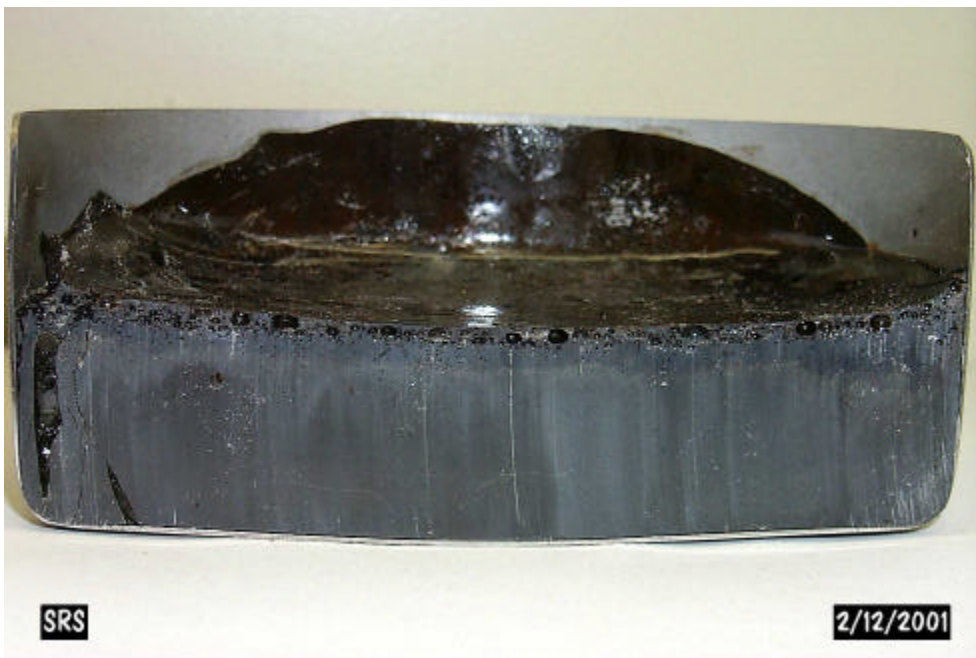


Figure C-13. 200-MB3-DRIED-4



Figure C-14. 200-MB3-DRIED-5



Figure C-15. 200-MB3-DRIED-6



Figure C-16. BONE-MB3-MRF



Figure C-17. KMA2-MB3-MRF



Figure C-18. BICK-MB3-MRF



Figure C-19. MIMI-MB3-MRF



Figure C-20. M-MB3-MRF



Figure C-21. G-MB3-MRF



Figure C-22. N-MB3-MRF



Figure C-23. D-MB3-MRF



Figure C-24. KMA2A-MB3-MRF



Figure C-25. C-MB3-MRF



Figure C-26. O-MB3-MRF



Figure C-27. BONE2-MB3-MRF



Figure C-28. 200-OVERWASHED-MRF

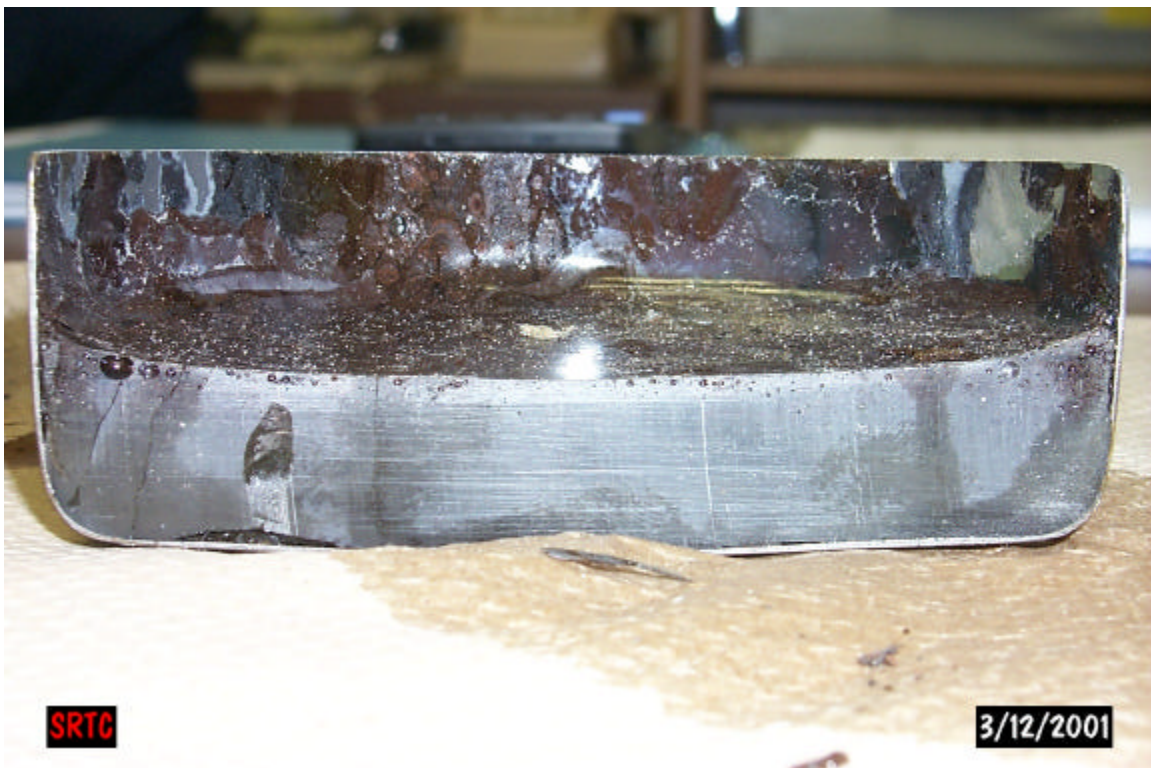


Figure C-29. 165-MB3-MRF-4



Figure C-30. 200-MB3-MRF-7



Figure C-31. 165(Silica Deficient)-MB3-MRF



Figure C-32. D-MB3-MRF-2

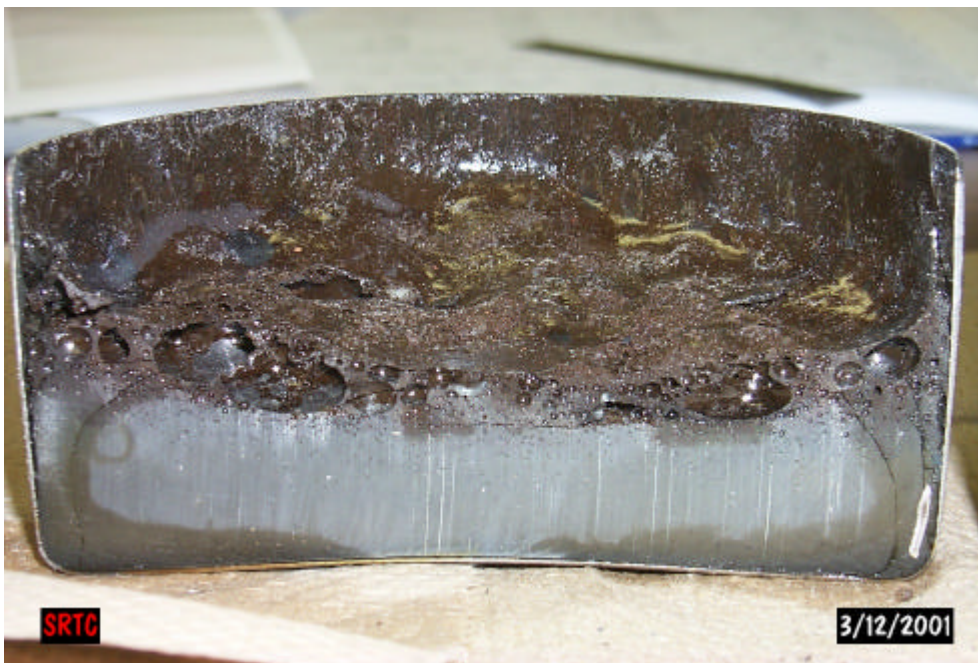


Figure C-33. 200-MB3-MRF-8



Figure C-34. 165-MB3-MRF-5

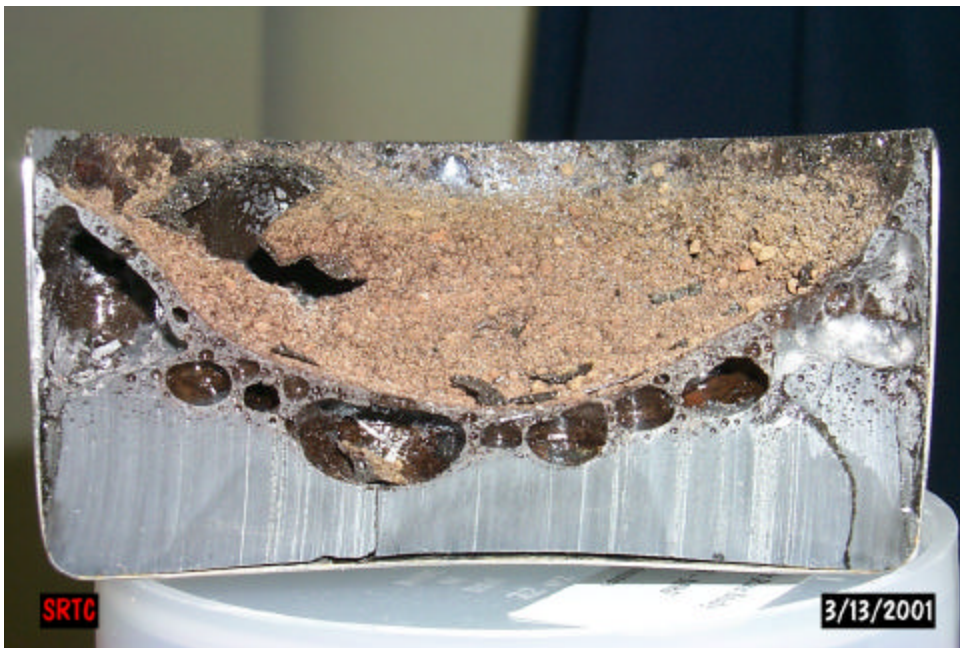


Figure C-35. M-MB3-MRF-2



Figure C-36. KMA2-MRF-2



Figure C-37. G-MB3-MRF-2



Figure C-38. BONE-MB3-MRF-2

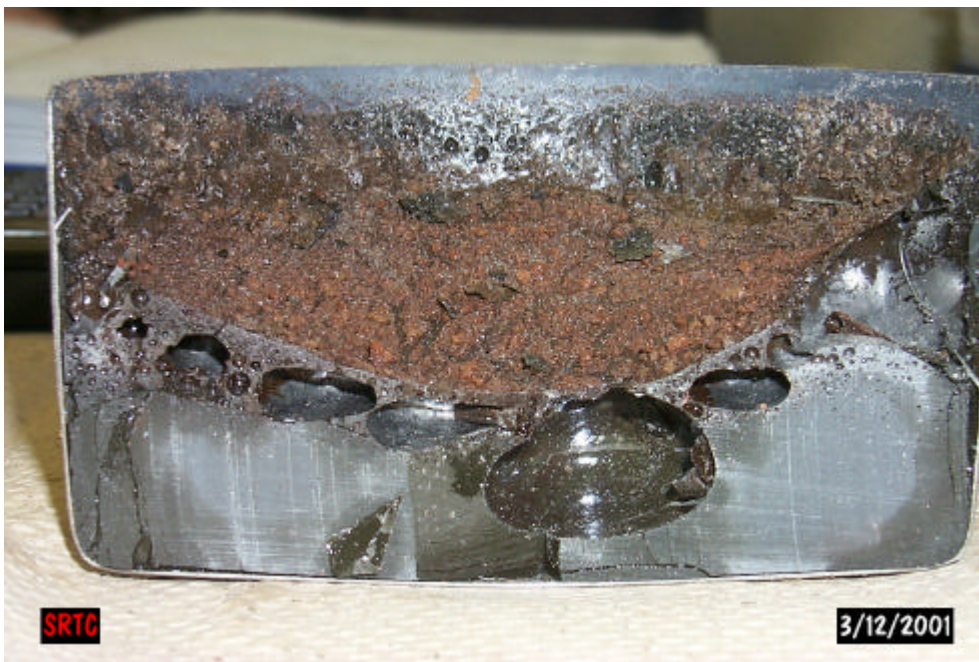


Figure C-39. BONE2-MB3-MRF-2



Figure C-40. 200-MB2-MRF

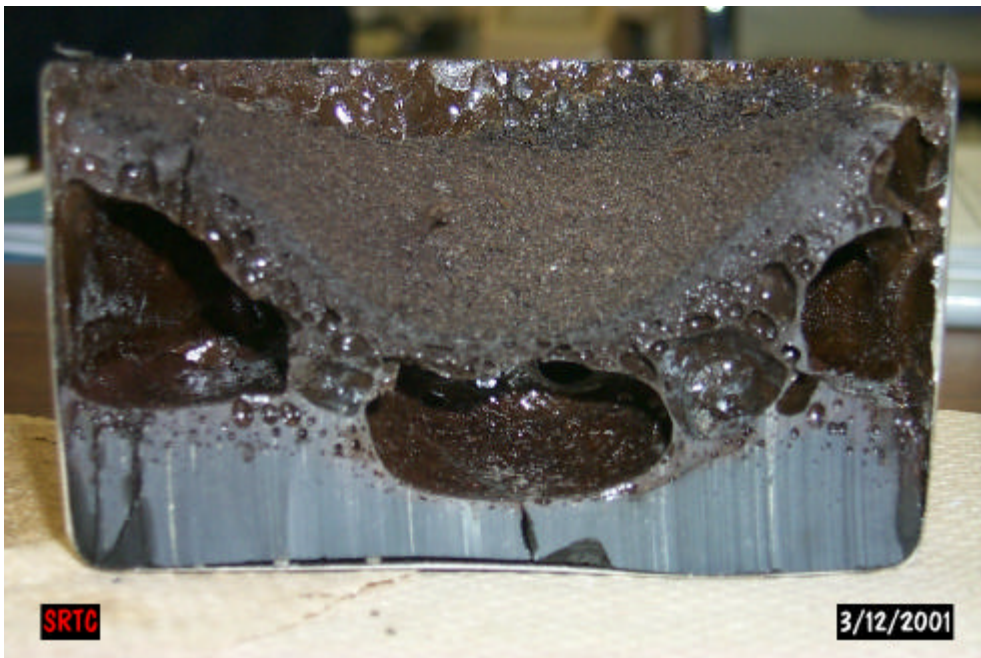


Figure C-41. 200-MB3-SUGAR-MRF



Figure C-42. 320A-MB3-MRF-2



Appendix D. Frit Compositions

Table D-1. Target Frit Compositions (Wt% Oxide)

Original Designation	165	165 (No Zr)	200	C	D	G	M	N
New Designation	165		200	303	304	307	313	314
Al₂O₃	0.0	0.0	0.0	2.29	2.29	0.0	0.0	0.0
B₂O₃	10.0	10.10	12.0	20.13	6.71	12.08	6.71	20.13
Li₂O	7.0	7.07	5.0	10.12	5.80	10.74	10.74	5.94
Na₂O	13.0	13.13	11.0	0.0	18.07	4.67	8.75	6.12
SiO₂	68.0	68.69	70.0	67.46	67.13	72.51	73.80	65.79
ZrO₂	1.0	0.0	0.0	0.0	0.0	0.0	0.0	2.01
MgO	1.0	1.01	2.00	0.0	0.0	0.0	0.0	0.0

Original Designation	O	BONE	MIMI	KMA2	KMA2A	BICK	BONE2	BONE3
New Designation	315	320	322	323	324	325	326	320-A
Al₂O₃	0.0	0.0	0.0	0.0	0.0	0.00	0.0	0.00
B₂O₃	20.13	8.00	8.00	15.00	15.00	8.55	8.00	8.00
Li₂O	10.03	8.00	5.00	5.19	8.28	7.55	8.00	11.00
Na₂O	0.0	12.00	10.00	8.28	5.19	9.10	11.00	9.00
SiO₂	69.84	72.00	77.00	71.53	71.53	72.80	72.00	72.00
ZrO₂	0.0	0.0	0.0	0.0	0.0	0.50	0.0	0.00
MgO	0.0	0.0	0.0	0.0	0.0	1.50	1.00	0.00

Table D-2. Measured Frit Compositions from Final Batch (Wt% oxide)

Original Designation	165	200	D	G	M	BONE	BONE2	BONE3	KMA2
New Designation	165	200	304	307	313	320	326	320-A	323
Al₂O₃	0.446	0.720	1.84	0.215	0.221	0.206	0.212	0.20	0.210
B₂O₃	9.76	11.2	6.96	12.4	6.79	8.02	8.28	8.08	14.9
Li₂O	6.58	4.34	5.65	10.5	10.4	7.63	7.80	11.5	4.88
Na₂O	12.8	11.6	17.2	4.84	8.68	11.8	10.2	8.83	8.29
SiO₂	67.8	68.3	66.6	72.8	72.8	70.8	72.8	73.0	70.8
ZrO₂	0.922	0.087	0.005	0.0	0.0	0.0	0.011	0.00	0.002
Fe₂O₃	0.098	0.098	0.063	0.063	0.055	0.074	0.116	0.686	0.057
Cr₂O₃	0.021	0.012	0.014	0.012	0.009	0.010	0.010	0.174	0.014
NiO	0.019	0.020	0.016	0.015	0.0	0.0	0.016	0.062	0.014
MgO	0.004	1.91	0.0	0.004	0.003	0.004	0.865	0.00	0.002

Appendix E. Photographs of Unsectioned Beakers

Figure E-1. Pre-fired Appearance of Melter Feed during Initial Tests



Figure E-2. Prefired Appearance of Dried Melter Feed (200-MB3-DRIED-MRF-1,2,3)



Figure E-3. Fired Appearance of Dried Melter Feed (200-MB3-DRIED-MRF-4)

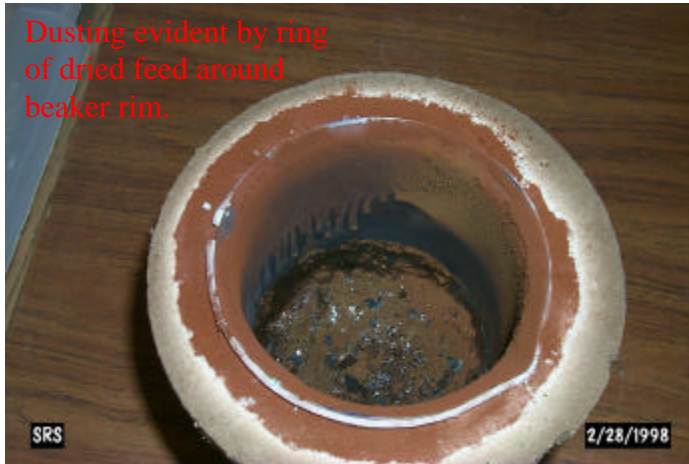


Figure E-4. Fired Appearance of Runs with Central Bubble (KMA2A-MB3-MRF)



Large central bubble. Note asymmetrical distribution of dust.

Figure E-5. Fired Appearance of Runs without Central Bubble (G-MB3-MRF)



Appendix F. Isotherm Charts from Selected Melt Rate Furnace Runs

Figure F-1. Isotherm Plot for 165-MB3-MRF-4

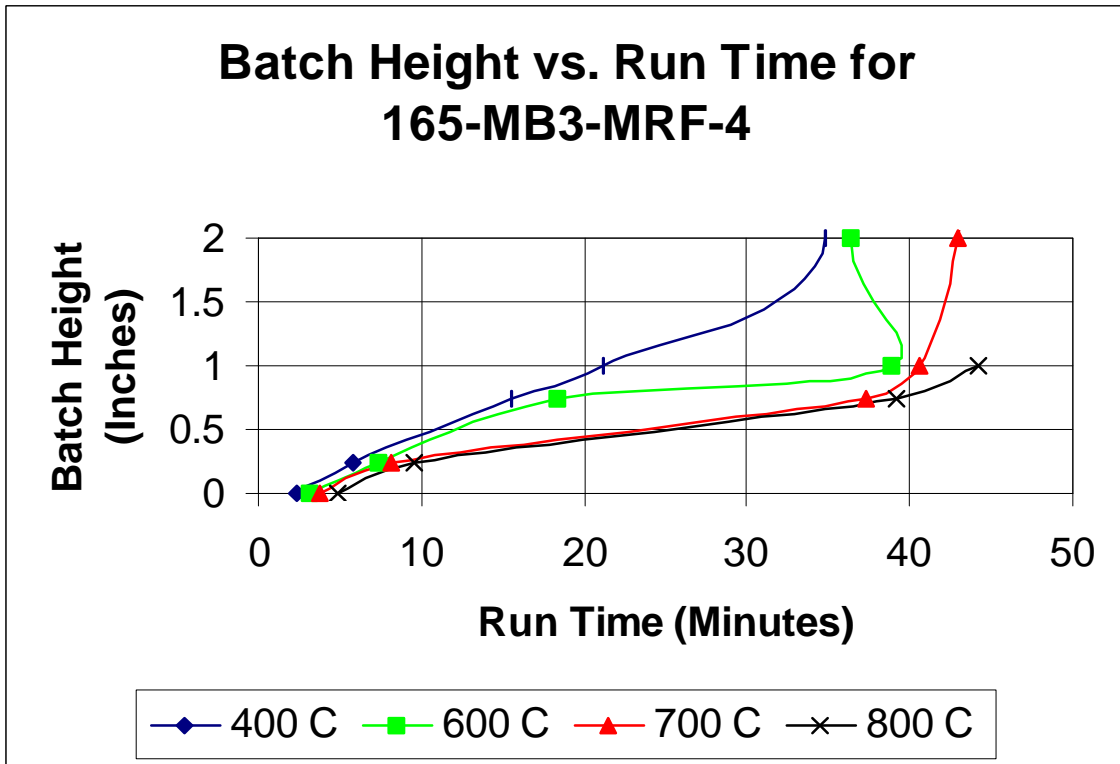


Figure F-2. Isotherm Plot for 200-MB3-MRF-7

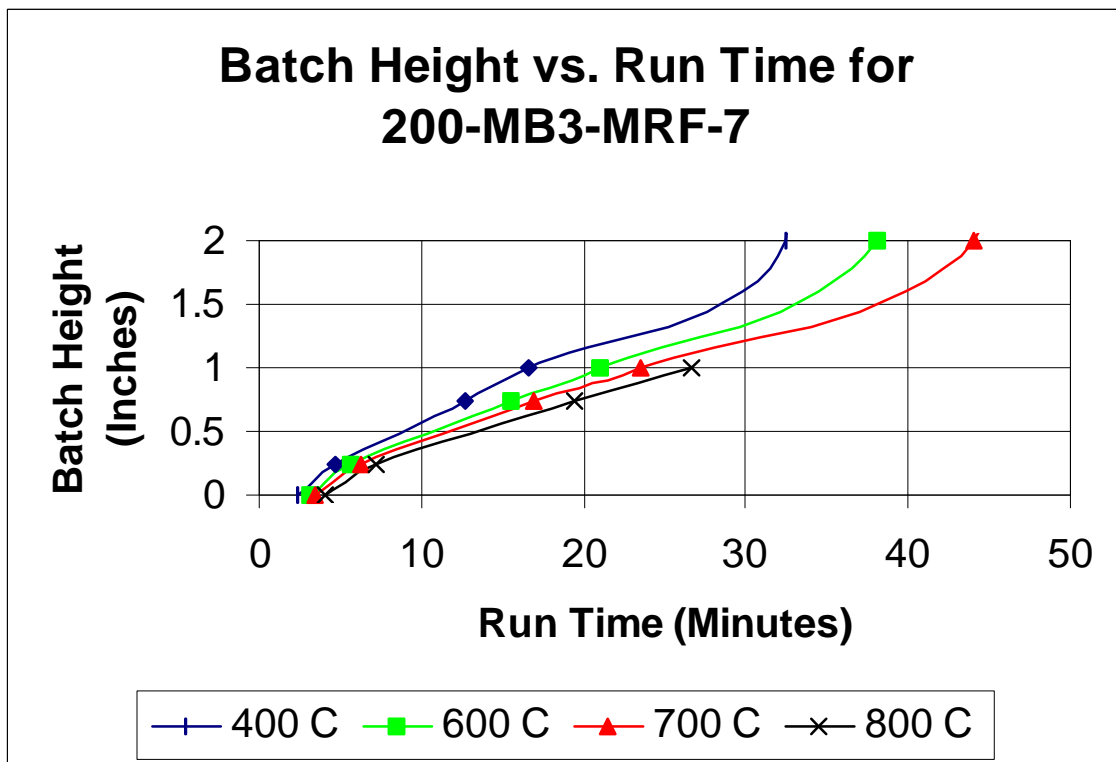


Figure F-3. Isotherm Plot for 165 (Si Def)-MB3-MRF

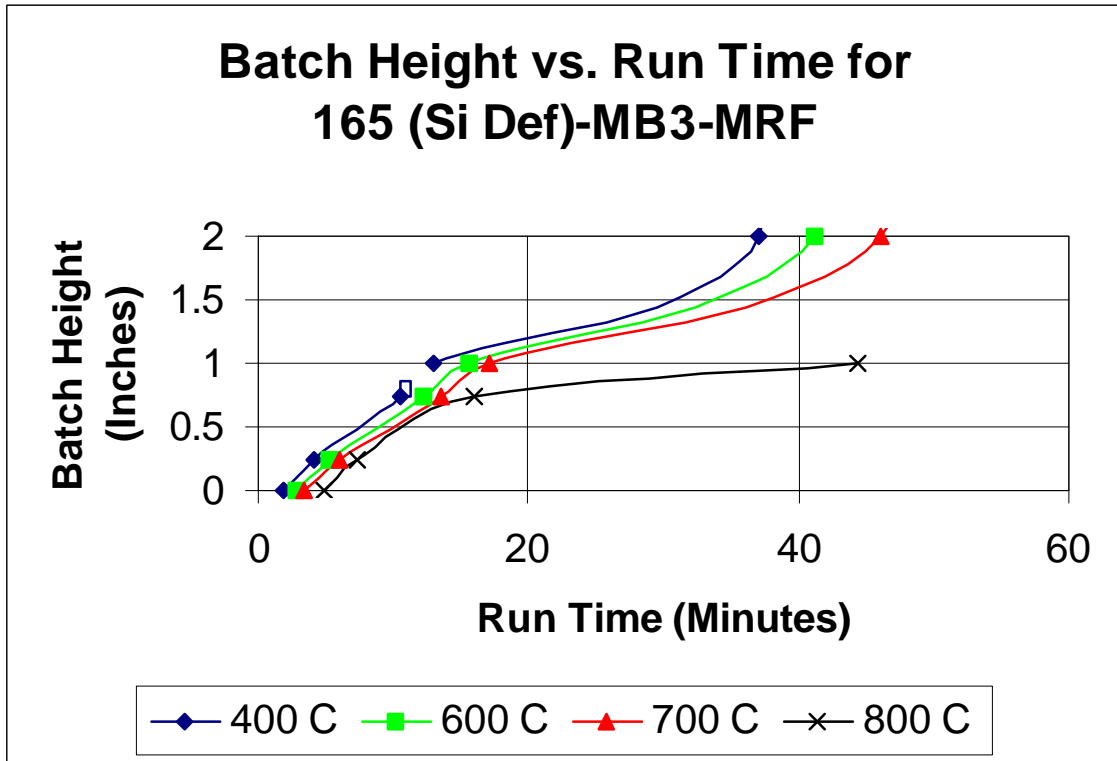


Figure F-4. Isotherm Plot for 200-MB3-MRF-1

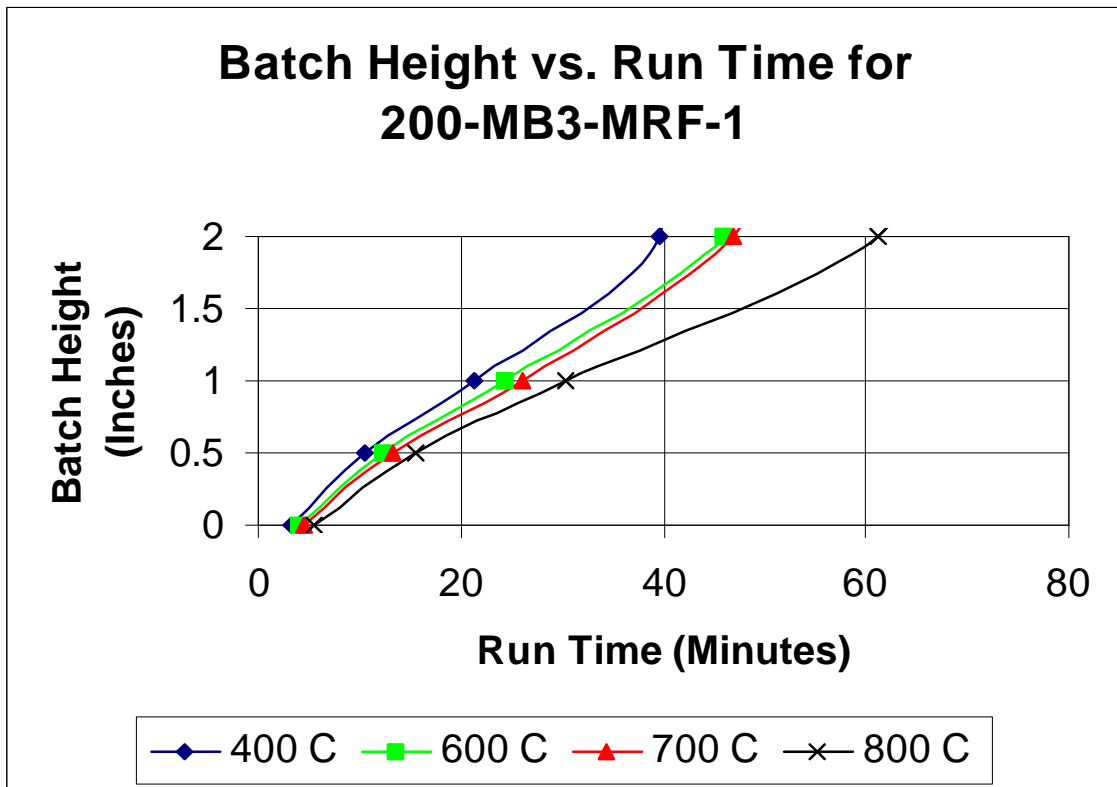


Figure F-5. Isotherm Plot for 200-MB3-Dried-MRF-2

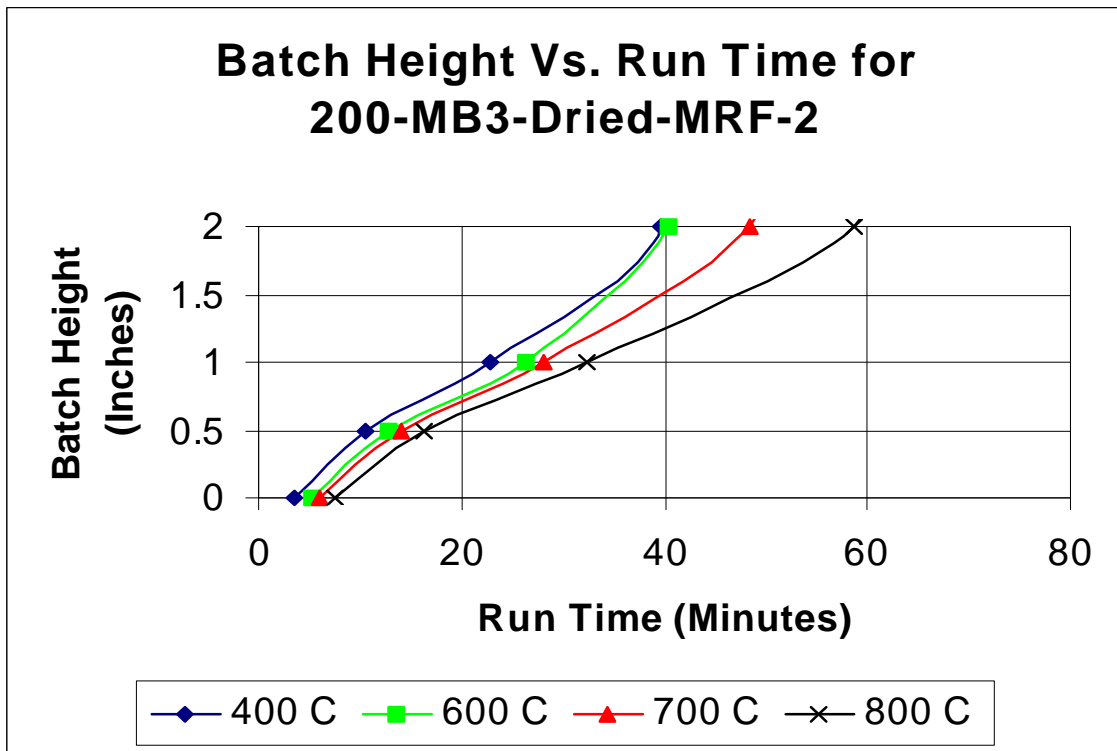


Figure F-6. Isotherm Plot for 200-MB3-Dried-MRF-3

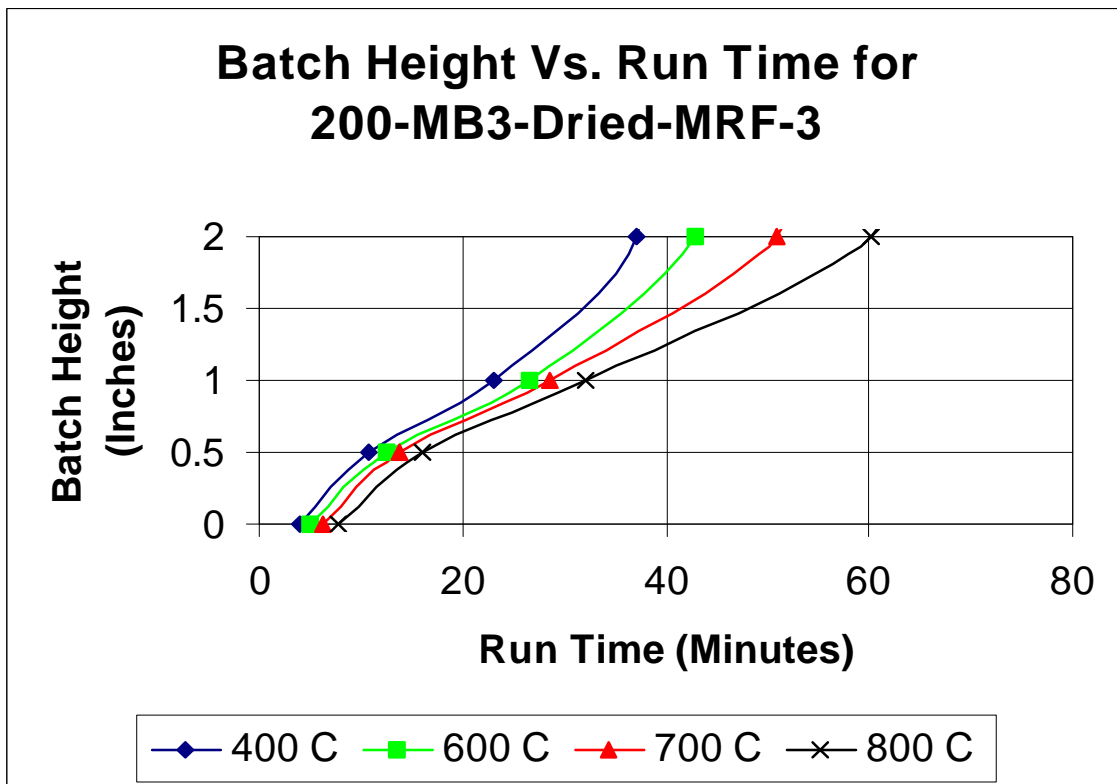


Figure F-7. Isotherm Plot for 200-MB3-Dried-MRF-4

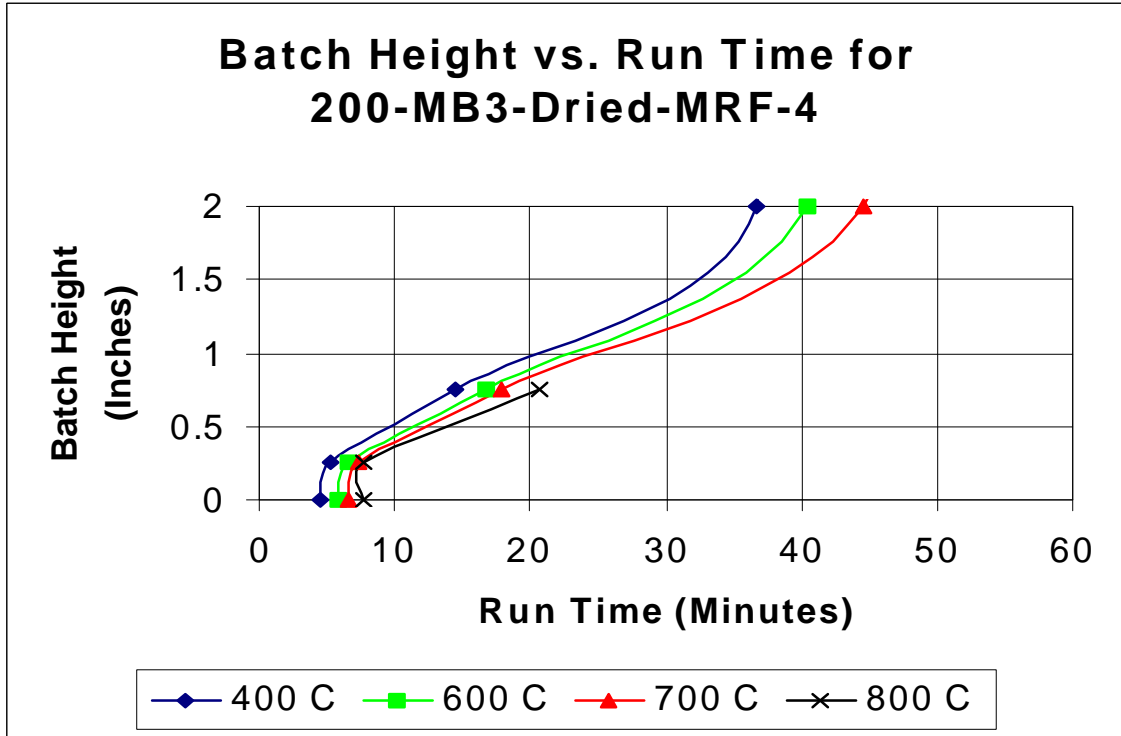


Figure F-8. Isotherm Plot for 200-MB3-MRF-5

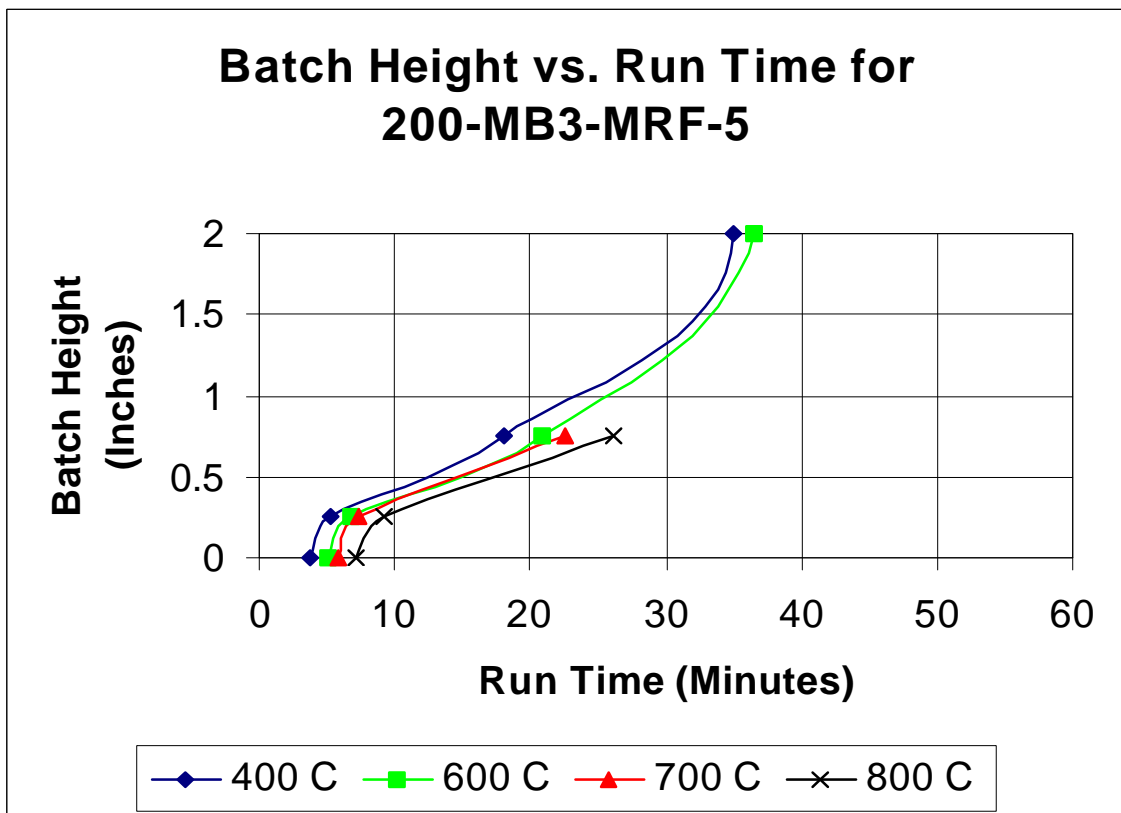


Figure F-9. Isotherm Plot for 200-MB3-MRF-6

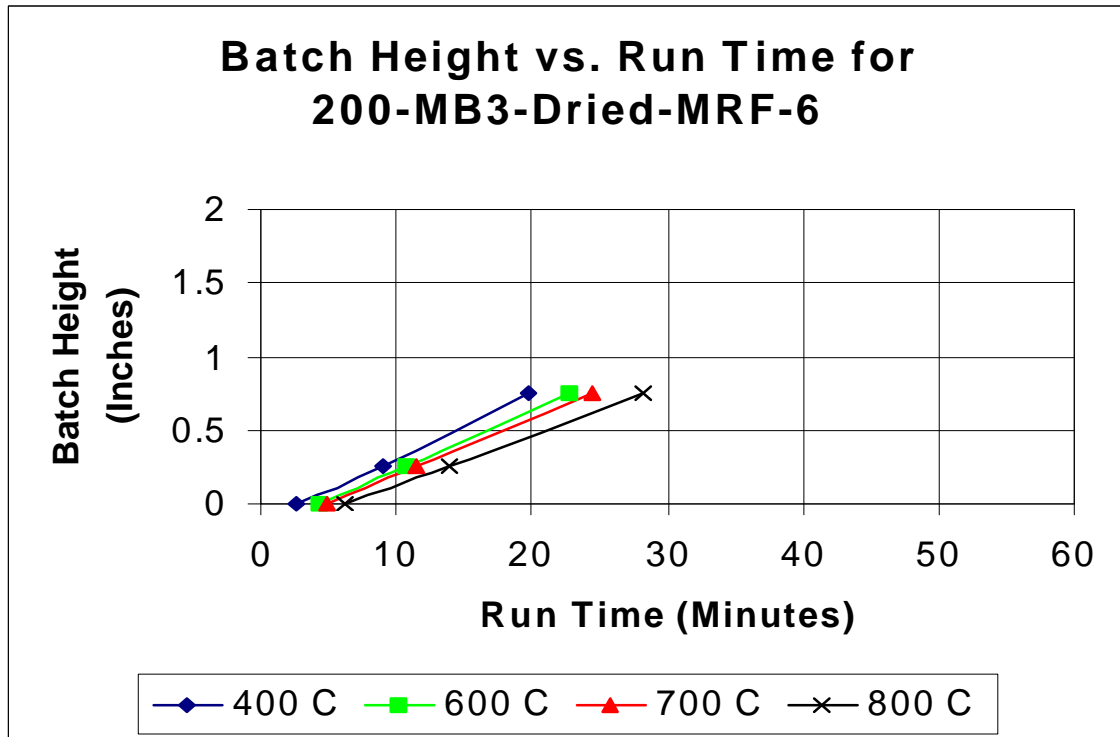


Figure F-10. Isotherm Plot for Bone-MB3-MRF

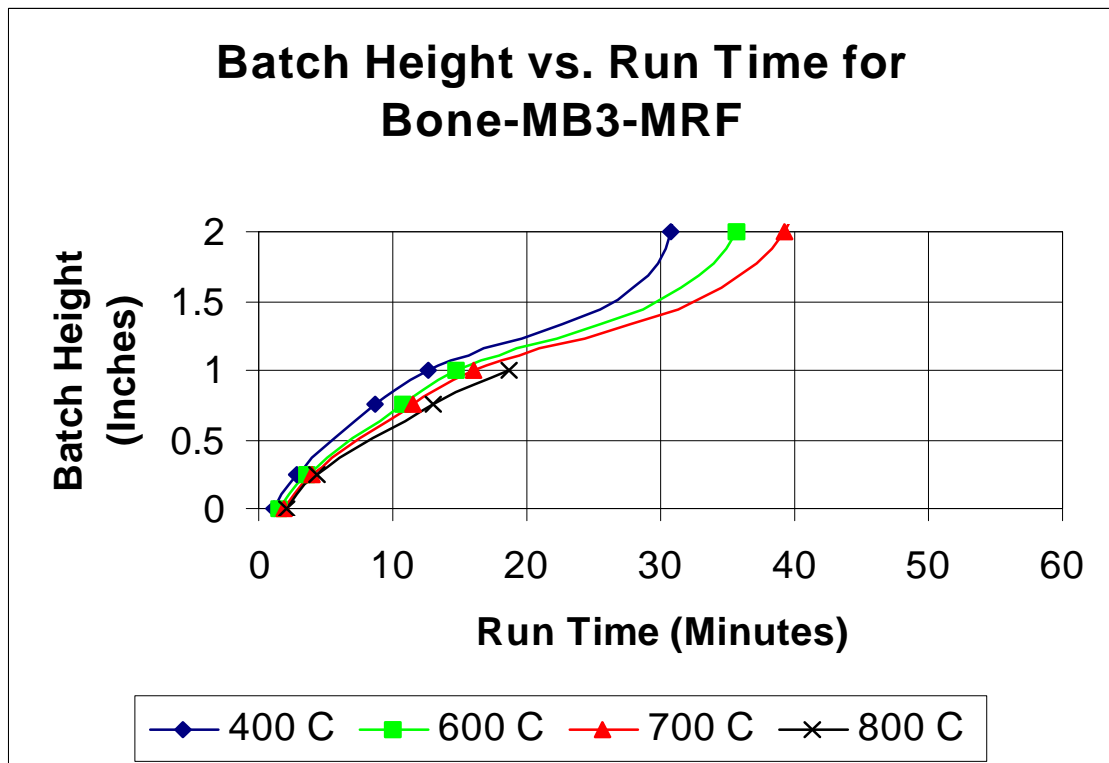


Figure F-11. Isotherm Plot for KMA 2-MB3-MRF

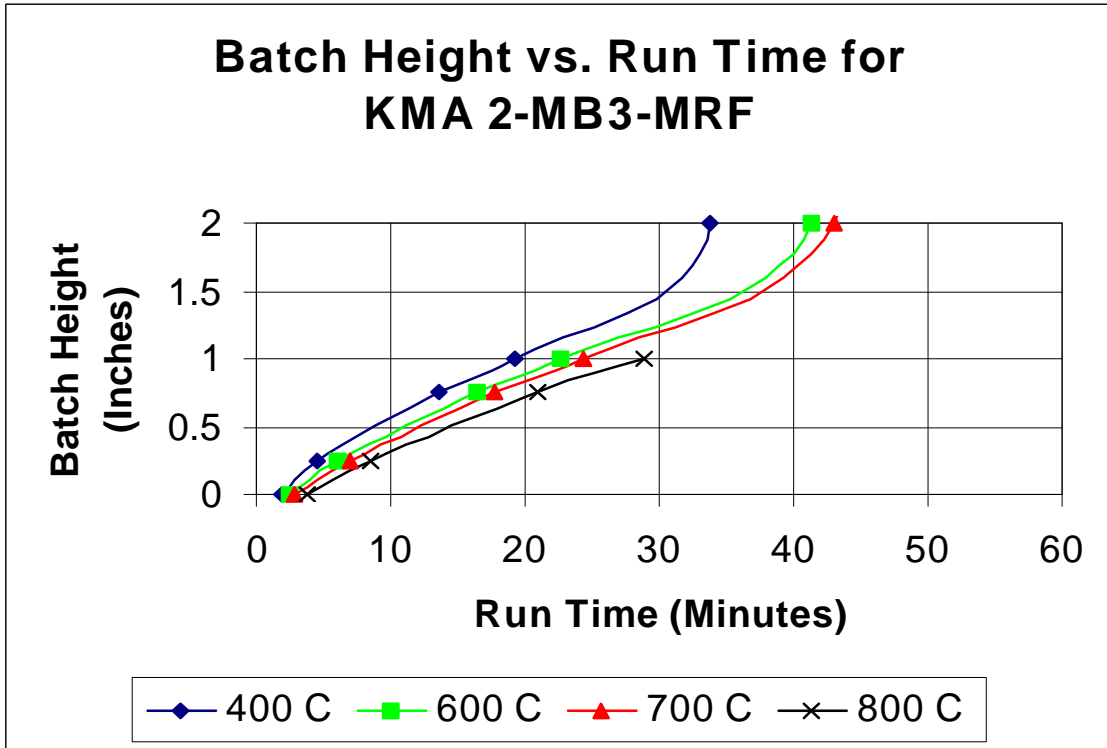


Figure F-12. Isotherm Plot for Bick-MB3-MRF

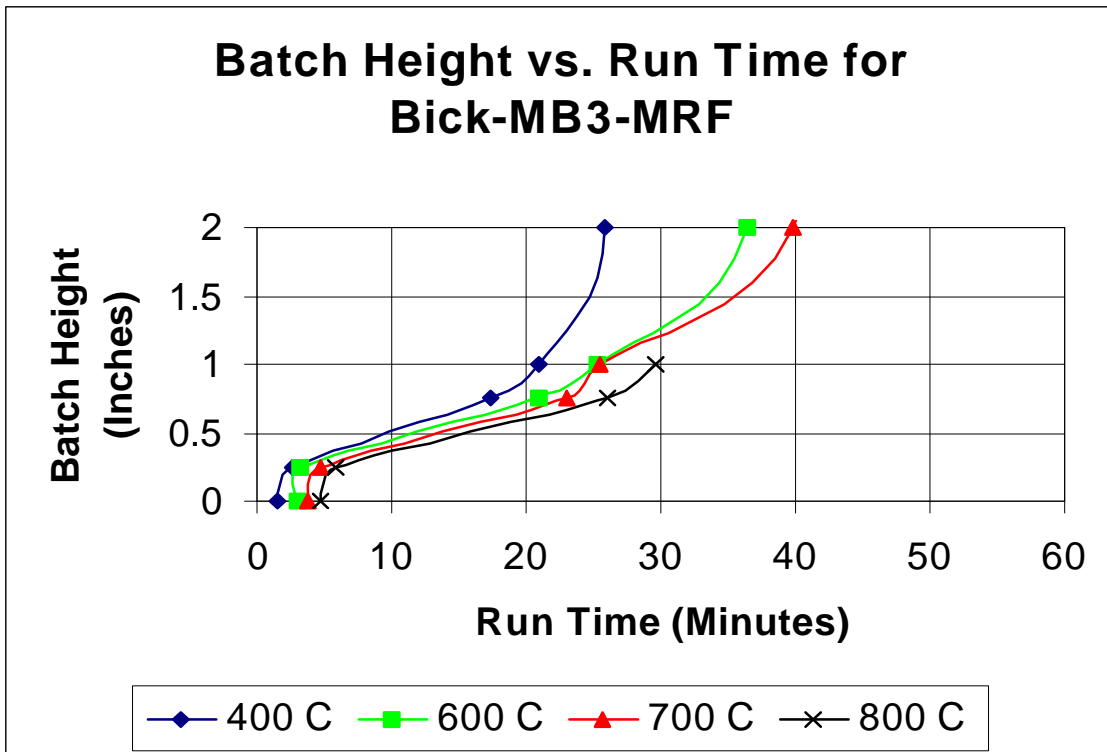


Figure F-13. Isotherm Plot for Mimi-MB3-MRF

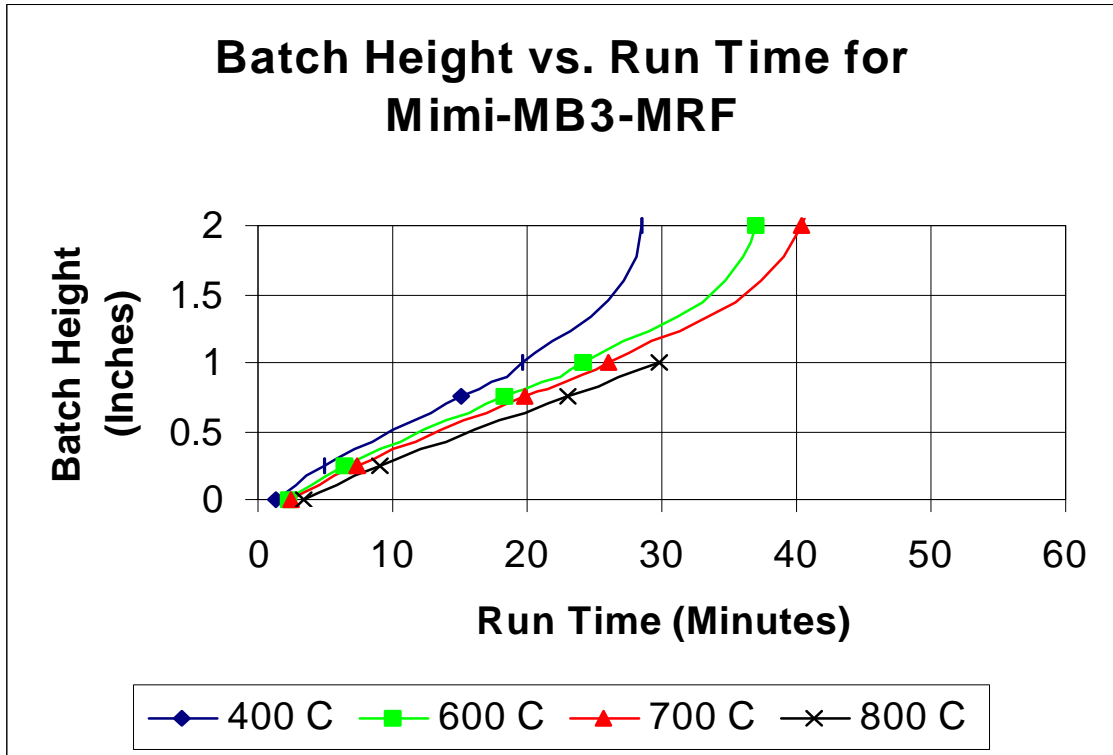


Figure F-14. Isotherm Plot for KMA 2A-MB3-MRF

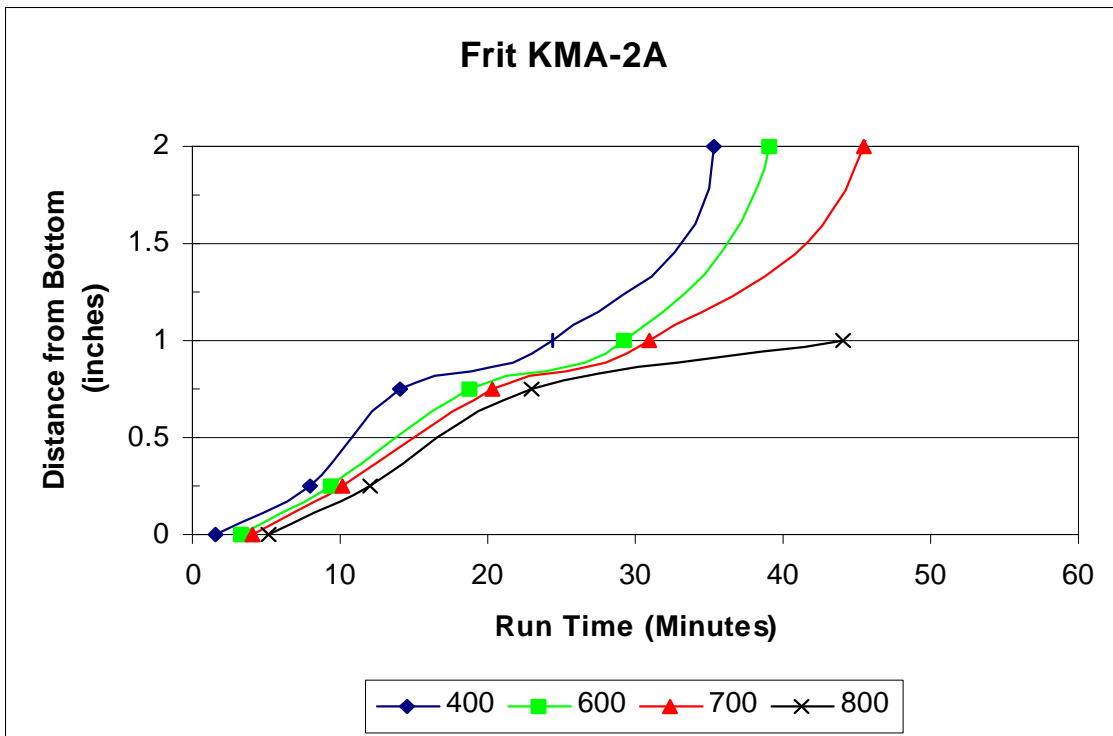


Figure F-15. Isotherm Plot for C-MB3-MRF

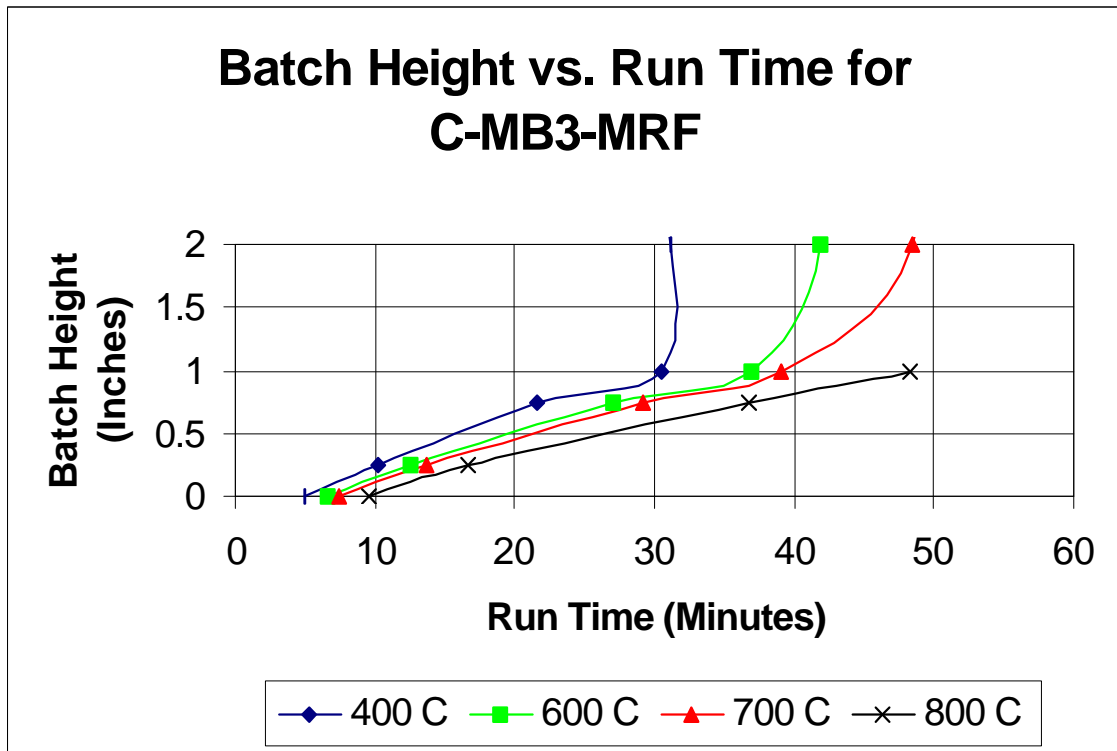


Figure F-16. Isotherm Plot for O-MB3-MRF

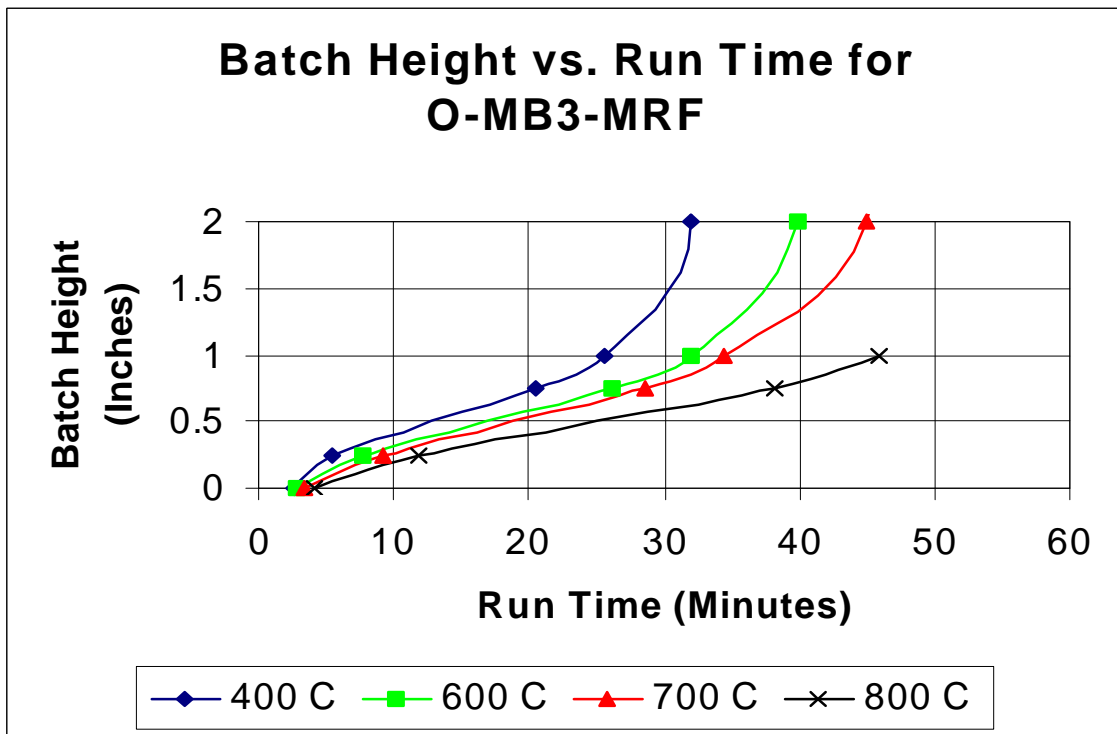


Figure F-17. Isotherm Plot for M-MB3-MRF

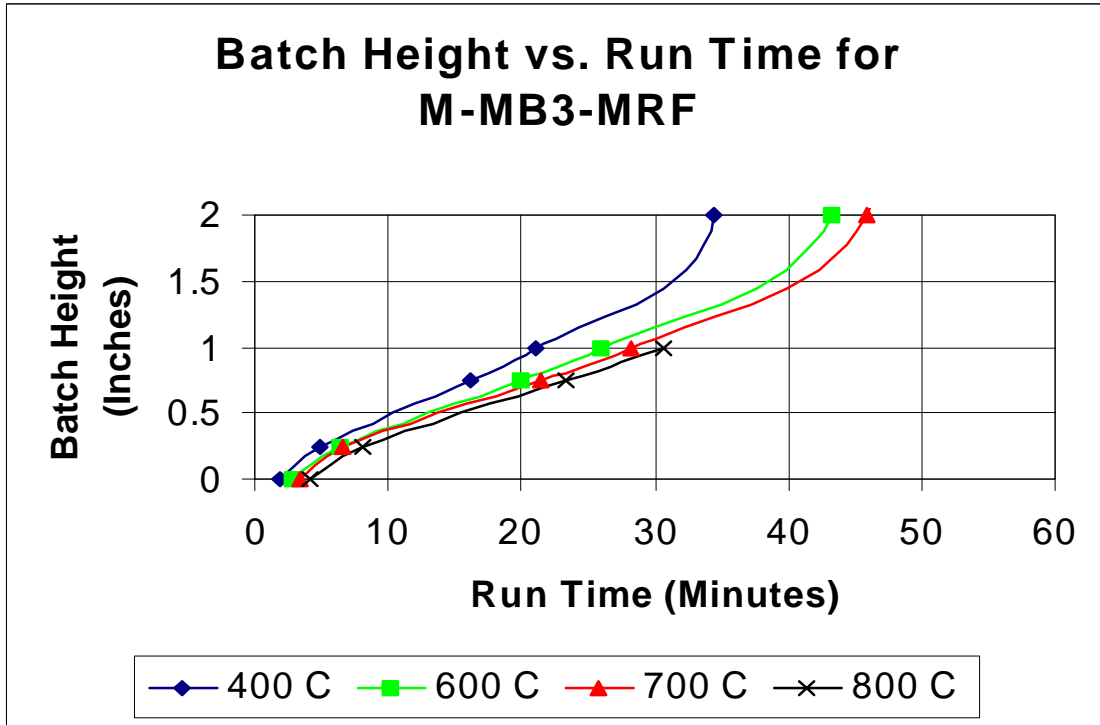


Figure F-18. Isotherm Plot for G-MB3-MRF

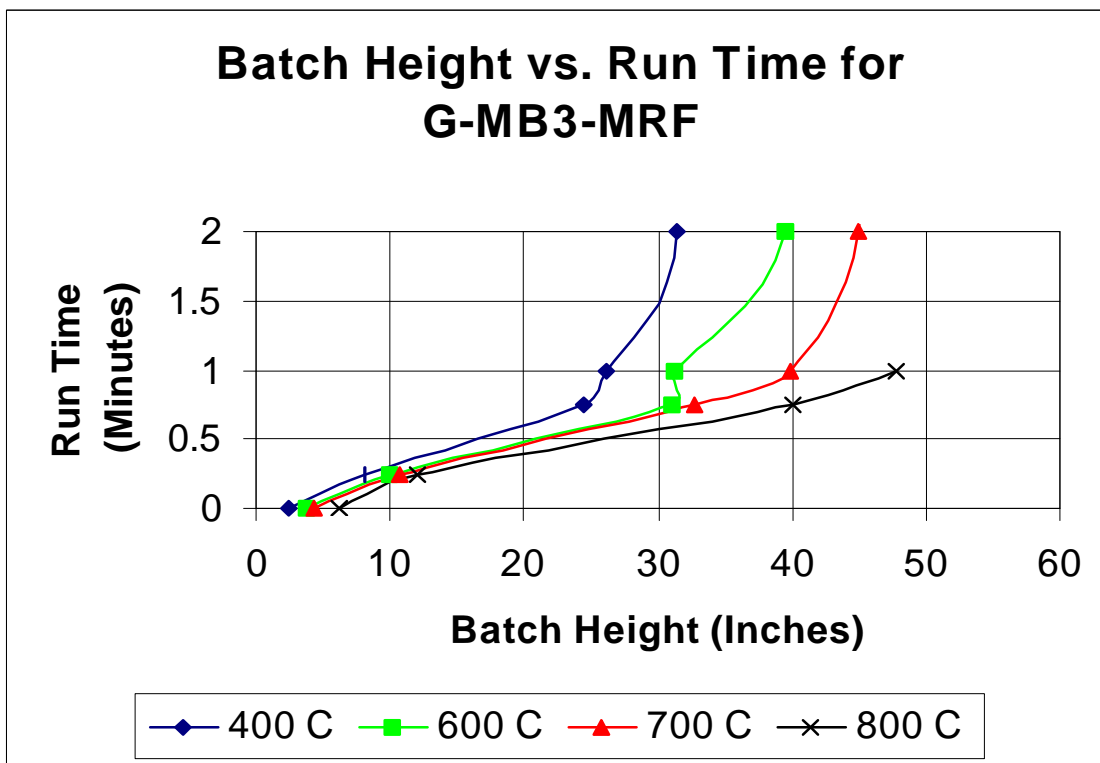


Figure F-19. Isotherm Plot for N-MB3-MRF

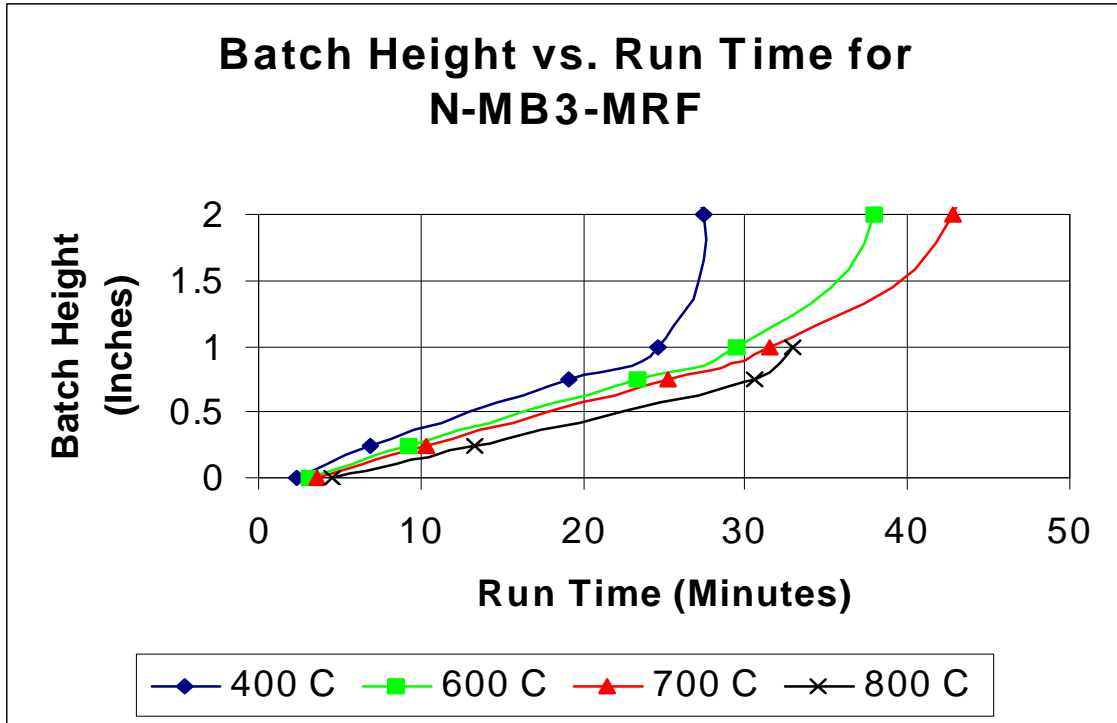


Figure F-20. Isotherm Plot for D-MB3-MRF

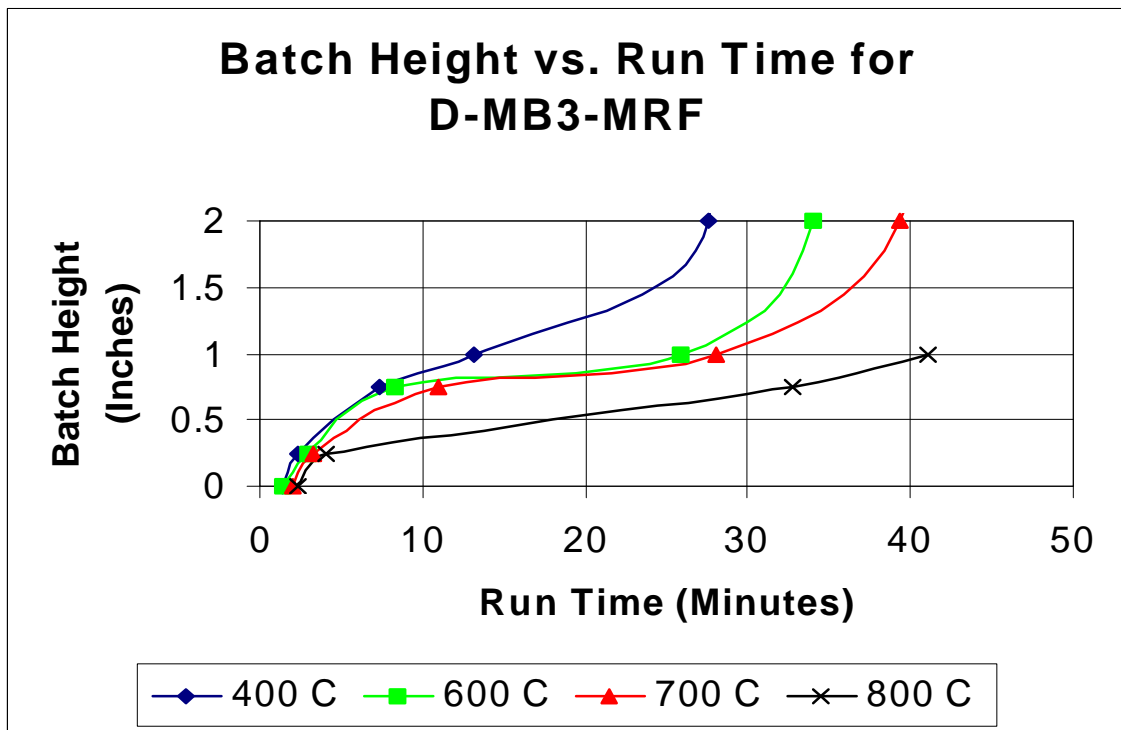


Figure F-21. Isotherm Plot for D-MB3-MRF-2

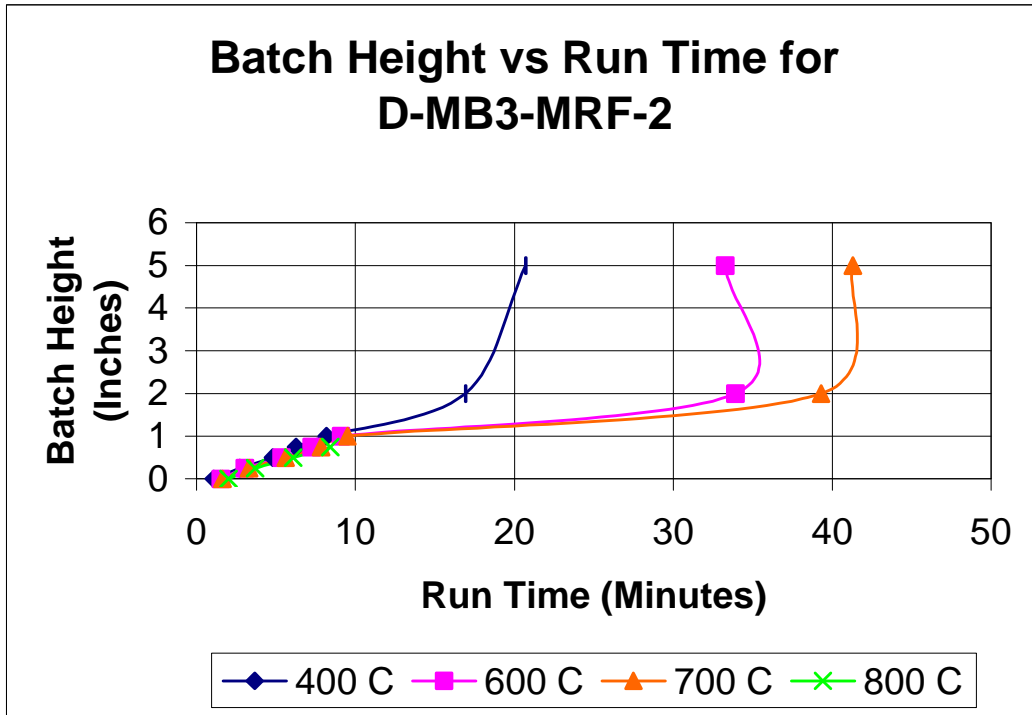


Figure F-22. Isotherm Plot for G-MB3-MRF-2

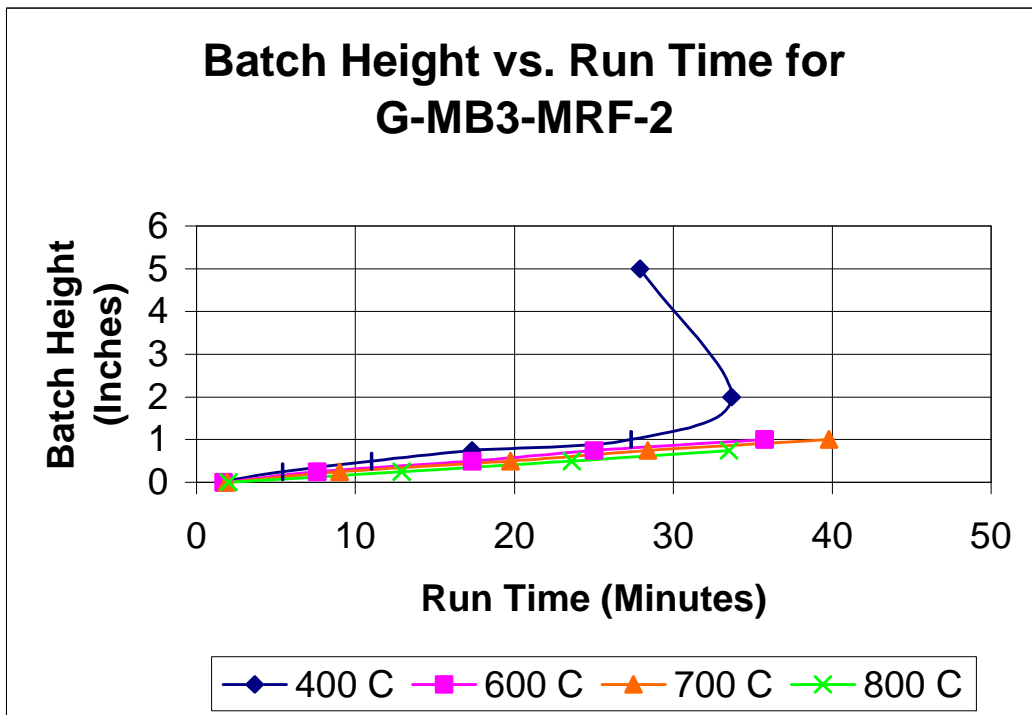


Figure F-23. Isotherm Plot for M-MB3-MRF-2

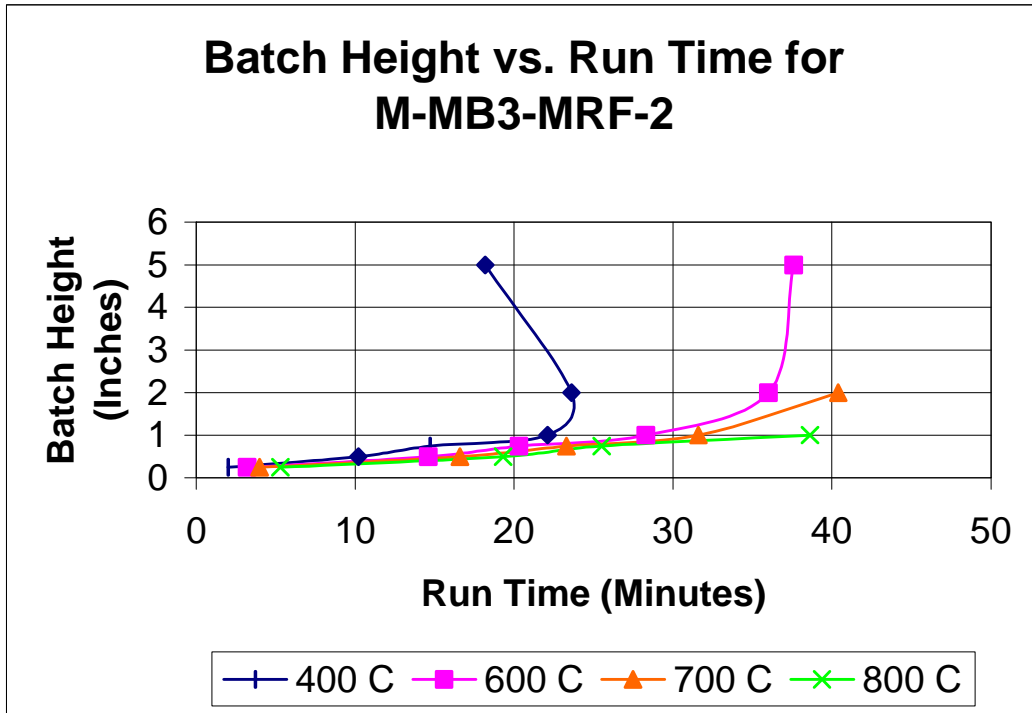


Figure F-24. Isotherm Plot for BONE-MB3-MRF-2

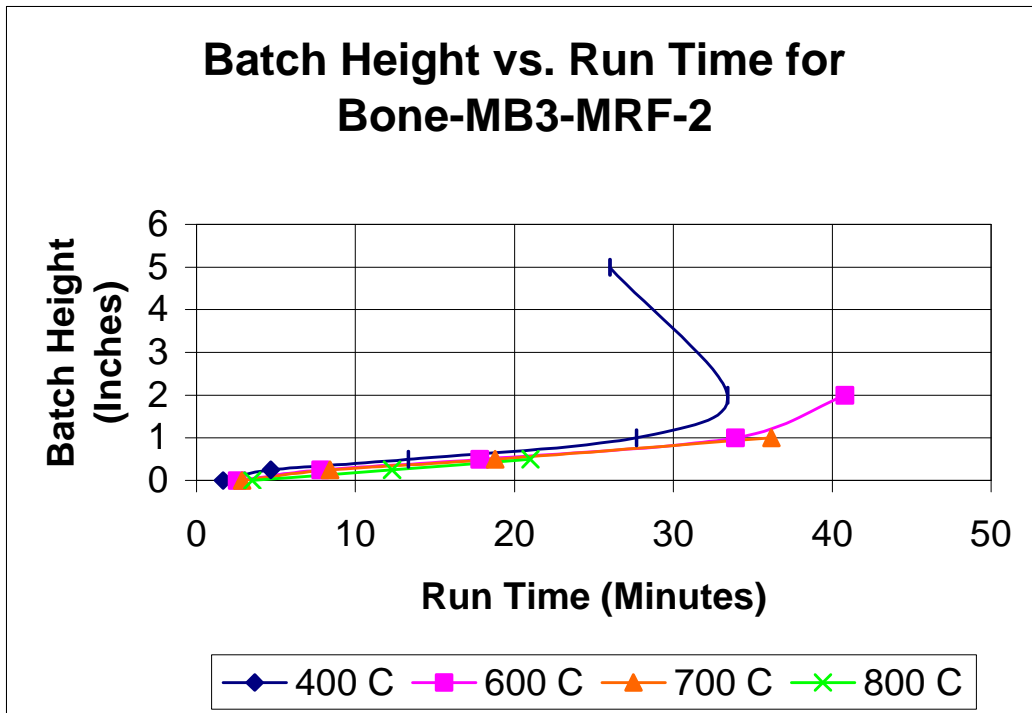


Figure F-25. Isotherm Plot for BONE2-MB3-MRF-2

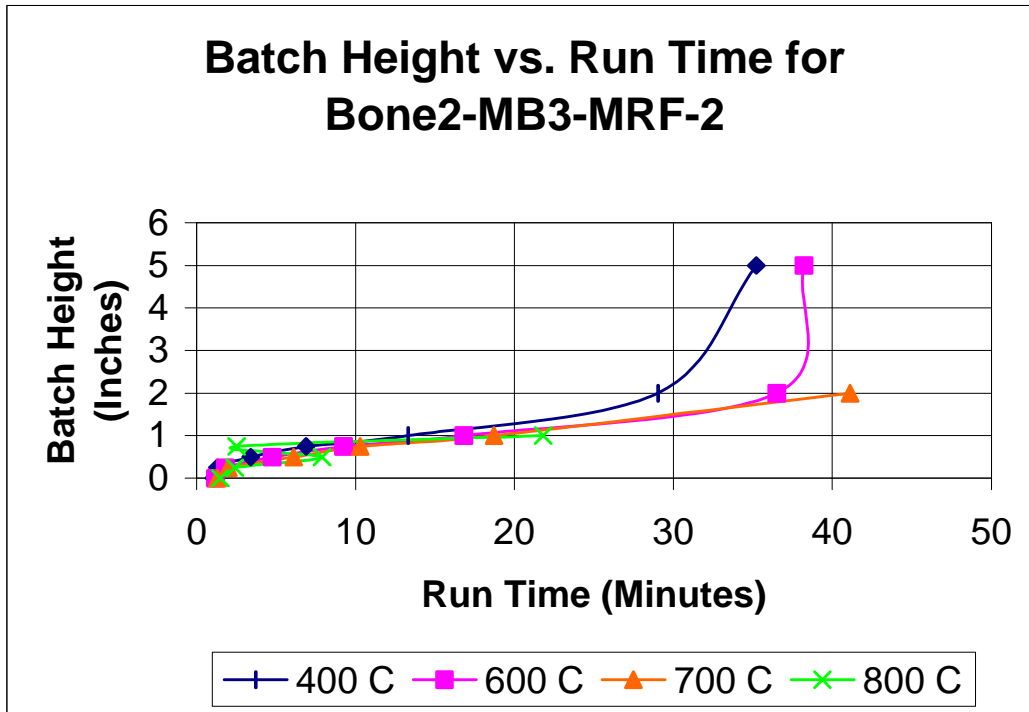


Figure F-26. Isotherm Plot for KMA2-MB3-MRF-2

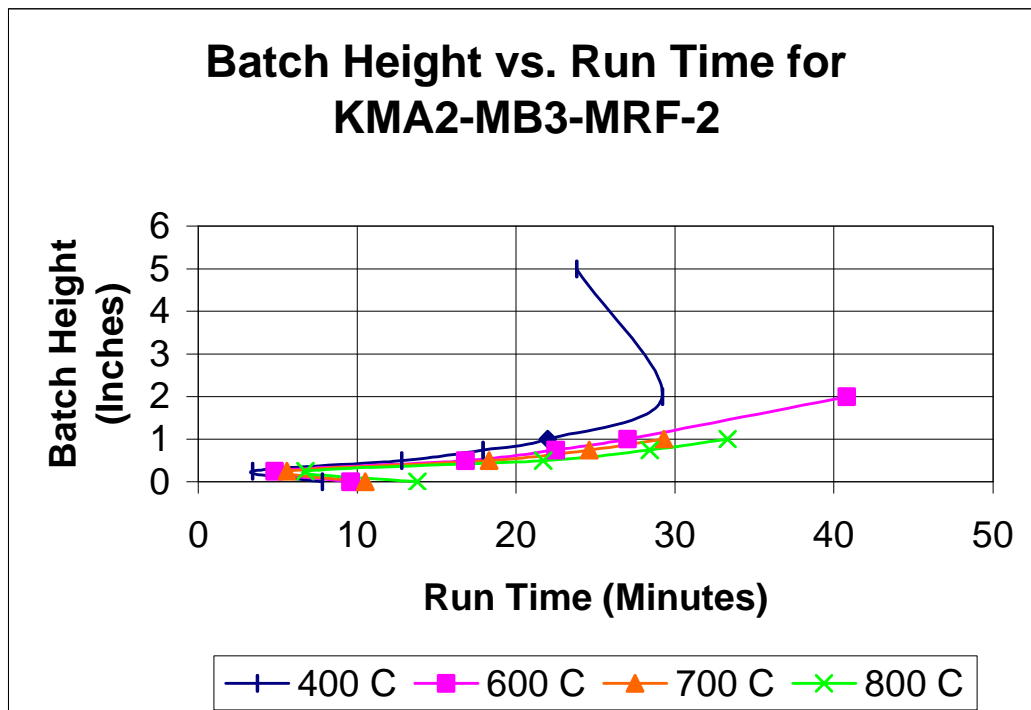


Figure F-27. Isotherm Plot for 200-MB3-MRF-8

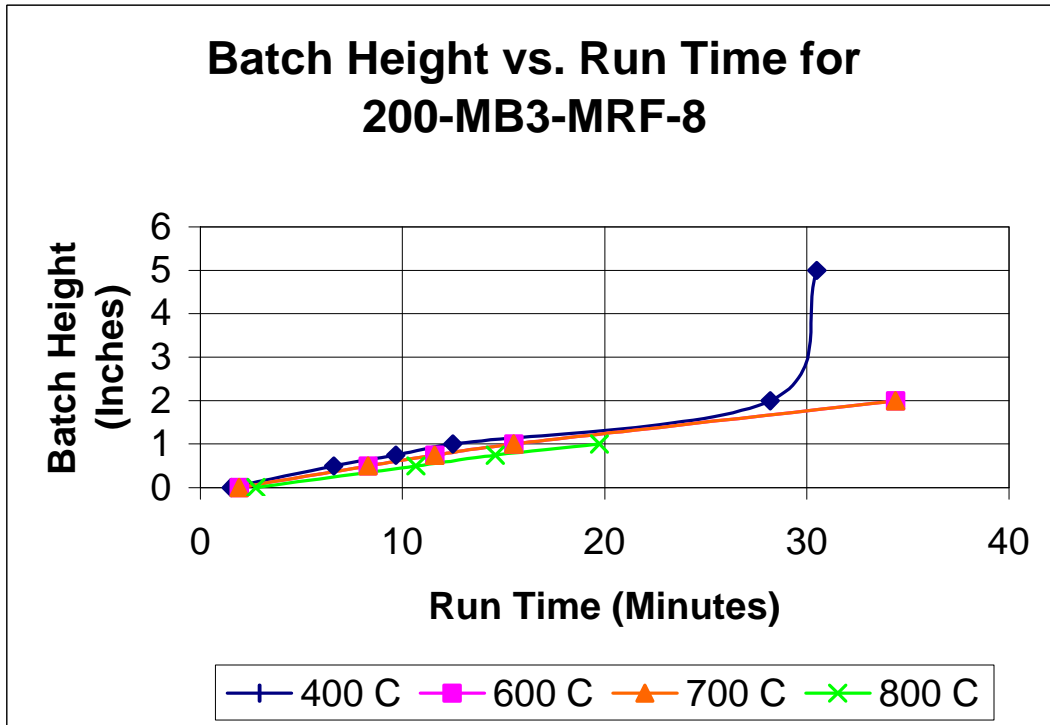


Figure F-28. Isotherm Plot for 165-MB3-MRF-5

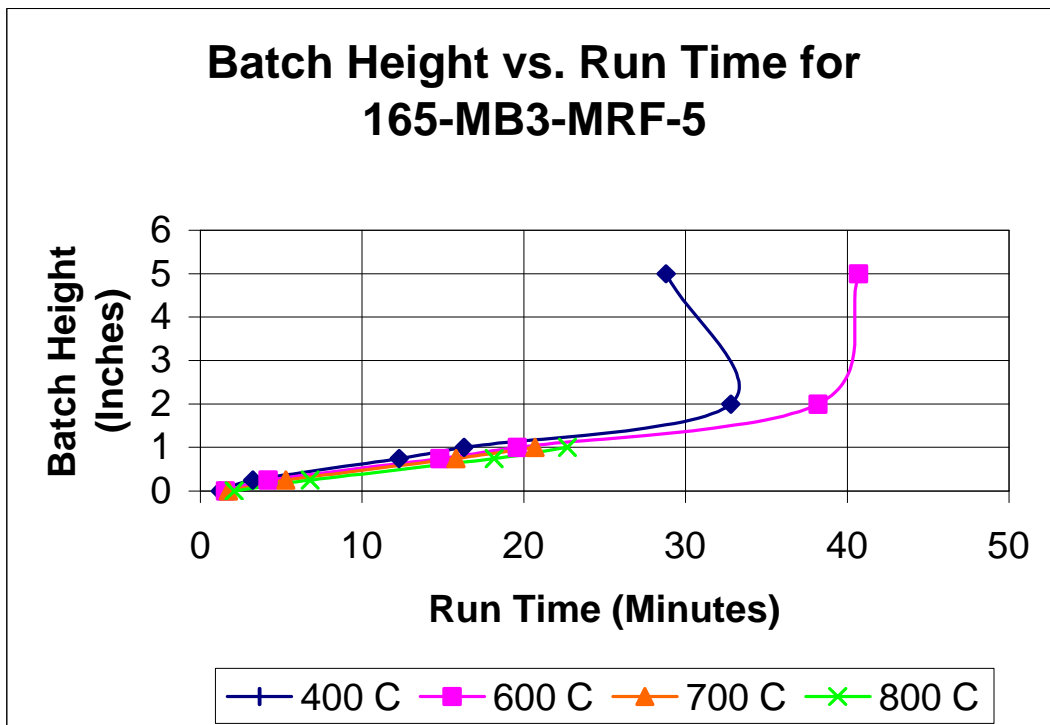


Figure F-29. Isotherm Plot for 200-MB2-MRF

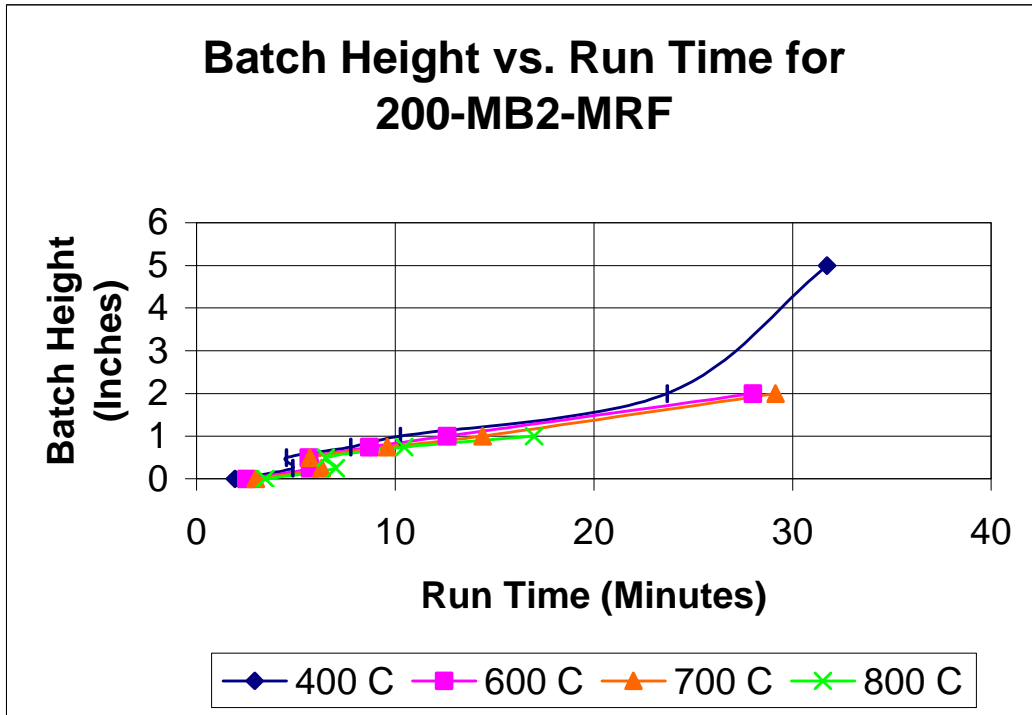
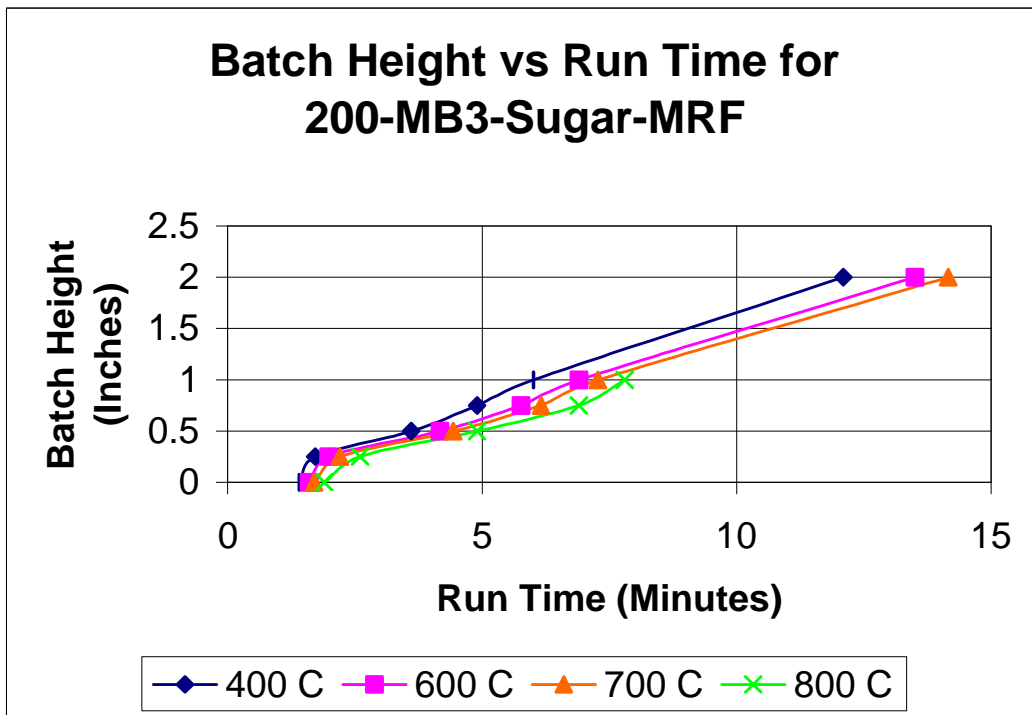


Figure F-30. Isotherm Plot for 200-MB3-SUGAR-MRF-2



Appendix G. Run Data and Melt Rate Determinations from Melt Rate Furnace Runs

Table G-1. Batch Weight and Run Times

Run #	Batch Height (inches)	Batch Weight (grams)	Run Time (minutes)	Glass Pool Height (inches)	Unreacted Feed (grams)
200-MB3-Baseline-MRF-1	2 3/8	794	82	0.70	0
200-MB3-Baseline-MRF-2	3	794	71	0.75	0
200-MB3-Baseline-MRF-3	X	794	80	0.75	0
165-MB3-Baseline-MRF-1	3.5	794	78	0.80	0
165-MB3-Baseline-MRF-2	3	794	78	0.80	0
165-MB3-Baseline-MRF-3	2.5	794	84	0.90	0
165-No Zr-Baseline-MRF	2.5	794	75	0.90	0
165 (Si Def)-MB3-MRF	3 1/8	566.3	49	0.87	0
200-MB3-Formic Only-MRF	2 1/2	798	82	0.80	0
200-MB3-Underwashed-MRF	2 1/2	794	72	0.82	0
200-MB3-Overwashed-MRF	2 1/2	794	90	0.70	0
200-MB3-Dried-MRF-1	2 15/16	582	66	0.80	0
200-MB3-Dried-MRF-2	2 15/16	582	65	0.85	0
200-MB3-Dried-MRF-3	3	582	66	0.85	0
200-MB3-Dried-MRF-4	3 1/16	575	50	0.85	2.7
200-MB3-Dried-MRF-5	3	574.5	36	0.45	30.0
200-MB3-Dried-MRF-6	3	574.9	30	0.35	165.8
0-MB3-MRF	3 3/8	555.1	48.5	0.50	0.5
N-MB3-MRF	3 1/16	546.3	46	0.51	1.4
M-MB3-MRF	3	548.5	49	0.79	3.4
KMA 2A-MB3-MRF	3 1/8	547.3	49	0.60	1.6
D-MB3-MRF	X	547.5	44	0.83	0.5
G-MB3-MRF	3 ¼	546.3	48	0.71	4.5
Bone-MB3-MRF	2 7/8	545	43	0.79	1.4
KMA 2-MB3-MRF	3 1/8	544.9	45.5	0.44	3.0
Bick-MB3-MRF	2 7/8	542.0	43	0.63	2.2
Mimi-MB3-MRF	2 3/4	542.3	45	0.65	0.5
C-MB3-MRF	3.1	548.6	51	0.43	2.0
Bone 2-MB3-MRF	2.88	546.0	44	0.73	2.5
165-MB3-MRF-4	3.13	543.7	47	0.75	X
200-MB3-MRF-7	3	540.7	48	0.57	X
D-MB3-MRF-2	X	545.2	42	0.79	0.3
200-MB3-MRF-8	3	545.1	42	0.55	46.2
165-MB3-MRF-5	3 1/4	546.2	42	0.66	15.6
M-MB3-MRF-2	2 3/4	545.4	42	0.73	10.3
KMA2-MB3-MRF-2	2 5/8	542.2	42	0.46	16.4
G-MB3-MRF-2	3 11/16	548.2	42	0.68	25.5
BONE-MB3-MRF-2	3 1/16	548.1	42	0.69	14.7
BONE2-MB3-MRF-2	3 1/16	546.9	42	0.68	5.2
200-MB2-MRF	3	572.8	42	0.56	33.4
200-MB3-SUGAR-MRF	2 11/16	550.7	42	0.5	55.8
320A-MB3-MRF-2	3	544.5	42	0.8	23.8

Note: X = Information not recorded.

Table G-2. Thermocouple and Camera Locations

Run #	Number of Lower T/C's	Location	Borescope Installed
200-MB3-Baseline-MRF-1	4	¾" Radius	
200-MB3-Baseline-MRF-2	4	¾" Radius	
200-MB3-Baseline-MRF-3	4	¾" Radius	
165-MB3-Baseline-MRF-1	4	¾" Radius	
165-MB3-Baseline-MRF-2	4	¾" Radius	
165-MB3-Baseline-MRF-3	4	¾" Radius	
165-No Zr-Baseline-MRF	4	¾" Radius	
165 (Si Def)-MB3-MRF	8	¾" Radius, Paired	
200-MB3-Formic Only-MRF	4	¾" Radius	
200-MB3-Underwashed-MRF	4	¾" Radius	
200-MB3-Overwashed-MRF	4	¾" Radius	
200-MB3-Dried-MRF-1	8	¾" Radius, Paired	
200-MB3-Dried-MRF-2	8	¾" Radius, Paired	
200-MB3-Dried-MRF-3	8	¾" Radius, Paired	
200-MB3-Dried-MRF-4	4	¾" Radius	
200-MB3-Dried-MRF-5	4	¾" Radius	
200-MB3-Dried-MRF-6	4	¾" Radius	
0-MB3-MRF	8	¾" Radius, Paired	
N-MB3-MRF	8	¾" Radius, Paired	
M-MB3-MRF	8	¾" Radius, Paired	
KMA 2A-MB3-MRF	8	¾" Radius, Paired	
D-MB3-MRF	8	¾" Radius, Paired	
G-MB3-MRF	8	¾" Radius, Paired	
Bone-MB3-MRF	8	¾" Radius, Paired	
KMA 2-MB3-MRF	8	¾" Radius, Paired	
Bick-MB3-MRF	8	¾" Radius, Paired	
Mimi-MB3-MRF	8	¾" Radius, Paired	
C-MB3-MRF	8	¾" Radius, Paired	
Bone 2-MB3-MRF	8	¾" Radius, Paired	
165-MB3-MRF-4	8	¾" Radius, Paired	
200-MB3-MRF-7	8	¾" Radius, Paired	
D-MB3-MRF-2	6	Central Bundle	YES
200-MB3-MRF-8	6	Central Bundle	YES
165-MB3-MRF-5	6	Central Bundle	YES
M-MB3-MRF-2	6	Central Bundle	YES
KMA2-MB3-MRF-2	6	Central Bundle	YES
G-MB3-MRF-2	6	Central Bundle	YES
BONE-MB3-MRF-2	6	Central Bundle	YES
BONE2-MB3-MRF-2	6	Central Bundle	YES
200-MB2-MRF	6	Central Bundle	YES
200-MB3-SUGAR-MRF	6	Central Bundle	YES
320A-MB3-MRF-2	6	Central Bundle	YES

Table G-3. Description of Sectioned Beakers.

Run #	Description of Sectioned Beaker
200-MB3-Baseline-MRF-1	Approximately 66 grams of foam stuck to thermocouples. Melt pool underneath foam is very flat with a 1/8" layer of small bubbles on surface.
200-MB3-Baseline-MRF-2	Dark, slightly convex, relatively uniform glass pool under 3/8" thick foam layer with medium to large bubbles.
200-MB3-Baseline-MRF-3	Glass pool with many cracks under a messy, flaky foam region plagued with small to medium sized bubbles.
165-MB3-Baseline-MRF-1	Neat, uniform glass pool with small, glass-like foam layer slightly greater than 1/16" thick.
165-MB3-Baseline-MRF-2	Neat, uniform glass pool with small, glass-like foam layer of ~1/16" thick with small to medium sized bubbles.
165-MB3-Baseline-MRF-3	Neat, uniform glass pool with virtually no foam layer, but a few small bubbles localized in pool's center. Top 1/16" layer of glass pool is darker than remainder of pool.
165-No Zr-Baseline-MRF	Neat, uniform glass pool with virtually no foam layer, but a few tiny bubbles localized near pool's center at top. Top 1/4" layer of glass pool is darker than remainder of pool.
165 (Si Def)-MB3-MRF	Neat, relatively uniform glass pool with thin, glass-like foam layer (a little thicker than 1/16") that is not really well-defined.
200-MB3-Formic Only-MRF	Neat, relatively uniform glass pool with slightly flaky, glass-like foam layer of ~1/6" thick. Foam layer contains small to a few medium sized bubbles.
200-MB3-Underwashed-MRF	Neat, uniform glass pool with small, glass-like foam layer of ~1/6" thick.
200-MB3-Overwashed-MRF	Neat, uniform glass pool with virtually no foam layer, but a few tiny bubbles in varied regions at top.
200-MB3-Dried-MRF-1	Neat, uniform glass pool under 1/8" thick glass-like foam layer which contains small bubbles.
200-MB3-Dried-MRF-2	Uniform glass pool with small, glass-like foam layer 1/8" thick. Top 1/8" layer of glass pool is darker than remainder of pool.
200-MB3-Dried-MRF-3	Neat, uniform glass pool with small, glass-like foam layer 1/8" thick. Top 1/8" layer of glass pool is darker than remainder of pool.
200-MB3-Dried-MRF-4	Dark, slightly convex glass pool under convex foam layer of 1/2" thickness at edge of beaker and 3/8" thickness around center of beaker. Foam layer contains small to large bubbles and is slightly messy.
200-MB3-Dried-MRF-5	Slightly convex, relatively uniform glass pool under foam layer. Foam layer (thickness of 1/6" with small to medium sized bubbles) underneath a 1/6" unreacted, brown, grainy feed layer.
200-MB3-Dried-MRF-6	Slightly convex, non-uniform glass pool. Large air passage around edge of beaker between glass pool and foam layer resulting in highly convex foam layer. Foam layer has small to medium sized bubbles. Thin unreacted, feed layer of grainy consistency covers foam layer.
0-MB3-MRF	Messy, convex foam layer ~1/2" thick and glass pool (which contains large, off-centered bubble). Foam layer has small to medium sized bubbles dispersed throughout.
N-MB3-MRF	Highly convex foam layer ~1/2" thick covers glass pool which contains large, slightly off-centered bubble. Foam layer has small to medium sized bubbles dispersed throughout.

M-MB3-MRF	Relatively neat, lightly colored, uniform glass pool under non-uniform foam layer. Foam layer is $\sim\frac{1}{4}$ " thick. Medium to large air passageway around side of beaker between foam layer and glass pool. Thin unreacted, feed layer of grainy consistency covers foam layer. Top $\frac{1}{8}$ " layer of glass pool darker than remainder of glass pool.
KMA 2A-MB3-MRF	Glass pool disrupted by large hole. Foam layer which is highly convex, due to medium sized air passageway around edge of beaker between glass pool and foam layer, has small to large sized bubbles dispersed throughout. Top of foam layer is also slightly flaky and covered with some unreacted feed. Foam layer is $\sim\frac{3}{8}$ " thick around center and almost 1" thick at the edge.
D-MB3-MRF	Messy, glass-like foam layer of $\sim\frac{1}{6}$ " thickness covers uniform glass pool. Foam layer contains small to medium sized bubbles.
G-MB3-MRF	Convex, relatively uniform glass pool disturbed at top by medium to large bubbles from foam layer of $\sim\frac{3}{8}$ " thickness. Unreacted feed layer sits on top of foam layer.
Bone-MB3-MRF	Bumpy foam layer of $\sim\frac{1}{4}$ " thickness covers a uniform glass pool. Foam layer contains medium sized bubbles.
KMA 2-MB3-MRF	Convex, non-uniform glass pool with large bubble (with ~ 2 " horizontal diameter) in bottom center. Large air passage around edge of beaker between glass pool and foam layer resulting in highly convex foam layer. Foam layer of $\sim\frac{1}{2}$ " (closer to center) to $\sim\frac{3}{4}$ " (closer to edge) thickness contains small to medium sized bubbles.
Bick-MB3-MRF	Glass pool disrupted by large bubble in center. Medium to large sized air passageway around edge of beaker between convex foam layer and glass pool. Foam layer is about $\frac{1}{8}$ to $\frac{1}{6}$ " thick.
Mimi-MB3-MRF	Convex glass pool disrupted by large bubble in center. Seems like upper $\frac{1}{2}$ " of glass pool has medium sized bubbles dispersed throughout. Messy, highly convex, non-uniform foam layer at least $\frac{1}{4}$ " thick. Also, medium sized air passageway around $\frac{1}{4}$ to $\frac{1}{2}$ of the circumference of beaker between foam layer and glass pool.
C-MB3-MRF	Smooth, convex foam layer of ~ 1 " thick covers glass pool which is disrupted by a large bubble/hole in the center. Bubble is about $\frac{1}{6}$ " above bottom of beaker. Medium to large sized bubbles form a discontinuous passageway around edge of beaker.
Bone 2-MB3-MRF	Glass pool under convex, smooth, thin foam layer of $\sim\frac{1}{8}$ " thickness with small to medium sized bubbles. One large bubble horizontally off-centered and $\sim\frac{1}{2}$ " from bottom of glass pool.
165-MB3-MRF-4	Relatively uniform glass pool under foam layer of $\sim\frac{1}{6}$ " thickness. Foam layer contains medium to large sized bubbles.
200-MB3-MRF-7	Convex foam layer $\sim\frac{1}{6}$ " thick and with small bubbles covers glass pool which is disrupted by large bubble in the center. Medium sized air passageway around edge of beaker separates foam layer from glass pool.
D-MB3-MRF-2	Bumpy, glass-like foam layer $\sim\frac{1}{6}$ " thick covers uniform glass pool. Foam layer contains small to medium sized bubbles.
200-MB3-MRF-8	Brown, highly bridged, convex, grainy foam layer is suspended $\frac{3}{4}$ " at center and 1.5" at edge above thin, relatively uniform glass pool which contains a few small bubbles in top middle. Foam layer contains small bubbles also.
165-MB3-MRF-5	Highly convex foam layer $\sim\frac{1}{6}$ " thick containing small to medium sized bubbles covers relatively uniform glass pool. Foam layer is covered by thin, brown, grainy unreacted feed layer. Convexity of foam layer caused by medium sized air passageway around edge of beaker.

M-MB3-MRF-2	Glass pool which contains a few large bubbles close to the edge has a small well in its center. Foam layer is ~1/6" thick and is covered by a very thin layer of unreacted feed.
KMA2-MB3-MRF-2	Brown, highly convex foam layer of grainy consistency and ~1/4" thick covers non-uniform glass pool which is disrupted by medium sized bubble. Large air passageway around edge of beaker separates foam layer and glass pool.
G-MB3-MRF-2	Crusty foam layer, ~1/4" thick, covers a convex glass pool. Foam layer contains medium to large sized bubbles.
BONE-MB3-MRF-2	Glass pool, disrupted by medium to large sized bubble, is covered by convex foam layer of at least 1/6" thickness and contains medium sized bubbles.
BONE2-MB3-MRF-2	Glass pool is disrupted by medium sized bubble that is slightly off-centered. Slightly convex foam layer of ~1/6" thick contains medium sized bubbles.
200-MB2-MRF	Large bubbles separate grainy, convex foam layer, of ~1/6" thickness, and glass pool. Top of glass pool contains small bubbles. Note: this is the only sample in which the foam layer is completely separated from glass pool by large bubbles.
200-MB3-SUGAR-MRF	Glass pool contains a small and medium sized bubble. Convex foam layer of ~1/6" thickness is rather grainy, almost rocky. Also, medium sized air passageway around edge of beaker between glass pool and foam layer.
320A-MB3-MRF-2	Glass pool is disrupted by medium sized bubble that is slightly off-centered. Slightly convex foam layer of ~1/6" thick contains medium sized bubbles.

Table G-4. Glass Pool Height and Melt Rate Determination

Linear Melt Rate Determination: in/hr

Distance from Center	D	D-2	BONE	M-2	BONE2	BONE-2	M	G-2
2	0.95	0.95	0.8	0.7	0.9	0.8	0.85	0.75
1.75	0.95	0.95	0.9	0.65	0.85	0.8	0.8	0.8
1.5	0.9	0.9	0.8	0.6	0.8	0.8	0.8	0.85
1.25	0.85	0.8	0.8	0.5	0.8	0.8	0.85	0.8
1	0.85	0.7	0.8	0.5	0.5	0.75	0.8	0.7
0.75	0.8	0.7	0.7	0.85	0.35	0.7	0.85	0.6
0.5	0.85	0.7	0.8	0.9	0.4	0.6	0.9	0.4
0.25	0.8	0.7	0.8	0.75	0.5	0.6	0.8	0.4
0.25	0.8	0.7	0.7	0.55	0.7	0.3	0.8	0.4
0.5	0.75	0.7	0.7	0.45	0.75	0.2	0.8	0.6
0.75	0.8	0.7	0.8	0.75	0.9	0.3	0.8	0.6
1	0.75	0.8	0.9	0.8	0.9	0.7	0.8	0.6
1.25	0.75	0.7	0.8	0.9	0.85	0.75	0.7	0.8
1.5	0.8	0.85	0.8	0.9	0.85	0.9	0.7	0.8
1.75	0.8	0.85	0.8	0.95	0.8	1	0.7	0.85
2	0.8	0.9	0.8	0.9	0.8	1	0.75	0.9
Average	0.83	0.79	0.79	0.73	0.73	0.69	0.79	0.68
Run Time	44	42	43	42	44	42	49	42
Melt Rate	1.13	1.13	1.11	1.04	0.99	0.98	0.97	0.97

Volumetric Melt Rate Determination: Cubic inches per hour

Distance from Center	D	D-2	BONE	M-2	BONE2	BONE-2	M	G-2
2	1.40	1.40	1.18	1.03	1.33	1.18	1.25	1.10
1.75	1.21	1.21	1.15	0.83	1.08	1.02	1.02	1.02
1.5	0.97	0.97	0.86	0.65	0.86	0.86	0.86	0.92
1.25	0.75	0.71	0.71	0.44	0.71	0.71	0.75	0.71
1	0.58	0.48	0.55	0.34	0.34	0.52	0.55	0.48
0.75	0.39	0.34	0.34	0.42	0.17	0.34	0.42	0.29
0.5	0.25	0.21	0.24	0.27	0.12	0.18	0.27	0.12
0.25	0.08	0.07	0.08	0.07	0.05	0.06	0.08	0.04
0.25	0.08	0.07	0.07	0.05	0.07	0.03	0.08	0.04
0.5	0.22	0.21	0.21	0.13	0.22	0.06	0.24	0.18
0.75	0.39	0.34	0.39	0.37	0.44	0.15	0.39	0.29
1	0.52	0.55	0.62	0.55	0.62	0.48	0.55	0.41
1.25	0.66	0.62	0.71	0.80	0.75	0.66	0.62	0.71
1.5	0.86	0.92	0.86	0.97	0.92	0.97	0.76	0.86
1.75	1.02	1.08	1.02	1.21	1.02	1.28	0.89	1.08
2	1.18	1.33	1.18	1.33	1.18	1.47	1.10	1.33
Sum	10.57	10.50	10.16	9.46	9.88	9.96	9.83	9.59
Run Time	42	42	44	42	43	42	42	44
Melt Rate	15.1	15.0	13.9	13.5	13.8	14.2	14.0	13.1

Linear Melt Rate Determination: in/hr

Distance from Center	165-4	165-5	BONE2-2	G	200-8	200-7	KMA2-2	KMA2
2	0.8	0.85	1	0.8	0.55	0.7	0.7	0.8
1.75	0.8	0.9	0.9	0.8	0.55	0.7	0.6	0.85
1.5	0.8	0.8	0.9	0.8	0.55	0.75	0.6	0.8
1.25	0.8	0.75	0.8	0.55	0.55	0.7	0.55	0.7
1	0.8	0.65	0.8	0.5	0.55	0.7	0.55	0.7
0.75	0.65	0.35	0.7	0.55	0.55	0.8	0.1	0.1
0.5	0.65	0.3	0.65	0.5	0.55	0.3	0.1	0.1
0.25	0.65	0.5	0.65	0.7	0.55	0.3	0.1	0.1
0.25	0.7	0.5	0.2	0.5	0.55	0.3	0.1	0.1
0.5	0.8	0.4	0.2	0.7	0.55	0.25	0.5	0.1
0.75	0.7	0.6	0.3	0.75	0.55	0.25	0.55	0.1
1	0.7	0.6	0.3	0.75	0.55	0.25	0.55	0.1
1.25	0.75	0.65	0.8	0.85	0.55	0.35	0.6	0.5
1.5	0.8	0.8	0.8	0.85	0.55	0.9	0.65	0.6
1.75	0.8	0.95	0.9	0.9	0.55	0.9	0.6	0.7
2	0.8	0.9	0.9	0.9	0.55	0.9	0.5	0.65
Average	0.75	0.66	0.68	0.71	0.55	0.57	0.46	0.44
Run Time	47	42	44	48	42	48	42	45.5
Melt Rate	0.96	0.94	0.92	0.89	0.79	0.71	0.66	0.58

Volumetric Melt Rate Determination: Cubic inches per hour

Distance from Center	165-4	165-5	BONE2-2	G	200-8	200-7	KMA2-2	KMA2
2	1.18	1.25	1.47	1.18	0.81	1.03	1.03	1.18
1.75	1.02	1.15	1.15	1.02	0.70	0.89	0.77	1.08
1.5	0.86	0.86	0.97	0.86	0.59	0.81	0.65	0.86
1.25	0.71	0.66	0.71	0.49	0.49	0.62	0.49	0.62
1	0.55	0.45	0.55	0.34	0.38	0.48	0.38	0.48
0.75	0.32	0.17	0.34	0.27	0.27	0.39	0.05	0.05
0.5	0.19	0.09	0.19	0.15	0.16	0.09	0.03	0.03
0.25	0.06	0.05	0.06	0.07	0.05	0.03	0.01	0.01
0.25	0.07	0.05	0.02	0.05	0.05	0.03	0.01	0.01
0.5	0.24	0.12	0.06	0.21	0.16	0.07	0.15	0.03
0.75	0.34	0.29	0.15	0.37	0.27	0.12	0.27	0.05
1	0.48	0.41	0.21	0.52	0.38	0.17	0.38	0.07
1.25	0.66	0.57	0.71	0.75	0.49	0.31	0.53	0.44
1.5	0.86	0.86	0.86	0.92	0.59	0.97	0.70	0.65
1.75	1.02	1.21	1.15	1.15	0.70	1.15	0.77	0.89
2	1.18	1.33	1.33	1.33	0.81	1.33	0.74	0.96
Sum	9.75	9.53	9.93	9.66	6.91	8.50	6.94	7.41
Run Time	45.5	44	49	48	42	42	47	48
Melt Rate	12.9	13.0	12.2	12.1	9.9	12.1	8.9	9.3

Linear Melt Rate Determination: in/hr

Distance from Center	O	KMA2A	C	N	MIMI	BICK	165 Si def	MB2	320A-2
2	0.8	0.9	0.65	0.75	0.75	0.9	0.9	0.7	0.85
1.75	0.8	0.9	0.7	0.7	0.7	0.9	0.9	0.7	0.8
1.5	0.2	0.9	0.7	0.7	0.6	0.9	0.9	0.7	0.8
1.25	0.15	0.8	0.65	0.6	0.6	0.9	0.85	0.6	0.8
1	0.1	0.2	0.2	0.3	0.5	0.75	0.85	0.6	0.85
0.75	0.1	0.2	0.2	0.1	0.5	0.7	0.85	0.6	0.7
0.5	0.15	0.2	0.2	0.1	0.2	0.2	0.85	0.3	0.65
0.25	0.45	0.3	0.2	0.1	0.15	0.2	0.85	0.3	0.6
0.25	0.5	0.3	0.2	0.1	0.15	0.2	0.85	0.3	0.65
0.5	0.6	0.3	0.2	0.45	0.2	0.22	0.85	0.3	0.3
0.75	0.55	0.7	0.2	0.55	0.2	0.25	0.85	0.4	0.4
1	0.6	0.75	0.2	0.65	3	0.7	0.85	0.6	0.75
1.25	0.7	0.75	0.3	0.7	0.65	0.8	0.85	0.65	0.8
1.5	0.7	0.8	0.7	0.7	0.75	0.8	0.9	0.75	0.9
1.75	0.8	0.8	0.8	0.75	0.73	0.8	0.9	0.8	0.9
2	0.8	0.8	0.85	0.85	0.7	0.8	0.9	0.7	0.9
Average	0.50	0.60	0.43	0.51	0.65	0.63	0.87	0.56	0.73
Run Time	48.5	45.5	51	46	45	43	49	42	42
Melt Rate	0.62	0.79	0.51	0.66	0.87	0.87	1.06	0.80	1.04

Volumetric Melt Rate Determination: Cubic inches per hour

Distance from Center	O	KMA2A	C	N	MIMI	BICK	165 Si-Def	MB2	320A-2
2	1.18	1.33	0.96	1.10	1.10	1.33	1.33	1.03	1.25
1.75	1.02	1.15	0.89	0.89	0.89	1.15	1.15	0.89	1.02
1.5	0.22	0.97	0.76	0.76	0.65	0.97	0.97	0.76	0.86
1.25	0.13	0.71	0.57	0.53	0.53	0.80	0.75	0.53	0.71
1	0.07	0.14	0.14	0.21	0.34	0.52	0.58	0.41	0.58
0.75	0.05	0.10	0.10	0.05	0.25	0.34	0.42	0.29	0.34
0.5	0.04	0.06	0.06	0.03	0.06	0.06	0.25	0.09	0.19
0.25	0.04	0.03	0.02	0.01	0.01	0.02	0.08	0.03	0.06
0.25	0.05	0.03	0.02	0.01	0.01	0.02	0.08	0.03	0.06
0.5	0.18	0.09	0.06	0.13	0.06	0.06	0.25	0.09	0.09
0.75	0.27	0.34	0.10	0.27	0.10	0.12	0.42	0.20	0.20
1	0.41	0.52	0.14	0.45	2.06	0.48	0.58	0.41	0.52
1.25	0.62	0.66	0.27	0.62	0.57	0.71	0.75	0.57	0.71
1.5	0.76	0.86	0.76	0.76	0.81	0.86	0.97	0.81	0.97
1.75	1.02	1.02	1.02	0.96	0.93	1.02	1.15	1.02	1.15
2	1.18	1.18	1.25	1.25	1.03	1.18	1.33	1.03	1.33
Sum	7.24	9.18	7.10	8.02	9.42	9.64	11.06	8.20	10.04
Run Time	48.5	45.5	51	46	45	43	49	42	42
Melt Rate	9.0	12.1	8.4	10.5	12.6	13.4	13.5	11.7	14.3

Appendix H. Statistical Regression using JMP4 Software

The JMP analysis of the melt rate response as a linear function of alkali, boron, and silica content and viscosity is shown below. The model fit is of the form:

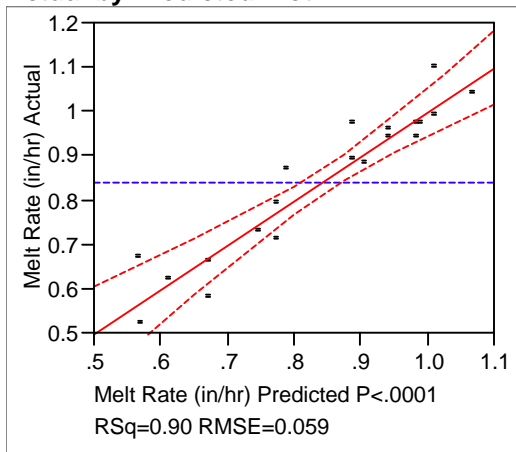
$$\text{Melt Rate} = \text{Intercept} + \text{Alkali} \cdot A + \text{Boron} \cdot B + \text{Silica} \cdot C + \text{Viscosity} \cdot D$$

Where A,B,C,D are parameter estimates for each effect (alkali, boron, silica, viscosity). The overall fit of this linear model is good with an adjusted Rsquare of 0.88 with 1.00 being a perfect fit.

Looking at the Parameter Estimates of this model fit, the intercept, alkali, boron, silica terms are probably zero based on the Student's t probabilities shown (Prob>|t|). These probabilities indicate the chance that the parameter estimate is zero. A desired probability of less than 0.05 is desired or there is a 95% chance that the parameter is not zero. Based on this overall model fit, another model fit was run with just viscosity to see if it produced a better model.

Response Melt Rate (in/hr) as Function of Alkali, Boron, Silica Content and Viscosity Whole Model

Actual by Predicted Plot



Summary of Fit

RSquare	0.901679
RSquare Adj	0.87546
Root Mean Square Error	0.059019
Mean of Response	0.84
Observations (or Sum Wgts)	20

Analysis of Variance

Source	DF	Sum of Squares	Mean Square	F Ratio
Model	4	0.47915214	0.119788	34.3903
Error	15	0.05224786	0.003483	Prob > F
C. Total	19	0.53140000		<.0001

Lack Of Fit

Source	DF	Sum of Squares	Mean Square	F Ratio
Lack Of Fit	9	0.03594786	0.003994	1.4703
Pure Error	6	0.01630000	0.002717	Prob > F
Total Error	15	0.05224786		0.3293
				Max RSq
				0.9693

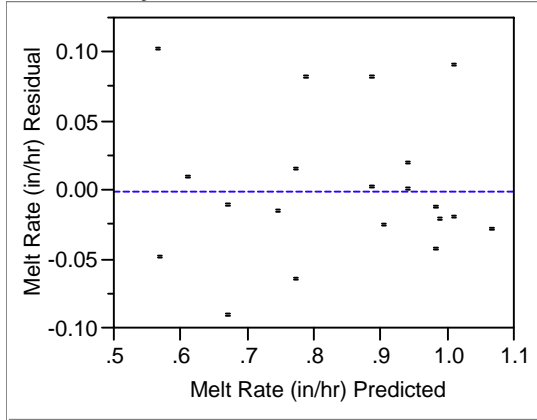
Parameter Estimates

Term	Estimate	Std Error	t Ratio	Prob> t
Intercept	0.0895555	1.004482	0.09	0.9301
Alkali (wt%)	0.0115723	0.016087	0.72	0.4830
Boron (wt%)	-0.019124	0.013413	-1.43	0.1744
Silica (wt%)	0.0138612	0.00945	1.47	0.1631
Viscosity (cP)	-0.004633	0.001488	-3.11	0.0071

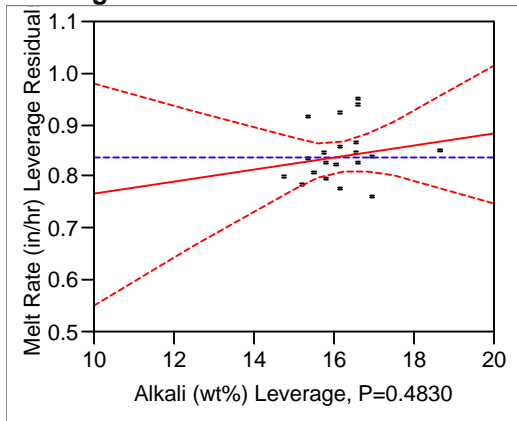
Effect Tests

Source	Nparm	DF	Sum of Squares	F Ratio	Prob > F
Alkali (wt%)	1	1	0.00180254	0.5175	0.4830
Boron (wt%)	1	1	0.00708050	2.0328	0.1744
Silica (wt%)	1	1	0.00749409	2.1515	0.1631
Viscosity (cP)	1	1	0.03377668	9.6971	0.0071

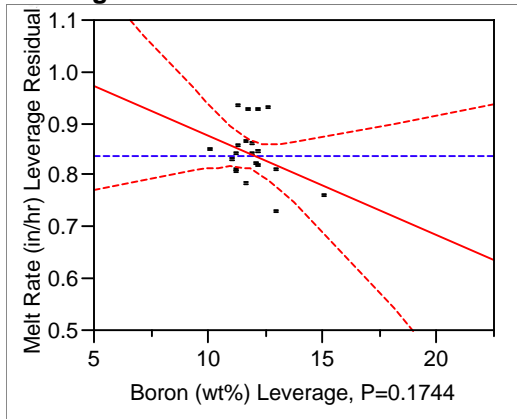
Residual by Predicted Plot



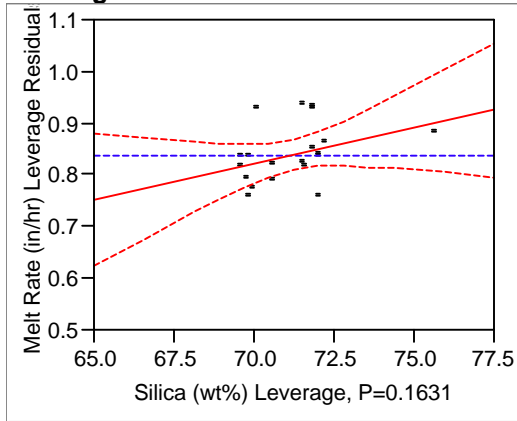
**Alkali (wt%)
Leverage Plot**



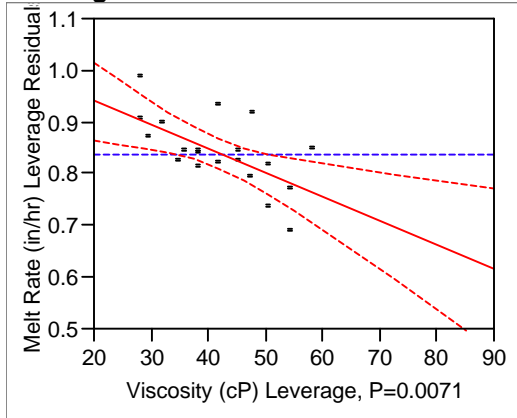
**Boron (wt%)
Leverage Plot**



**Silica (wt%)
Leverage Plot**



**Viscosity (cP)
Leverage Plot**



Just fitting a melt rate model as a linear function of viscosity is shown below. The model fit is of the form:

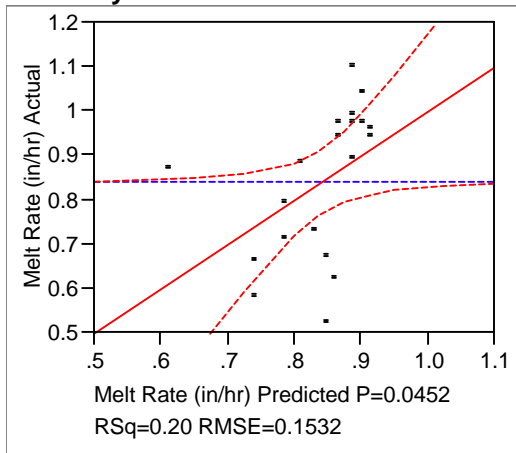
$$\text{Melt Rate} = \text{Intercept} + \text{Viscosity} * D$$

Where D is the parameter estimate for the viscosity effect. The fit of this linear model is very poor with an adjusted Rsquare of 0.16 with 1.00 being an ideal fit. Looking at the Parameter Estimates of this model fit, the intercept and viscosity terms are not probably zero based on the Student's t probabilities shown (Prob>|t|). However, the model is lacking some effects or does not explain the majority of error between the actual and predicted melt rate values. Based on this viscosity only model fit, another model analysis was run with viscosity and alkali to see if it produced a better model.

Response Melt Rate (in/hr) as Function of Viscosity Only

Whole Model

Actual by Predicted Plot



Summary of Fit

RSquare	0.204642
RSquare Adj	0.160455
Root Mean Square Error	0.153234
Mean of Response	0.84
Observations (or Sum Wgts)	20

Analysis of Variance

Source	DF	Sum of Squares	Mean Square	F Ratio
Model	1	0.10874670	0.108747	4.6313
Error	18	0.42265330	0.023481	Prob > F
C. Total	19	0.53140000		0.0452

Lack Of Fit

Source	DF	Sum of Squares	Mean Square	F Ratio
Lack Of Fit	10	0.39265330	0.039265	10.4708
Pure Error	8	0.03000000	0.003750	Prob > F
Total Error	18	0.42265330		0.0014
				Max RSq
				0.9435

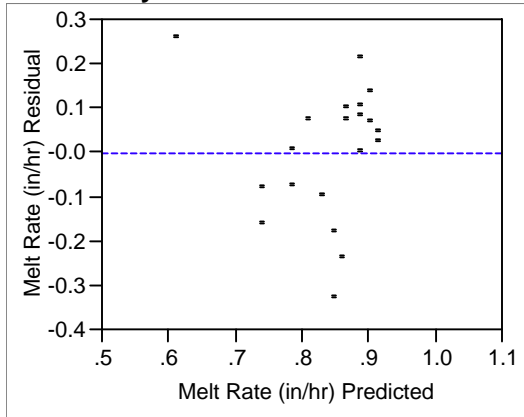
Parameter Estimates

Term	Estimate	Std Error	t Ratio	Prob> t
Intercept	1.0704243	0.112421	9.52	<.0001
Viscosity (cP)	-0.005475	0.002544	-2.15	0.0452

Effect Tests

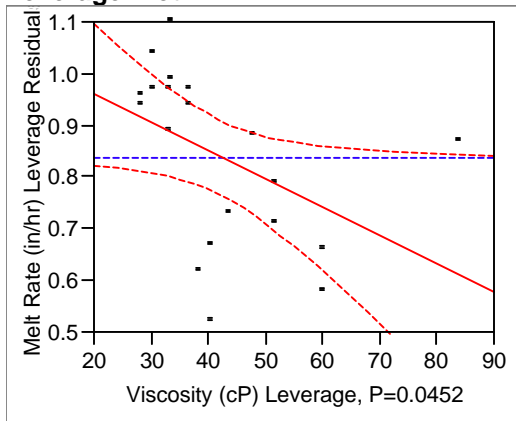
Source	Nparm	DF	Sum of Squares	F Ratio	Prob > F
Viscosity (cP)	1	1	0.10874670	4.6313	0.0452

Residual by Predicted Plot



Viscosity (cP)

Leverage Plot



The JMP analysis of the melt rate response as a linear function of alkali content and viscosity is shown below. The model fit is of the form:

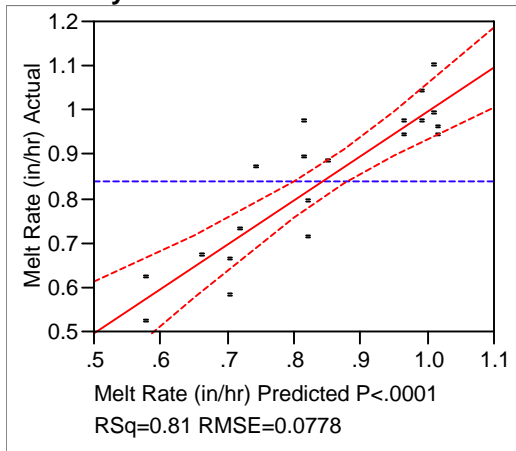
$$\text{Melt Rate} = \text{Intercept} + \text{Alkali} * A + \text{Viscosity} * D$$

Where A and D are parameter estimates for each effect (alkali and viscosity). The overall fit of this linear model is fair with an adjusted Rsquare of 0.78 with 1.00 being a perfect fit. Looking at the Parameter Estimates of this model fit, the intercept and viscosity terms are probably zero based on the Student's t probabilities shown (Prob>|t|). As stated before these probabilities indicate the chance that the parameter estimate is zero and a probability less than 0.05 is desired. This model fit indicates that the biggest effect is from alkali or that the alkali content is more important than viscosity. To confirm this hypothesis, another model fit was run with just alkali to see if it produced a better model.

Response Melt Rate (in/hr) as Function of Alkali and Viscosity

Whole Model

Actual by Predicted Plot



Summary of Fit

RSquare	0.806362
RSquare Adj	0.783581
Root Mean Square Error	0.0778
Mean of Response	0.84
Observations (or Sum Wgts)	20

Analysis of Variance

Source	DF	Sum of Squares	Mean Square	F Ratio
Model	2	0.42850069	0.214250	35.3963
Error	17	0.10289931	0.006053	Prob > F
C. Total	19	0.53140000		<.0001

Lack Of Fit

Source	DF	Sum of Squares	Mean Square	F Ratio
Lack Of Fit	10	0.08414931	0.008415	3.1416
Pure Error	7	0.01875000	0.002679	Prob > F
Total Error	17	0.10289931		0.0711
				Max RSq
				0.9647

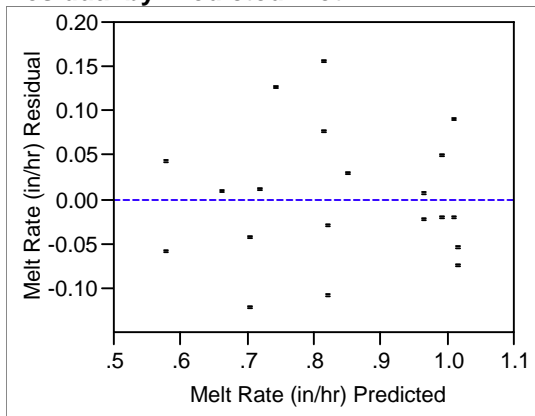
Parameter Estimates

Term	Estimate	Std Error	t Ratio	Prob> t
Intercept	0.1895747	0.133961	1.42	0.1751
Alkali (wt%)	0.0428719	0.005899	7.27	<.0001
Viscosity (cP)	-0.001051	0.001428	-0.74	0.4716

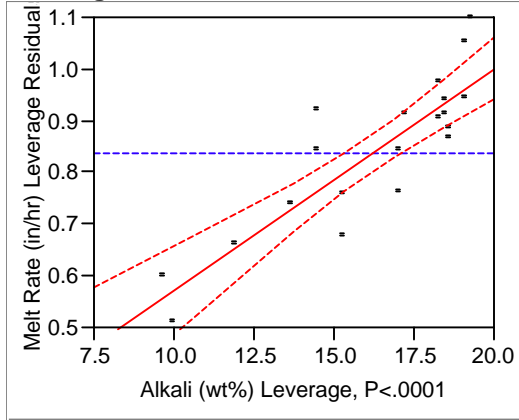
Effect Tests

Source	Nparm	DF	Sum of Squares	F Ratio	Prob > F
Alkali (wt%)	1	1	0.31975399	52.8266	<.0001
Viscosity (cP)	1	1	0.00328172	0.5422	0.4716

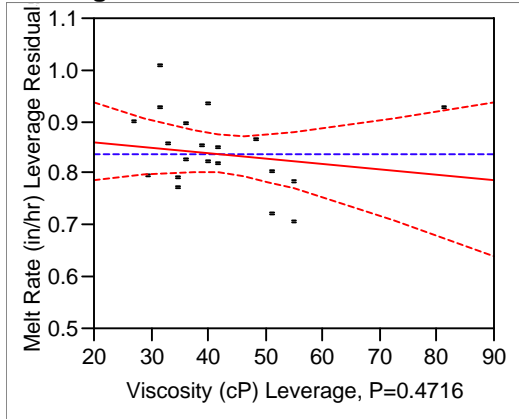
Residual by Predicted Plot



**Alkali (wt%)
Leverage Plot**



**Viscosity (cP)
Leverage Plot**



The JMP analysis of the melt rate response as a linear function of just alkali content is shown below. The model fit is of the form:

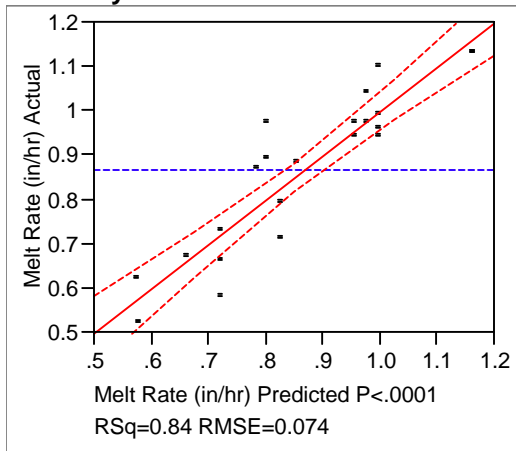
$$\text{Melt Rate} = \text{Intercept} + \text{Alkali} \cdot A$$

Where A is the parameter estimate for the alkali effect. The overall fit of this linear model is good with an adjusted Rsquare of 0.83 with 1.00 being a perfect fit. Looking at the Parameter Estimates of this model fit, the intercept and alkali terms are significant or have 95% chance of not being zero based on the Student's t probabilities shown (Prob>|t|). This model fit with its overall Rsquare shows that indeed the biggest effect is from alkali and that the viscosity effect is minimal in comparison. To confirm this hypothesis, more experiments could be devised focusing on viscosity and alkali as the primary effects.

Response Melt Rate (in/hr) as Function of Alkali Only

Whole Model

Actual by Predicted Plot



Summary of Fit

RSquare	0.839892
RSquare Adj	0.831887
Root Mean Square Error	0.074015
Mean of Response	0.866364
Observations (or Sum Wgts)	22

Analysis of Variance

Source	DF	Sum of Squares	Mean Square	F Ratio
Model	1	0.57474590	0.574746	104.9159
Error	20	0.10956319	0.005478	Prob > F
C. Total	21	0.68430909		<.0001

Lack Of Fit

Source	DF	Sum of Squares	Mean Square	F Ratio
Lack Of Fit	10	0.07372153	0.007372	2.0569
Pure Error	10	0.03584167	0.003584	Prob > F
Total Error	20	0.10956319		0.1355
				Max RSq
				0.9476

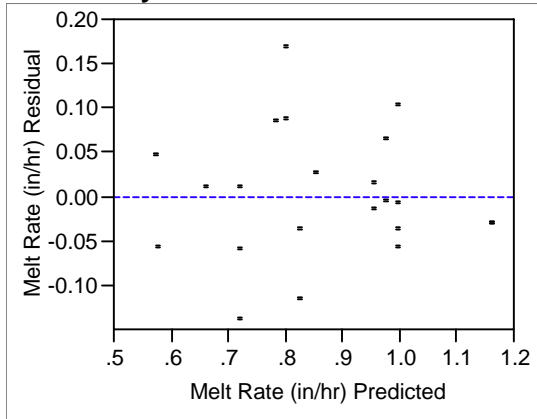
Parameter Estimates

Term	Estimate	Std Error	t Ratio	Prob> t
Intercept	0.1495098	0.071743	2.08	0.0502
Alkali (wt%)	0.0424162	0.004141	10.24	<.0001

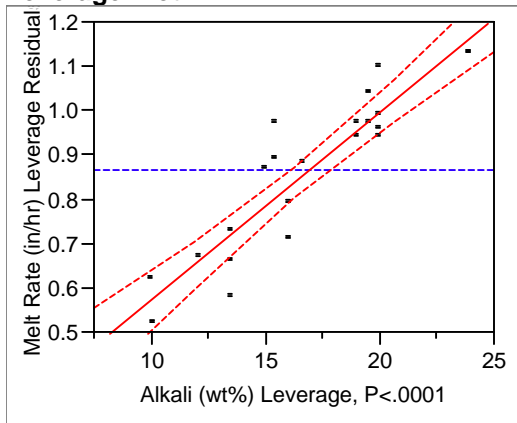
Effect Tests

Source	Nparm	DF	Sum of Squares	F Ratio	Prob > F
Alkali (wt%)	1	1	0.57474590	104.9159	<.0001

Residual by Predicted Plot



**Alkali (wt%)
Leverage Plot**



Distribution

W. D. Kerley, 704-S
J. F. Ortaldo, 704-S
R. E. Edwards, 704-3N
M. R. Norton, 704-27S
J. E. Occhipinti, 704-27S
J. F. Sproull, 704-30S
D. C. Iverson, 704-30S
R. J. O'Driscoll, 704-30S
L. M. Papouchado, 773-A
E. W. Holtzscheiter, 773-A
R. H. Spires, 773-A
D. A. Crowley, 773-43A
S. L. Marra, 704-1T
D. F. Bickford, 773-43A
C. M. Jantzen, 773-A

D. C. Witt, 704-1T
M. E. Stone, 704-1T
D. P. Lambert, 704-1T
M. F. Williams, 704-1T
D. C. Koopman, 704-1T
T. K. Snyder, 773-42A
J. J. Connelly, 773-41A
K. G. Brown, 704-1T
D. R. Best, 773-41A
D.K. Peeler, 773-43A
T.H. Lorier, 773-23A
D. H. Miller, 786-1A
T. B. Edwards, 773-42A
J.C. George, 773-43A
Records (4)
VT QA File